ARYL-SUBSTITUTED IMINO-N-HETEROCYCLIC CARBENE COMPLEXES OF LATE TRANSITION METALS: SYNTHESIS AND REACTIVITY STUDIES

ANNA CANDACE BADAJ

A DISSERTATION SUBMITTED TO THE FACULTY OF GRADUATE STUDIES IN PARTIAL FULFILLMENT OF THE REQUIREMENT FOR THE DEGREE OF

DOCTOR OF PHILOSOPHY

GRADUATE PROGRAM IN CHEMISTRY

YORK UNIVERSITY

TORONTO, ONTARIO

June 2014

ABSTRACT

N-heterocyclic carbenes (NHCs) have found enormous success as ancillary ligands in catalysts in many areas of organometallic chemistry. Surprisingly, their use in olefin polymerization, until recently, was not widely explored. The focus of this thesis is to investigate the synthesis of a bidentate ligand scaffold that incorporates an NHC moiety and to study the ability of the resulting complexes to catalyze chemical transformations such as olefin polymerization.

The synthesis and characterization of several *N*-aryl substituted imino-imidazolin-2-ylidene (C^Imine$_R$) ligand precursors was achieved following one of two synthetic protocols. Coordination of these ligands was explored with Group 11 metals in order to develop synthetic protocols which were later extended to prepare complexes of ruthenium, cobalt, iron, nickel, palladium and zinc.

The coordination of C^Imine$_R$ ligands to nickel using new copper carbene dimers as the transmetalating agent was established. All the nickel complexes were structurally characterized and the size of the iminic carbon substituent was found to have a profound impact on the bond angles and bond lengths around the metal center. However, when tested for ethylene polymerization activity at standard temperature and pressure, the nickel complexes were found to be inactive.

With the discovery the nickel complexes of these C^Imine$_R$ ligands were inactive for ethylene polymerization, the research focus was extended to the diamagnetic palladium-methyl complexes in order to gain insight into their thermal stability and

insertion chemistry. The nature of the iminic substituent profoundly affects the thermal stability of the neutral palladium complexes. While inactive for ethylene polymerization, these palladium methyl complexes react with CO and isocyanides to form various coordination and insertion products.

ACKNOWLEDGEMENT

I would like to thank my supervisor, Professor Gino G. Lavoie, for providing me with the opportunity of being a part of his research group. Dr. Lavoie has been a great mentor over these years, not only providing me with direction but also encouragement at difficult points of this journey. I would like to thank my examining committee members for their valuable time and contribution to my thesis defense.

I would like to thank those that have provided assistance with my research. I would like to thank Dr. Howard Hunter for his help with spectroscopic techniques. Many thanks to Dr. Alan Lough and Dr. Jim Britten for their help with structure determination. The Lavoie research group, whom on a daily basis, provided me with ideas, encouragement, laughter and friendship: Jameel Al Thagfi, Edwin Alvarado, Sarim Dastgir, Michael Harkness, Delwar Hossain, Tim Larocque, Richard Morris and Barbara Skrela. It has been a great pleasure to have worked together with all of you.

I would like to thank my parents for the love and support they have given me all these years.

Table of Contents

List of Tables

List of Figures

List of Abbreviations

Å	angstrom
ArNC	aryl isocyanide
atm	atmosphere
Ar	aryl
BARF	tetrakis[3,5-bis(trifluoromethyl)phenyl]borate
br	broad
^{13}C	carbon-13
calc	calculated
C^Imine$_{Me}$	1-(1-(2,6-dimethylphenylimino)ethyl)-3-(2,4,6-trimethylphenyl)imidazol-2-ylidene
C^Imine$_{Me'}$	1-(1-(2,6-diisopropylphenylimino)ethyl)-3-(2,4,6-trimethylphenyl)imidazol-2-ylidene
C^Imine$_{Me''}$	1-(1-(2,6-dimethylphenylimino)ethyl)-3-(2,6-diisopropylphenyl)imidazol-2-ylidene
C^Imine$_{Ph}$	1-(1-(2,4,6-trimethylphenylimino)benzyl)-3-(2,4,6-trimethylphenyl)imidazol-2-ylidene
C^Imine$_{t\text{-}Bu}$	1-(1-(2,6-dimethylphenylimino)-2,2-dimethylpropyl)-3-(2,4,6-trimethylphenyl)imidazol-2-ylidene
CO	carbon monoxide
COD	1,5-cyclooctadiene

DCM	dichloromethane
DIPP	diisopropylphenyl
DME	dimethyoxyethane
d	doublet
Et	ethyl group
^{1}H	proton
{^{1}H}	proton decoupled
HMBC	heteronuclear multiple-bond correlation
HSQC	heteronuclear single quantum coherence
m	meta
Me	methyl group
NHC	*N*-heterocyclic carbene
NMR	nuclear magnetic resonance
o	*ortho*
ORTEP	Oak Ridge Thermal Ellipsoid Program
p	para
Ph	phenyl group
rt	room temperature
s	singlet
*t*Bu	*tert*-butyl group
THF	tetrahydrofuran
TMSCl	trimethylsilyl chloride

Chapter 1 – General Introduction

1.1 Polymerization Catalysts – An Introduction

The discovery of titanium halides and alkylaluminum reagents by Ziegler and Natta[1] to be used in the polymerization of ethylene and propylene has led to the development of several new homogeneous single-site catalysts.[2-4] Studies of group 4 metallocenes have provided a mechanistic understanding of the critical elementary steps involved in the formation of polyolefins.[5] As a result, various ligand scaffolds and their corresponding complexes have been developed with enhanced activity and control over the properties of the polymer.[6] This work in the field of organometallic chemistry and polymer science has led to the development of commercial protocols to prepare polyolefins varying in microstructure and properties. Unfortunately, aside from radical polymerization, commercial processes for the preparation of new materials from copolymerization of ethylene and polar monomers (such as acrylate, vinyl acetate and acrylonitrile) do not currently exist.

Polymerization catalysts based on early transition metals have proven to be excellent catalysts for the polymerization of ethylene and propylene. However in the presence of polar monomers, the high oxophilicity of early transition metals causes these catalysts to be poisoned and leads to catalyst deactivation. Late transition metals are more tolerant towards functional groups and therefore are more appealing candidates to be used in the development of catalysts for copolymerization. Therefore it is no surprise late transition metal catalysts have attracted a great deal of attention not only for the polymerization of α-olefins[7] but also for copolymerization with polar monomers.[8] For the purpose of this

thesis, the literature background moving forward will concentrate on late transition metal oligomerization and polymerization catalysts. An emphasis will be placed on identifying the key features crucial for the development of an active, robust catalyst and examining the ability of several late transition metal catalysts to copolymerize α-olefins with polar monomers.

1.2 α-Diimine Neutral Chelating Systems of Late Transition Metals

Prior to the 1990s, the field of polymerization was heavily dominated by early transition metal-based catalysts. An important discovery in the mid 1990s by Brookhart revealed α-diimine nickel and palladium pre-catalysts were active in ethylene polymerization to give high molecular weight polyolefins (Figure 1).[7] This new found knowledge created renewed interest in the field of polymerization for late transition metals. A key component of this system is the α-diimine ligand. Features of the α-diimine ligand include: they are bidentate neutral ligands that enforce a *cis* geometry in square planar complexes,[9,10] they are good σ–donors and π–acceptors,[11] and it is possible to prepare extensive libraries of the ligand that have varying steric and electronic properties at the backbone and aryl positions.[12]

The effect of the substitution pattern on catalyst activity and polymer properties has been investigated by many research groups. This work led to a series of important observations: 1) As the bulk of the *ortho* substituents is increased, the molecular weights of the polymer increase;[13] 2) Catalysts containing the 2,3-butanedione back bone produce polymers with molecular weights higher than those obtained from catalysts based on a

planar aromatic acenaphthyl backbone;[13] 3) Greater electron-donating ligands on the metal center result in more stable catalysts;[14] 4) Catalysts with greater electron-donating ligands gave higher molecular weight polymers;[14] and 5) Catalysts with greater electron-donating ligands produced ethylene-acrylate copolymers with greater polar monomer incorporation.[14]

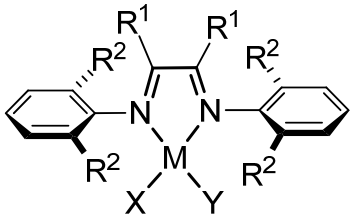

M = Ni, Pd

Figure 1. Nickel(II) and Palladium(II) α-diimine precatalysts.

In addition to being active catalysts for ethylene polymerization, Brookhart published findings that revealed cationic palladium complexes containing α-diimine ligands showed activity toward the copolymerization of ethylene with acrylates.[7,8] However, the palladium catalysts did not exhibit high turnover frequencies (TOF) and the level of acrylate incorporation was mainly found at the end of the polymer chains rather than into the polyethylene chain. Another shortcoming of these systems was the carbonyl group of the polar monomer would inhibit the catalyst by binding to the metal and occupying the vacant site thus not allowing for subsequent insertion to occur.[8]

1.3 Mechanism of Olefin Polymerization

With all the research surrounding nickel and palladium α-diimine complexes, one area of focus has been the mechanism of ethylene polymerization. A cationic species is considered the active species responsible for polymerization, therefore starting from the neutral precatalysts (species **1.3a** in Figure 2) activation is usually achieved *in situ* using several possible routes.[15] The most common route for nickel complexes is achieved by treating the dihalide species with methylaluminoxane (MAO).[16] Although the exact details of how MAO generates the active species is not clear, a probable sequence of events are the aluminum reagent alkylates the complex forming a dialkyl species which is followed by a mono-dealkylation from the nickel. This results in the formation of a cationic species containing a vacant site *cis* to the alkyl group which is able to accommodate binding of a substrate (Figure 2).[6]

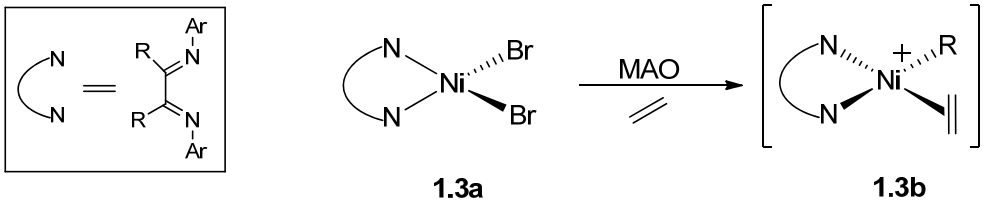

1.3a **1.3b**

Figure 2. General representation for the activation of a Ni(II) α-diimine polymerization catalyst.

For palladium alkyl precatalysts, generation of the active species is easily achieved by abstraction of the chloride by either silver reagents or sodium tetrakis(3,5-

bis(trifluoromethyl)phenylborate (NaBARF) (Figure 3) and can be performed in the presence of a coordinating solvent such as acetonitrile.[17]

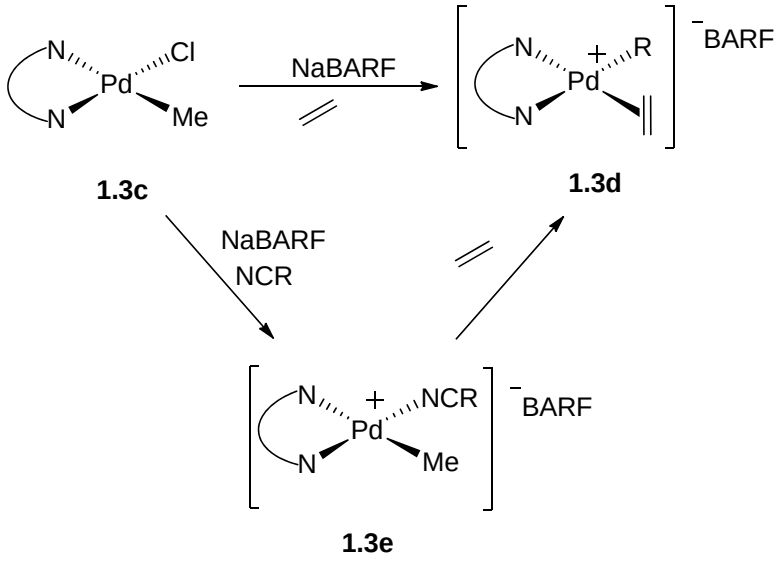

Figure 3. General representation for the activation of a Pd(II) α-diimine polymerization catalyst.

The mechanism of polymerization is outlined in Figure 4.[7,17,18] Upon formation of a cationic species, coordination of an olefin gives rise to an alkyl olefin complex, structure **I**. Migratory insertion results in the formation of **II**. Polymerization proceeds with repeated coordination of ethylene, followed by migratory insertion to grow the polymer chain continuously cycling between structures **I** and **II**. Instead of ethylene coordination, complex **II**, can undergo a β–hydride elimination to form an olefin hydride species, **III**. Complex **III** can undergo hydride reinsertion to form a branched alkyl group on the polymer chain (structure **V**) which can further proceed in polymer growth. The

other possibility is complex **III** can undergo a chain transfer via an associative displacement[19,20] of the polymer by ethylene from the olefin hydride species which initiates a new chain.

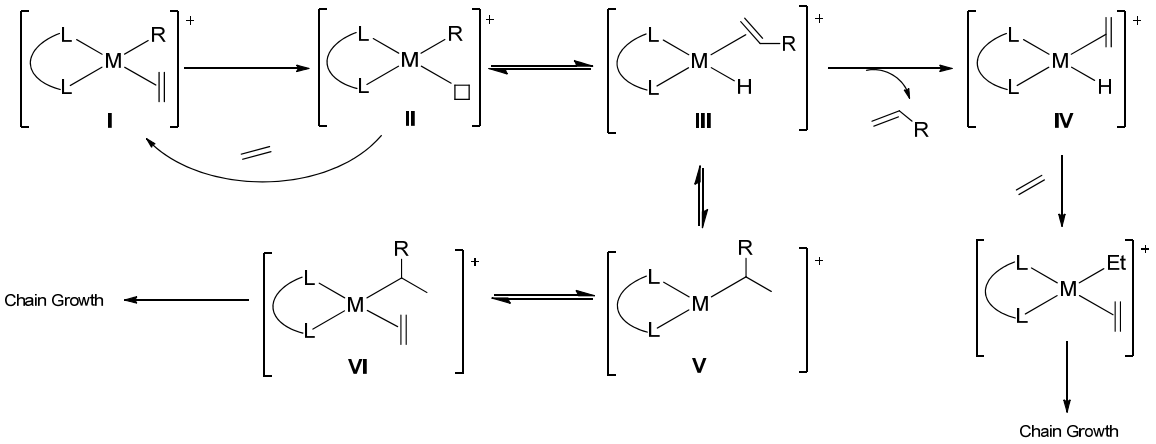

Figure 4. General representation of mechanism of ethylene polymerization.

1.4 Iminophosphine Chelating Systems of Late Transition Metals

Despite the significant progress made by Brookhart, most α-diimine-based nickel and palladium catalysts are thermally unstable and decompose[17,21] rapidly at elevated temperatures.[13] Therefore it is no surprise a lot of interest has been directed to improve the thermal stability of this class of catalysts which has led to alternative ligands with an N-N, N-O and P-P binding motif.[4,22] Of particular interest is the work with the related iminophosphine ligand Brookhart and Marshall reported (Figure 5). The iminophosphine ligand is similar to the α-diimine scaffold except one imine group is replaced with a

phosphine group. The results of this alteration were the iminophosphine-based catalysts were less productive than the α-diimine-based catalysts but showed significantly improved thermal stability upon activitation.[23,24] This was an important observation, indicating that greater electron-donating ligands can enhance the thermal stability of their corresponding complexes.

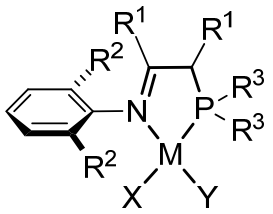

M = Ni, Pd

Figure 5. Nickel (II) and Palladium (II) iminophosphine precatalysts.

1.5 Monoanionic Chelating Systems of Late Transition Metals

In addition to neutral ligands, monoanionic ligands have proven to be valuable in the area of oligomerization and polymerization. An example is the Shell Higher Olefin Process which uses nickel complexes bearing a monoanionic chelating [PO] ligand for the oligomerization of ethylene.[25-27] The catalysts, depicted in Figure 6, produce linear α-olefins from ethylene. Extensive research of these systems have revealed that the activity of SHOP-type catalysts can be controlled by the architecture of the ligand;[28] large bulky groups next to the oxygen atom lead to an increase in activity of the resulting catalysts[29]

and the molecular weights of the oligomer can be increased by the addition of greater bulk as well as greater electron density on the substitutents on the phosphorous atom.[27]

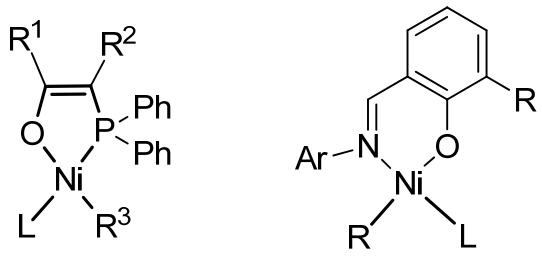

Figure 6. Nickel(II) precatalysts with monoanionic [PO] and [NO] ligands.

With the immergence of monoanionic [PO] ligands, several related anionic chelates have also been introduced. Grubbs reported complexes of nickel bearing monoanionic salicylaldinaminato [NO] ligands that exhibited high activities towards ethylene polymerization (Figure 6).[30] The bulky substitutents at the *ortho* position of the N-aryl rings result in an increase in the molecular weights of the polymer and bulky substitutens on the phenoxy group are an important feature as they deter the formation of bis-ligand complexes which lead to catalyst deactivation.[4] In addition to be active catalysts for ethylene, salicylaldiminato complexes of nickel have also been found active in the copolymerization of ethylene with other α-olefins.

1.6 Chelating Ligands for Copolymerization Catalysts of Late Transition Metals

In the last two decades, the emergence of polymerization catalysts capable of incorporating polar monomers into a linear ethylene chain have been reported (Figure

7).[31] Drent demonstrated neutral palladium catalysts that contain an anionic chelating sulfonate phosphine ligand can produce linear copolymers that incorporate acrylates. [31] Unlike Brookhart's work that also demonstrated palladium complexes bearing α-diimine ligands can copolymerize ethylene with acrylates, the polymers produced were branched polyethylene chains where the acrylate incorporation was mainly found at the end of the polymer chains, Drent's system demonstrated acrylate incorporation within the polyethylene chain. In addition, these palladium catalysts have also been shown to copolymerize vinyl ethers,[32] vinyl fluoride and acrylamides.[33] Although Drent's initial report was based on a palladium catalyst generated *in situ*, research groups have successfully been able to prepare and characterize the isolated precatalyst. [34]

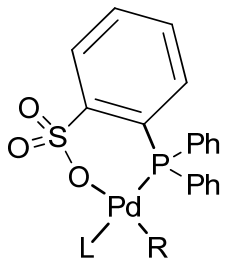

Figure 7. Palladium(II) precatalysts with monoanionic ligands.

1.5 *N*-Heterocylic Carbenes – Introduction

N-heterocyclic carbenes (NHCs) were first explored by Wanzlick several decades ago in the early 1960s[35] and independently coordinated to transition metals by Wanzlick[36] and Ofele[37] in 1968. It was only until Arduengo[38] reported the synthesis and isolation of

an NHC in 1991 that it became an area of immense research interest in the field of transition metal chemistry.[39]

1.6 Features of NHC Ligands

The attractive features that have made NHCs so ubiquitous in the field of organometallic chemistry include their electronic properties and their ability to impart thermal stability in their corresponding complexes. NHCs are neutral strong sigma-donors.[40,41] Comparison studies using carbonyl complexes bearing either an NHC or phosphine have revealed NHCs are in fact more electron-donating than even the most basic phosphines.[42-46] It is possible to alter the electronic character of an NHC by altering the electronic nature of the azole ring.[47] Being the strong sigma donors as they are, NHCs form very strong bonds with metals [41,48] resulting in the formation of very robust metal-carbene complexes. Despite the strength of a metal-carbon bond, there are reported cases where migratory insertion into a metal-carbene bond,[49,50] reductive elimination,[51] and carbene displacement by another ligand[52] has occurred proving the metal-carbene bond is not exempt from decomposition pathways.

1.7 Synthetic Routes to Prepare Metal-Carbene Complexes

There are a number of ways to prepare transition metal imidazol-2-ylidene complexes. The synthetic methodologies that were followed to prepare compounds in this thesis are generically represented in Figure 8. One of the most common methods to prepare NHC complexes involves the complexation of an isolated *N*-heterocyclic carbene

ligand via the ligand displacement reaction using a suitable metal precursor. This method has been successfully employed for a variety of transition metal precursors and used to displace several neutral ligands to include phosphines,[53] carbonyls,[43] amines[54] and coordinated solvent molecules.[55] When it is not possible to isolate the carbene, another method that can be employed is reaction of the imidazolium salt with a metal precursor that contains a basic ligand.[56] Basic metal precursors are commercially available or can be prepared *in situ*.[57,58] Another methology that can be used when isolation of the free carbene is not possible is the use of an isolated or *in situ* generated transmetalating agent such as a silver NHC complex, to transfer the ligand from silver to a suitable target metal precursor.[59] In cases where the imidazolium precursors contain functional groups that are sensitive to deprotonation by a strong base, the use of transfer agents becomes a viable alternative. Lastly, oxidative addition of the imidazolium salt with appropriate metal precursors can be used to prepare metal carbene hydride species.[60]

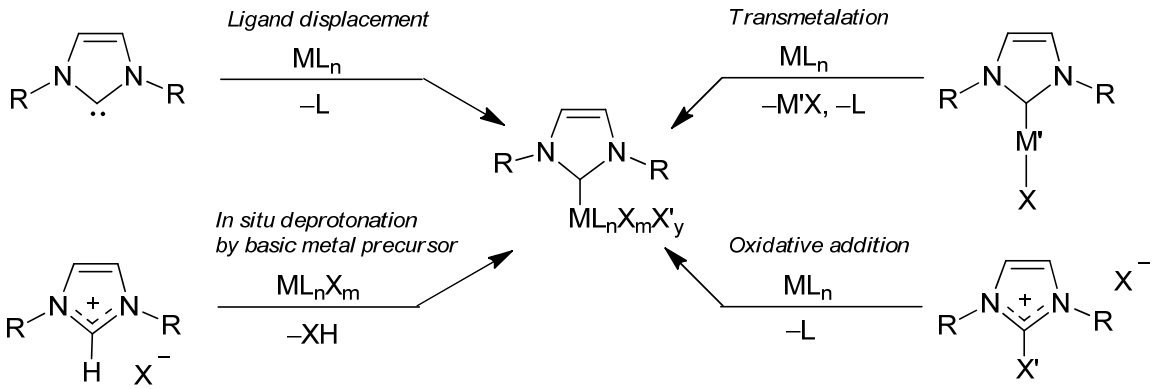

Figure 8. General routes to prepare NHC metal complexes.

1.8 Plan of Study

In the last few years, much effort has been made to synthesize novel *N*-heterocyclic ligands and the corresponding metal complexes since the strong sigma donor ability of the NHC leads to complexes that are more thermodynamically robust than phosphine ligands.[61] Until recently, their use in olefin polymerization was not widely explored.[62,63] Considering the improved thermal stability of group 10 complexes with bulky iminophosphine ligands over those with the related α-diimines,[23,24] it became of interest to investigate the synthesis of a bidentate ligand scaffold that incorporates an *N*-heterocyclic carbene moiety (Figure 9) and study the ability of the resulting complexes to catalyze chemical transformations such as olefin polymerization.

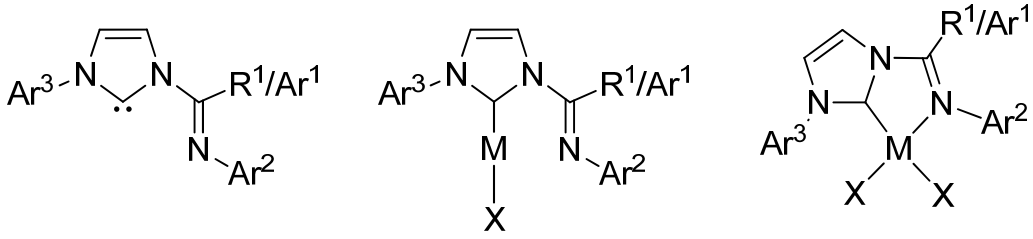

Figure 9. Design concept for *N*-heterocyclic carbene ligands and their corresponding metal complexes.

The ligand scaffold of interest in our research group has several advantages over other bidentate imino-,[64] pyridyl-,[65-67] and oxazolinyl-functionalized[68] carbene ligands (Figure 10).[64,69-71]

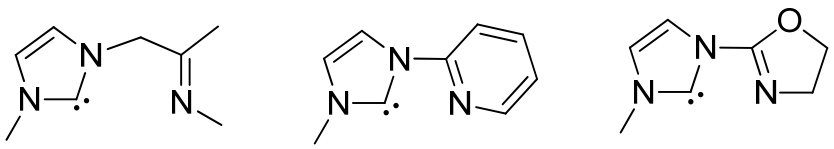

Figure 10. Functionalized carbene ligands.

The absence of any carbon spacers between the carbene and imine group will avoid tautomerisation of the imine moiety to an enamine upon coordination with a metal precursor.[64] In addition, the removal of the carbon spacer may prevent decomposition of the ligands during attempts to prepare the free carbenes.[72] The bulky aryl subsitutents on both the imidazolin-2-ylidene and the imine nitrogen atoms will stabilize coordinatively-unsaturated species, such as square-planar d^8 complexes, and protect the axial sites against unwanted coordination or associative displacement of other loosely bound ligands. Bulky aryl substituents, not present in other related systems, turned out to be critical for the group 10 α-diimine system in producing high molecular weight polymers.[7] In addition, the presence of bulky aryl groups at various locations along the ligand scaffold will allow fine-tuning of sterics and electronics of the active site. This is achieved by reaction of various easily prepared *N*-aryl-substituted imidazoles with *N*-aryl-substituted imidoyl chlorides.

Chapter 2. Aryl-Substituted Imino-*N*-Heterocyclic Carbene Ligands: Synthesis, Characterization and Coordination with Silver(I), Copper(I) and Gold(I)

Preface

A part of the research presented in this chapter has been published in several papers.[73-75] Any work presented in these papers that was completed by other research colleagues does not appear in this thesis.

2.1 Introduction

The use of NHCs as an ancillary ligand in the area of organometallic chemistry has grown immensely since Arduengo reported the isolation of an NHC. Due to the strong σ–donor ability of the carbene, complexes are more thermodynamically robust compared to those with phosphine ligands. To explore the application of NHC ligands in olefin polymerization, the synthesis of a bidentate ligand that would have an NHC imbedded into the scaffold was investigated along with the coordination chemistry. This chapter describes the synthesis and characterization of the first *N*-aryl substituted imino-imidazolin-2-ylidene ligand precursors, isolation of the free carbenes and coordination to Group 11 metals.

2.2 Results and Discussion

2.2.1 Synthesis of imidazolium salts and imino-N-heterocyclic carbene ligands

In order to prepare a library of complexes bearing structurally and electronically distinct ligands, a synthetic protocol to easily prepare a variety of ligand precursor

scaffolds first needed to be established. Following a modified synthetic approach from the literature,[72,76] a series of imino imidazolium salts can be prepared by reaction of a substituted arylimidazole with *N*-(aryl)acetimidoyl chloride (Scheme 1).

Scheme 1. Synthesis of imino-NHC ligand precursors (**1a–1a"**).

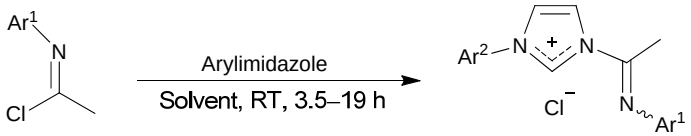

a: Ar^1 = 2,6-dimethylphenyl; Ar^2 = 2,4,6-trimethylphenyl — **1a** ($C^{\wedge}Imine_{Me}$·HCl)
a': Ar^1 = 2,6-diisopropylphenyl; Ar^2 = 2,4,6-trimethylphenyl — **1a'** ($C^{\wedge}Imine_{Me'}$·HCl)
a":Ar^1 = 2,6-dimethylphenyl; Ar^2 = 2, 6-diisopropylphenyl — **1a"**($C^{\wedge}Imine_{Me"}$·HCl)

The imidazolium salt **1a** is readily prepared from 1-(2,4,6-trimethylphenyl)imidazole and *N*-(2,6-dimethylphenyl)acetimidoyl chloride in THF at room temperature (Scheme 1). In the ^{1}H NMR ($CDCl_3$) spectrum, the resonance of the central imidazolium proton (NC*H*N) for the *E*-isomer resonance is observed at δ 11.98 and the backbone protons of the heterocycle (NC*H*C*H*$N_{mesityl}$) appear at δ 8.51 and δ 7.24. In the ^{13}C NMR spectrum, the iminic carbon (*C*=N) resonance and the central imidazolium carbon (N*C*N) appear at δ 150.1 at δ 140.2, respectively. The FTIR $\upsilon_{C=N}$ absorption for the imine group of **1a** is 1691 cm^{-1}. The ^{1}H NMR spectrum of a freshly prepared DMSO-d_6 solution initially shows the presence of both geometric isomers (*E*/*Z*) in approximately a 15:1 ratio, with the major isomer assigned unambiguously as the *E*-isomer by 1D NOESY experiments using selective excitations. Slow isomerization to the

Z-isomer was observed at room temperature. In contrast, isomerization in $CDCl_3$ at 333K was very slow, with no observable change in the initial ratio of isomers over 24 hours.

The solid-state structure of compound **1a** was determined by X-ray crystallography and the molecular structure is shown in Figure 11 along with select bond lengths and angles. Compound **1a** crystallized in the centrosymmetric P –1 space group. Analysis reveals that the *E*-isomer preferentially crystallized out of the mixture of isomers. The solid-state structure shows that the mean plane passing through C5–C4–N3–C6 is slightly twisted off from the imidazol-2-ylidene ring by 0.78º. The 2,6-dimethylphenyl and the 2,4,6-trimethylphenyl rings are twisted 99.37º and 71.23º with respect to the 5-membered ring, respectively (Figure 11).

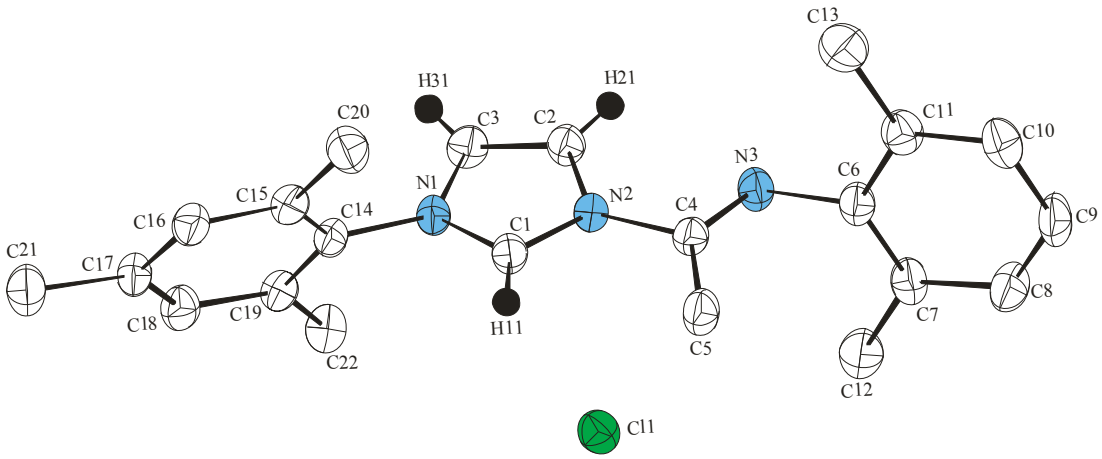

Figure 11. ORTEP plot of (C^Imine$_{Me}$H·Cl) **(1a)** (30% probability level). Hydrogen atoms and dichloromethane molecules are omitted for clarity. Select bond lengths (Å) and angles (º): N1–C1 1.323(4), N2–C1 1.338(4), N1–C3 1.398(4), N2–C2 1.391(4), C2–C3 1.344(5), N3–C4 1.262(4), N1–C1–N2 108.1(3), C1–N1–C14 125.8(3), C1–N2–C4 126.1(3).

An analogous imino imidazolium salt, C^Imine$_{Me'}$·HCl (**1a'**), was synthesized by replacing the 2,6-dimethylphenyl ring with a 2,6-diisopropylphenyl fragment by reaction of 2,4,6-trimethylphenylimidazole with *N*-(2,6-diisopropylphenyl)acetimidoyl chloride in toluene for a total of 19 h (Scheme 1). The ^{1}H NMR ($CDCl_3$) spectrum of **1a'** shows the presence of only one isomer. In the ^{1}H NMR spectrum, the central imidazolium proton (NC*H*N) is observed at δ 12.20 and the remaining backbone protons of the heterocycle (NC*H*C*H*N$_{mesityl}$) appear at δ 8.51 and δ 7.28. In the ^{13}C NMR spectrum, the iminic carbon (*C*=N) resonance and the central imidazolium carbon (N*C*N) appears at δ 149.8 and δ 140.3, respectively. The FTIR $\nu_{C=N}$ absorption for the imine group of **1a'** is 1698cm^{-1}. To introduce a different substitution pattern on the aryl substitutent bound to the azole nitrogen, compound **1a"** C^Imine$_{Me"}$·HCl, was prepared in a similar manner to **1a** from 1-(2,6-diisopropylphenyl)imidazole and *N*-(2,6-dimethylphenyl)acetimidoyl chloride in THF at room temperature (Scheme 1). Similar to **1a'**, compound **1a"** also shows the presence of only one isomer.

Having found success at preparing several ligand precursors of different aryl substituents at the imine and 3-azole positions, the next step was to replace the methyl substituent at the iminic position for a *tert*-butyl and phenyl group. Reactions of *N*-(2,6-dimethylphenyl)pivalimidoyl chloride or *N*-(2,4,6-trimethylphenyl)benzimidoyl chloride with 2,4,6-trimethylimidazole under similar reaction conditions used for compounds **1a** and **1a'** unfortunately did not produce the desired imidazolium chloride. Numerous attempts were made varying the ratio between reagents, solvents, reaction time and temperature but no success was reached with this synthetic approach. The imidoyl

chloride was thus activated by first reacting it with sodium tetrafluoroborate to form the corresponding nitrilium ion and sodium chloride. Addition of 2,4,6-trimethylphenylimidazole to the highly electrophilic nitrilium ion produced the targeted products (Scheme 2).

Scheme 2. Synthesis of imino imidazolium salts **1b** and **1c**.

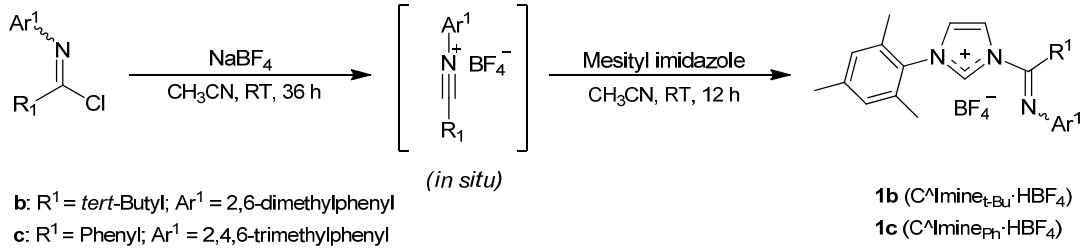

Solution ^{1}H NMR spectroscopy of **1b** in $CDCl_3$ showed that a single geometric isomer was formed, unambiguously assigned to the *E* conformer by a series of 1D NOESY NMR experiments. In the ^{1}H NMR spectrum, the central imidazolium proton for the major isomer resonance is observed at δ 8.39 and the remaining backbone protons of the heterocycle appear at δ 7.70 and 7.25. In the $^{13}C\{^{1}H\}$ NMR spectrum, the iminic carbon (*C*=N) resonance appears at δ 154.6 and the central imidazolium carbon appears at δ 134.8. The phenyl derivative C^Imine$_{Ph}$·HBF_4 (**1c**) also necessitated activation of the imidoyl chloride by reaction with sodium tetrafluoroborate to form the corresponding nitrilium salt *in situ* (Scheme 2). The ^{1}H NMR ($CDCl_3$) resonance for the central imidazolium proton of **1c** is observed at δ 8.81, while those for the inequivalent backbone protons of the heterocycle appear at δ 8.09 and 7.52. The iminic and the central

imidazolium carbon nuclei resonate at δ 148.1 and 136.1, respectively. The FTIR stretching frequency for the imine group of **1c** was observed at 1675 cm^{-1}. With several salts in hand, the next step was to generate the free carbene.

Reaction of the imidazolium salt (**1b**) with sodium bis(trimethylsilyl)amide cleanly gave the free carbene **2b**, C^Imine$_{t\text{-Bu}}$, in 91% yield (Scheme 3). The ^{1}H and ^{13}C NMR spectra are in agreement with the desired product. The ^{1}H NMR resonance for the central imidazolium proton of **1b** vanished and a new ^{13}C NMR resonance appeared at 218.3 ppm, characteristic of central carbon nuclei of NHCs.[72] 1D NOESY NMR spectoscopy showed that **2b** exists as the *Z* conformer in solution.

Scheme 3. Synthesis of free carbenes C^Imine$_{t\text{-Bu}}$ (**2b**) and C^Imine$_{Ph}$ (**2c**).

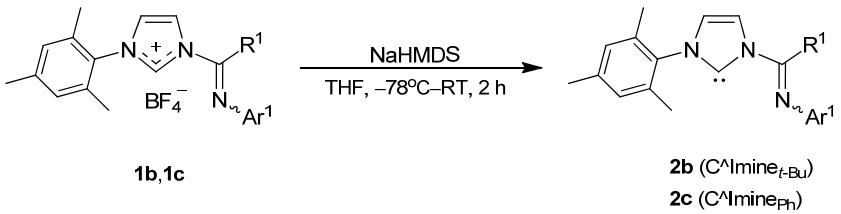

1b,**1c**

2b (C^Imine$_{t\text{-Bu}}$)
2c (C^Imine$_{Ph}$)

Crystals of the C^Imine$_{t\text{-Bu}}$ (**2b**) suitable for X-ray diffraction studies were grown at –35 °C from a saturated pentane solution and crystallized in the centrosymmetric P –1 space group. Single crystal X-ray diffraction analysis confirmed generation of the free carbene **2b.** The molecular structure is shown in Figure 12 along with select bond lengths and angles. The imine group also adopts the *Z*-conformation in the solid-state,

with a 54.03° angle between the mean planes formed by C14, C13, N3 and C18 and by the imidazol-2-ylidene ring. The 2,4,6-trimethylphenyl ring is twisted off by 82.95° with respect to the azole ring.

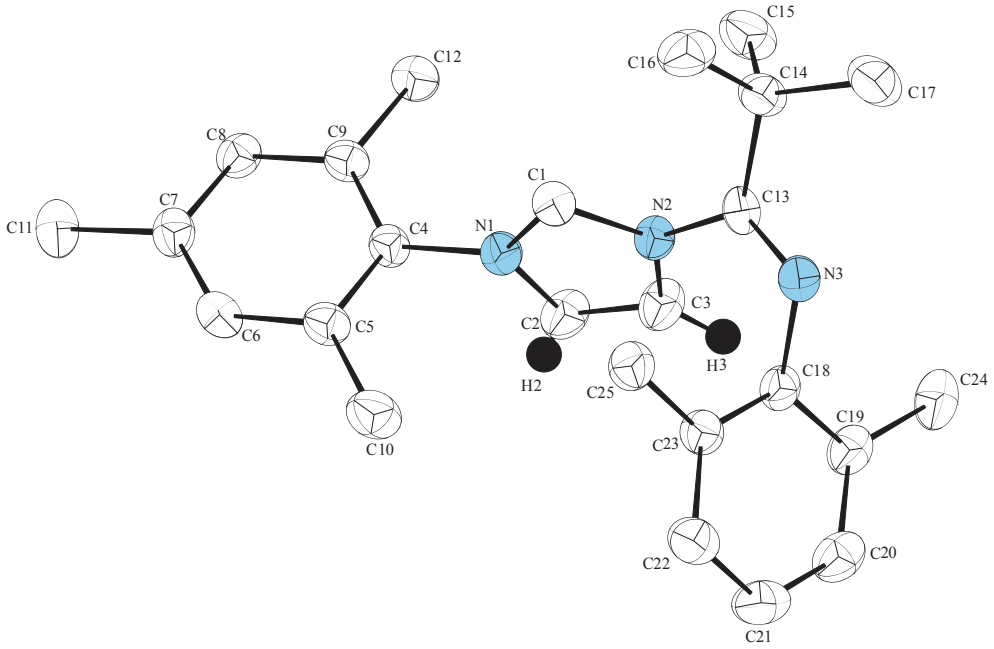

Figure 12. ORTEP plot of (C^Imine$_{t\text{-Bu}}$) **(2b)** (50% probability level). Hydrogen atoms and solvent molecules are omitted for clarity. Selected bond lengths (Å) and angles (°):N1–C1 1.354(3), N2–C1 1.380(3), N1–C2 1.393(3), N2–C3 1.388(3) , C2–C3 1.338(3) , N3–C13 1.266(3), N1–C1–N2 101.48(19).

Deprotonation of **1c** with bis(trimethylsilyl)amide under similar conditions also cleanly gave the corresponding free carbene C^Imine$_{Ph}$ (Scheme 3) in 72% yield, with ^{1}H and ^{13}C NMR spectra consistent with the desired product. The stretching frequency of the imine group is observed for **2c** at 1652 cm^{-1}.

2.2.2 Synthesis of group 11 imino-N-heterocyclic carbene complexes

Attempts to deprotonate C^Imine$_{Me}$·HCl (1a) with common bases, such as potassium *tert*-butoxide, bis(trimethylsilyl)amide, and hydride, to form the corresponding free carbene were unsuccessful and led to a mixture of unidentified products, possibly due to competing deprotonation of the iminic methyl group with subsequent decomposition. Similar observations were reported in other related systems.[77] The preparation of the corresponding silver complex was thus investigated. This approach is valuable as silver complexes can effectively transmetalate the coordinated carbene to other transition metals and would allow us to prepare the corresponding group 10 complexes as initially intended. C^Imine$_{Me}$·HCl (1a) shows no reactivity towards silver(I) oxide under various experimental conditions, in contrast, reaction of 1a with silver carbonate at room temperature cleanly generated the silver chloride complex (C^Imine$_{Me}$)AgCl (3a) in 77% yield (Scheme 4).

Scheme 4. Synthesis of silver(I) complexes (**3a–3a"**).

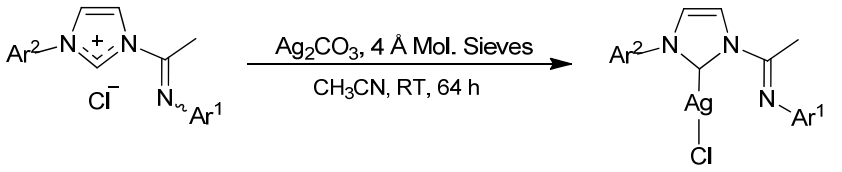

1a–**1a"**

3a (C^Imine$_{Me}$)AgCl
3a' (C^Imine$_{Me'}$)AgCl
3a" (C^Imine$_{Me"}$)AgCl

The ^{1}H and ^{13}C NMR spectra are in agreement with the desired product. 1D NOESY ($CDCl_3$) experiments using selective excitations confirm the presence of only

the *E* isomer in solution. The FTIR stretching frequency for the imine group of **3a** was observed at 1682 cm^{-1} comparable to that of C^Imine$_{Me}$·HCl (**1a**) ($\nu_{C=N}$ 1691 cm^{-1}) which is an indication of no coordination of the iminic arm.[69]

X-ray diffraction studies on a single crystal show the complex also adopts the *E*-configuration in the solid-state (Figure 13), in agreement with that observed in solution. As expected, the ligand is coordinated to silver through the carbene center. The Ag1–C1 and Ag1–Cl1 bond lengths are 2.074(3) and 2.3346(9) Å, respectively, with a C1–Ag1–Cl1 angle of 176.29(9)º. Those values are in agreement with the corresponding values observed in related compounds.[69,76,78,79] In contrast to C^Imine$_{Me}$·HCl (**1a**), the imine nitrogen N3 in (C^Imine$_{Me}$)AgCl (**3a**) is positioned so as to allow possible interactions with the metal center. However, the measured Ag(1)···N(3) distance (2.866 Å) is too great for any significant interaction. The elevated FTIR $\nu_{C=N}$ absorption at 1682 cm^{-1}, further confirms the absence of any dative bond between N(3) and the metal center. This value is in fact comparable to that observed for the imidazolium salt precursor **1a**, with a $\nu_{C=N}$ absorption at 1691 cm^{-1}. Coordination of N3 would have decreased the $\nu_{C=N}$ value to ca. 1610 cm^{-1}.[69] The angles between the mean planes formed by the imidazol-2-ylidene ring and those of the 2,6-dimethylphenyl and of the 2,4,6-trimethylphenyl rings are 52.15 and 74.87°, respectively.

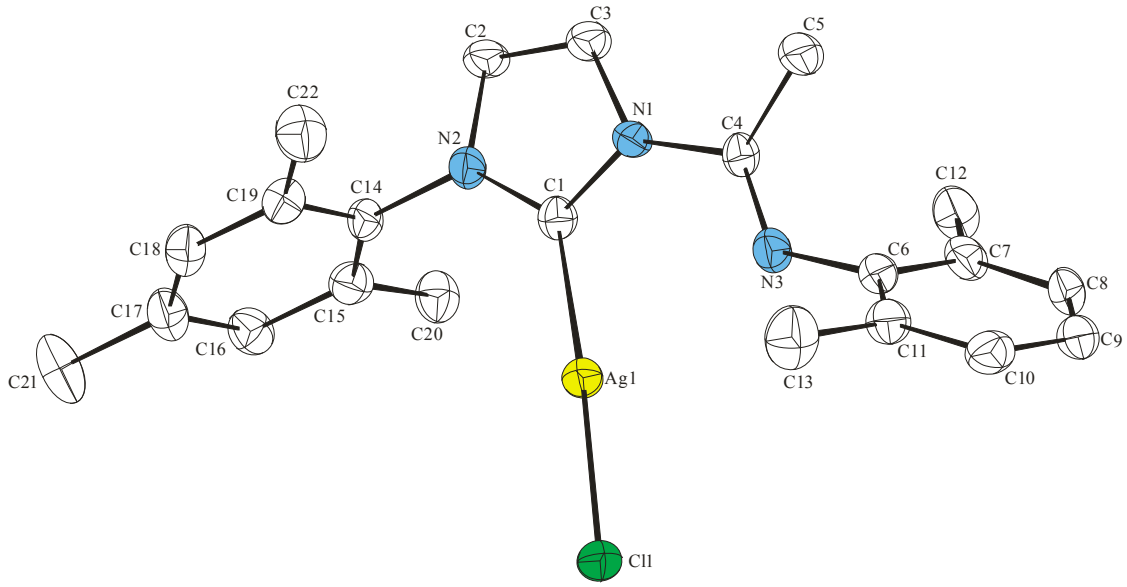

Figure 13. ORTEP plot of [(C^Imine$_{Me}$)AgCl] **(3a)** (30% probability level). Hydrogen atoms and dichloromethane molecules are omitted for clarity. Select bond lengths (Å) and angles (º): Ag1–Cl1 2.3346(9), Ag1–C1 2.074(3), N3–C4 1.263(5), C1–Ag1–Cl1 176.29(9), N1–C4–N3 116.8(3).

Once a set of conditions to successfully coordinate the C^Imine$_{Me}$ ligand to silver was established, this same synthetic protocol was used to prepare the other analogous silver carbene complexes 3a' and 3a".

The ^{1}H NMR ($CDCl_3$) spectrum for compounds 3a' and 3a" shows the presence of only one isomer. The ^{1}H NMR spectrum is consistent with the formation of the carbene and coordination to silver. In the ^{13}C NMR spectrum, the iminic carbon (*C*=N) resonance appears at δ 153.3 and 152.2 for 3a' and 3a", respectively. The carbene carbon (N*C*N) appears at δ 182.5 and 182.8 for 3a' and 3a", respectively.

Despite being initially interested in group 10 transition metal complexes, it was important to first prepare and study the coordination chemistry of the ligand to group 11 metals, as the resulting complexes would be diamagnetic and would allow for characterization by NMR spectrometry. Cu(C^Imine$_{Me}$)$_2$Cl (**4**) was synthesised in 69% yield as the expected sole product of the reaction of silver complex **3a** with CuI in dichloromethane (Scheme 5).

Scheme 5. Synthesis of Copper(I) Complex **4**.

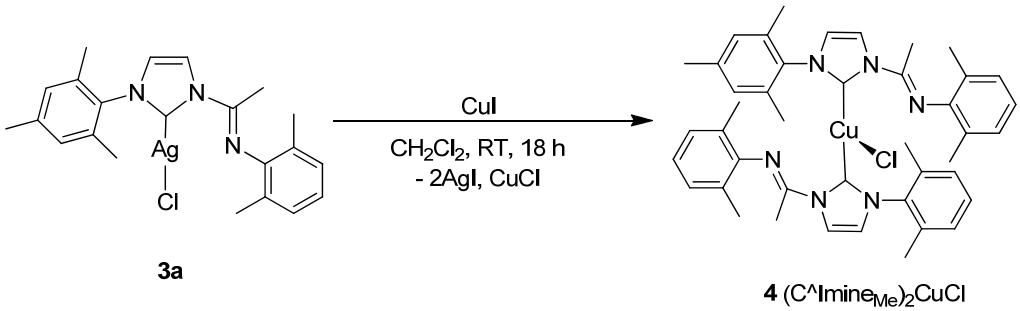

The crystal structure of **4** shows a distorted T-shaped complex with Cu1, Cl1, C1 and C23 forming a plane where both carbenes are approximately *trans* to each another (Figure 14). The C1–Cu1–C23 bond angle is 155.34(14)°, with C1–Cu1–Cl1 and C23–Cu1–Cl1 bond angles of 105.35(10) and 99.29(10)º, respectively. No interaction between the iminic nitrogen to the metal center is observed, in agreement with the observed $\nu_{C=N}$ absorption at 1678 cm^{-1}. Biscarbene copper complexes normally adopt a linear conformation.[80] To the best of my knowledge, only two T-shaped three-coordinate complexes of Cu(I)[71] and Ag(I)[81] containing two monodentate *N*-heterocyclic carbene

ligands coordinated to a metal center have been characterized by X-ray diffraction. Unlike Ag(C^Imine$_{Me}$)Cl (**3a**), no interaction between the imine nitrogen atoms and the copper center is possible as the iminic arm points away from the copper metal center.

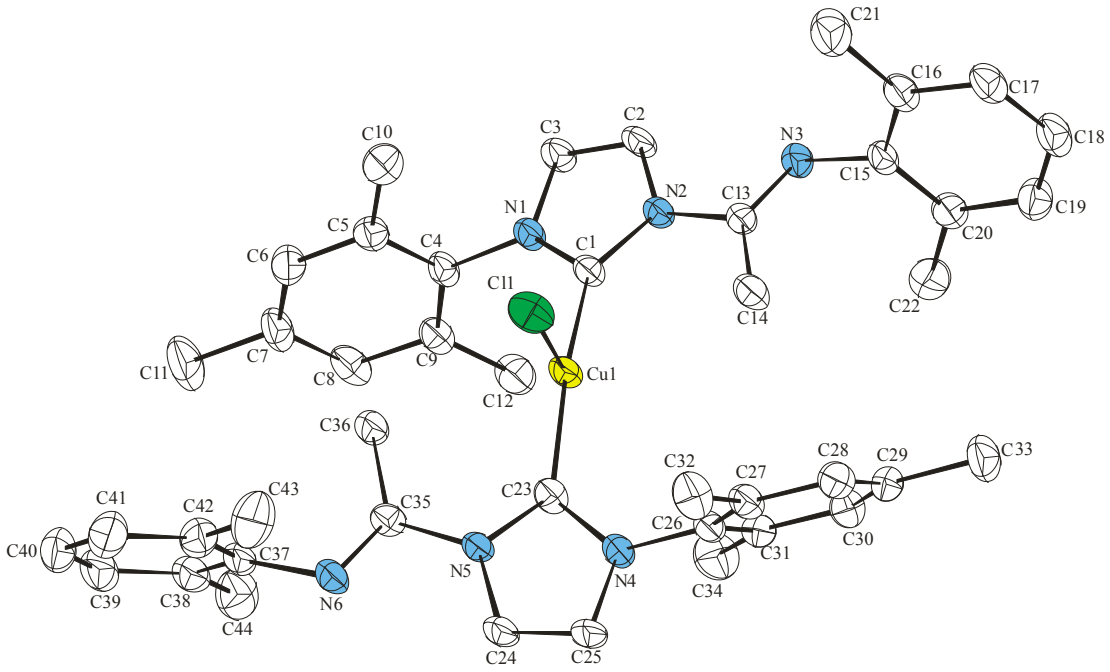

Figure 14. ORTEP plot of [(C^Imine$_{Me}$)$_2$CuCl] **(4)** (30% probability level). Hydrogen atoms and dichloromethane molecules are omitted for clarity. Select bond lengths (Å) and angles (º): Cu1–Cl1 2.4313(10), Cu1–C1 1.937(3), Cu1–C23 1.933(3), N6–C35 1.259(4), Cl1–Cu1–C(1) 105.35(10), Cl1–Cu1–C23 99.29(10), C1–Cu1–C23 155.34(14).

The average Cu-carbene bond length of 1.935(3) Å in (C^imine)$_2$CuCl (**4**) is slightly shorter compared to the bond length (1.953 Å) observed for IPrCuCl[82] but it is in close agreement with the corresponding bond length of 1.930(2)Å reported by Albecht

for a three-coordinate biscarbene copper halide complex (*bis*[1,3-dihydro-1-methyl-3-(1-methylethyl)-2H-imidazol-2-ylidene]iodocopper).[71] The Cu1–Cl1 bond length of 2.4313(10) Å is also long compared to other copper carbene complexes.

Interested to see if using different conditions would allow the preparation of a mono-ligand copper structure, another synthetic approach was tested to prepare additional imino-NHC copper(I) complexes. Complexes **5a** and **5b** were synthesized in 81% and 95% yield, respectively, by reaction of the respective imidazolium salts with CuI and sodium hexamethyldisilazide (Scheme 6). Complex **5b** was also independently prepared by addition of the free carbene **2b** to a solution of copper(I) iodide.

Scheme 6. Synthesis of (C^Imine)CuI Dimers (**5a** and **5b**).

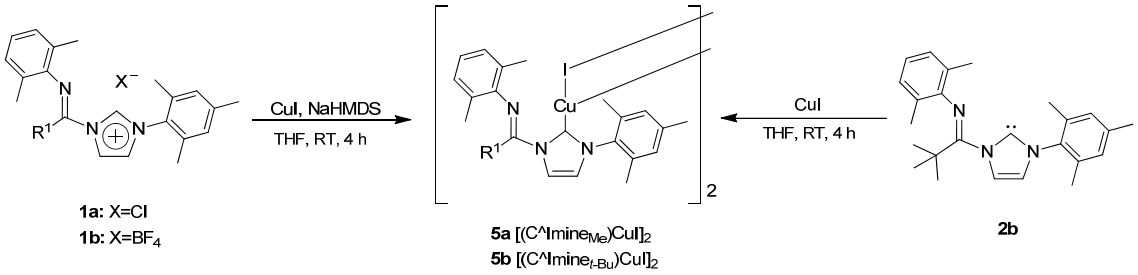

As expected, the characteristic downfield resonance for the central imidazolium proton of **1a** and **1b** in the ^{1}H NMR spectra is no longer present and resonances for the backbone (–NC*H*C*H*N–) protons move upfield to δ 8.19 and 6.83 for **5a** and to δ 6.89 and 6.69 for **5b**. The ^{13}C NMR resonances for the carbenoid carbon (–N*C*N–) and the iminic carbon nuclei of **5a** are observed at δ 186.0 and 153.6, respectively, a significant downfield shift from that of the corresponding salt. A similar trend to higher frequency

was observed in **5b**, for which the carbenoid carbon and iminic carbon nuclei resonate at δ 178.8 and 159.9, respectively. The FTIR $\nu_{C=N}$ absorption for **5a** and **5b** were observed at the expected 1678 and 1664 cm^{-1}, respectively.

Crystals suitable for X-ray diffraction studies were obtained by slow vapor diffusion of pentane into a concentrated solution of dichloromethane. Complex **5a** crystallized in the centrosymmetric P –1 space group as a dimer with two bridging iodide ligands forming a slightly puckered four-membered ring metallacycle (Figure 15). The geometry about each copper atom is best described as a slightly disordered trigonal planar structure, with angles about the metal centers ranging from 113.20(10) to 126.69(11)°. The Cu1–C1 and Cu2–C23 bond distances of 1.926(3) and 1.936(3) Å, respectively, comparable to that reported in a related carbene copper dimeric structure.[83] Although N3 is positioned as to allow coordination to Cu1, the distance between Cu1 and N3 is 2.465(3) Å, slightly longer than the sum of the covalent radii of both atoms, suggests that no interaction actually exists and is likely due to crystal packing within the lattice.[84] This is further supported by the statistically equivalent bond lengths for both iminic bonds N3–C4 and N6–C26, at 1.264(5) and 1.263(4) Å, respectively.

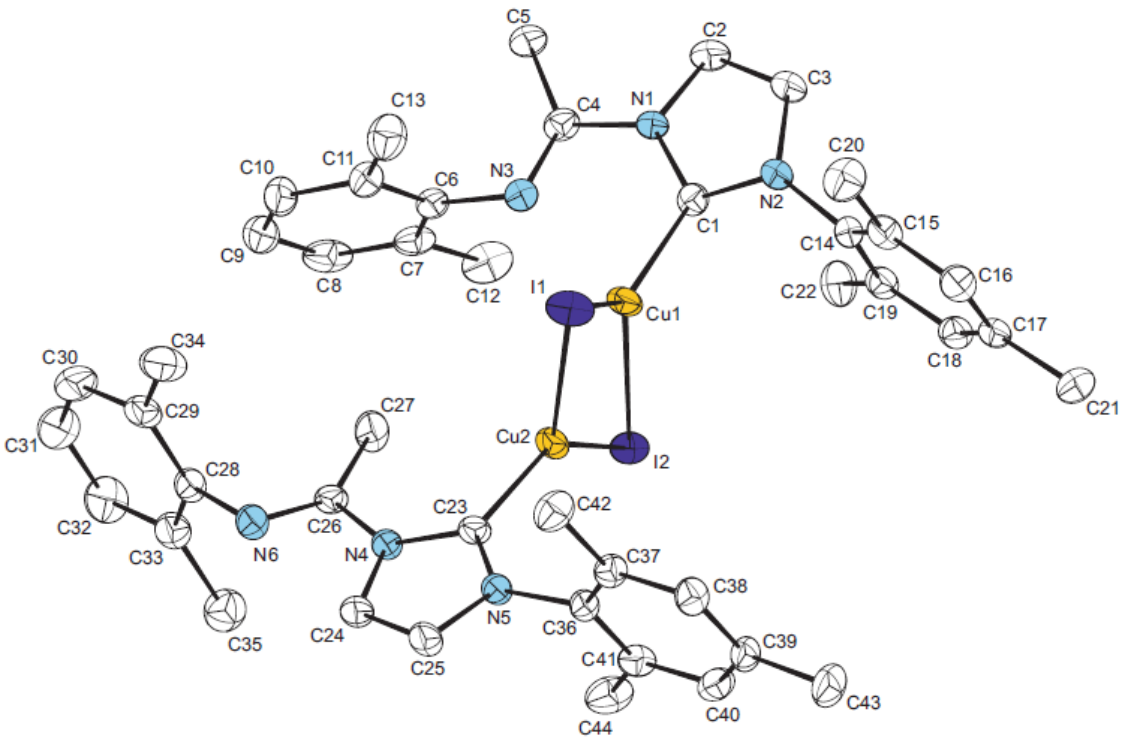

Figure 15. ORTEP plot of $[(C\text{^}Imine_{Me})CuI]_2$ **(5a)** (thermal ellipsoids at 50% probability). Hydrogen atoms omitted for clarity. Selected bond lengths (Å) and angles (°): Cu1–C1 1.926(3), Cu1–I1 2.6288(5), Cu1–I2 2.6047(5), Cu1–N3 2.465(3), N1–C1 1.370(4), N2–C1 1.350(4), N3–C4 1.264(5), N2–C1–N1 103.0(3).

The homologous *tert*-butyl complex **5b** crystallized in the $P2_1/c$ space group also as a dimer with two bridging iodide ligands and $C\text{^}Imine_{t\text{-}Bu}$ bound to copper in a monodentate fashion through the carbene center (Figure 16). The molecule lies on an inversion center. Similar to **5a**, the geometry about the metal center is best described as slightly distorted trigonal plane, with C1–Cu1–I1, C1–Cu1–I1a and I1–Cu1–I1a bond angles of 120.83(9)°, 122.28(9)° and 116.516(14)°, respectively.

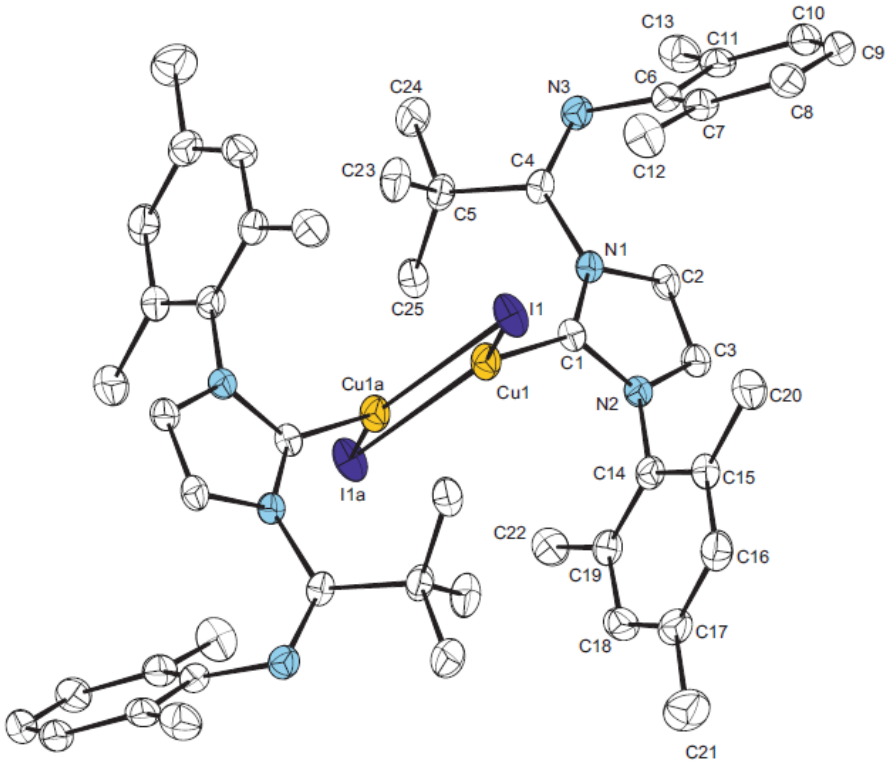

Figure 16. ORTEP plot of [(C^Imine$_{t\text{-Bu}}$)CuI]$_2$ **(5b)** (thermal ellipsoids at 50% probability). Hydrogen atoms omitted for clarity. Selected bond lengths (Å) and angles (°): Cu1–C1 1.945(3), Cu1–I1 2.5688(4), Cu1–I1a 2.6030(4), N3–C4 1.259(4), C1–Cu1–I1 120.83(9), I1–Cu1–I1a 116.516(14), C1–Cu1–I1a 122.28(9).

Reaction of C^Imine$_{t\text{-Bu}}$ (**2b**) with Au(SMe$_2$)Cl resulted in the formation of an off-white solid providing proton and carbon spectra consistent with the target (C^Imine$_{t\text{-Bu}}$)AuCl (**6b**) compound (Scheme 7). The FTIR $\nu_{C=N}$ stretching frequency of 1664 cm^{-1} found for **6b** suggests no chelation of the iminic arm to the metal center.[57,73]

Scheme 7. Synthesis of (C^Imine$_{t\text{-Bu}}$)AuCl (**6b**) with subsequent rearrangement to [(C^Imine$_{t\text{-Bu}}$)$_2$Au][AuCl$_2^{-1}$] (**7b**).

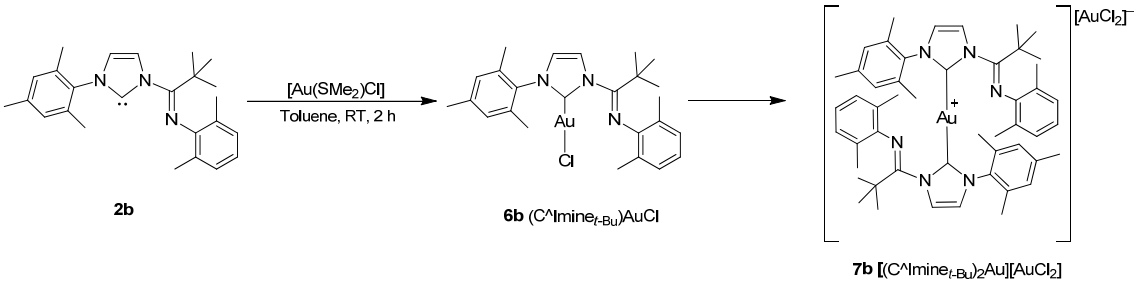

X-ray quality crystals were grown at room temperature by slow vapour diffusion of pentane into a saturated THF solution. The complex crystallized in a triclinic crystal system in the *P* –1 space group. The solid-state structure showed a coordination complex, in which two carbenes are bound to a cationic gold(I) metal center with dichloroaurate as the counteranion (Figure 17). The C1–Au1–C26 bond angle is 172.6(2)° with the imidazole rings approximately orthogonal to each other at 87.4°. The Au1–C1 and Au1–C26 bond lengths are equivalent with an average value of 2.029(7) Å , this is slightly longer compared to (IMes)AuCl (1.998 Å) but expected considering the strong σ-donation of both carbenes.[85] The C^Imine$_{t\text{-Bu}}$ ligands coordinate to gold in a monodentate fashion through the carbenoid carbon with the iminic bond length (1.262(8) Å) statistically equivalent to that of C^Imine$_{t\text{-Bu}}$ (**2b**).

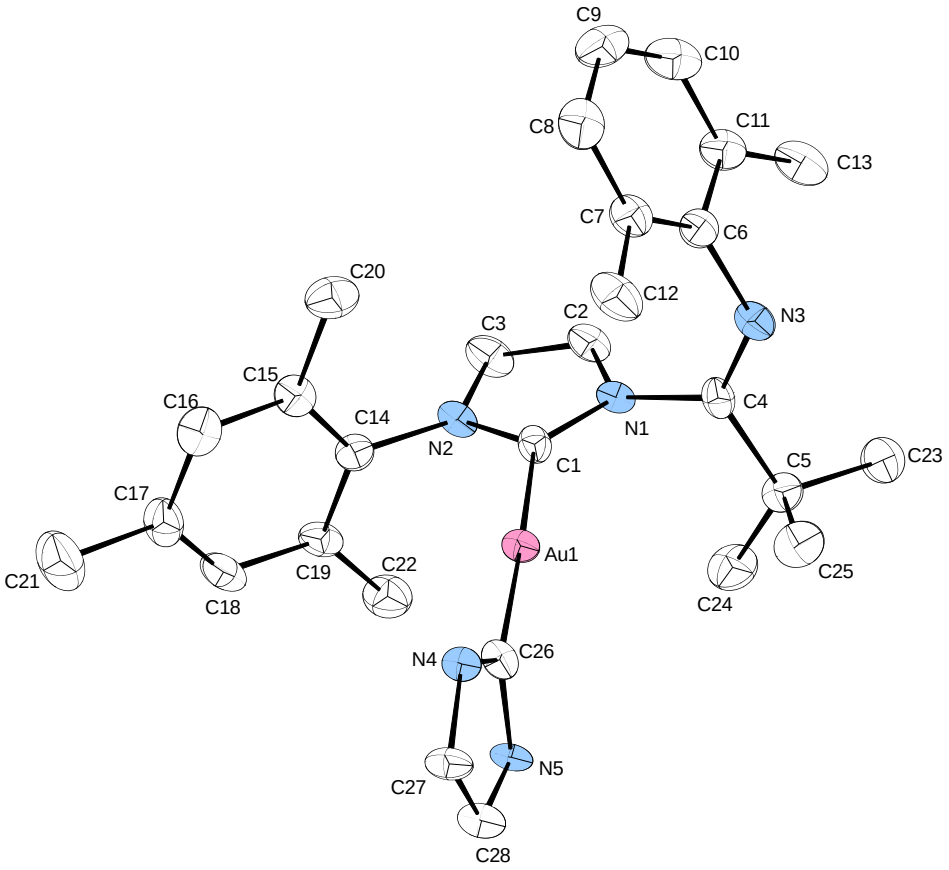

Figure 17. ORTEP plot of [(C^Imine$_{t\text{-Bu}}$)$_2$Au][AuCl$_2$] (**7b**) (50% probability level). Two THF solvent molecules, the [AuCl$_2$]$^-$ counteranion, hydrogen atoms, and N4/N5 substituents are omitted for clarity. Select bond lengths (Å) and angles (º) are average values observed for both C^Imine$_{t\text{-Bu}}$ ligands present in the complex: N1–C1 1.363(8), N2–C1 1.354(8), C2–C3 1.341(9), N1–C4 1.464(8), N3–C4 1.262(8), Au–C1 2.029(7), Au–Cl1 2.262(2), N1–C1–N2 104.2(7)°, N1–C1–Au1 133.0(5)°, C26–Au1–C1 172.6(2)°.

The chemical shift for the carbenoid carbon observed in the ^{13}C NMR spectrum (δ 172.7) is in closer agreement to a (carbene)Au(halide) neutral complex (δ 173.4–175.1) [85]

than to a (carbene)$_2$Au$^+$ cationic one (δ 180.3–186.1). This information suggests that complex **6b** is not in fact formed in the reaction of the free carbene **2b** with Au(SMe$_2$)Cl but upon crystallisation, disproportionation occurs to yield complex **7b** (Scheme 7). This behaviour has been observed with related gold and silver systems.[59,86-89]

Reaction of (C^Imine$_{Me}$)AgCl (**3a**) with Au(SMe$_2$)Cl gave (C^Imine$_{Me}$)AuCl (**6a**) in 85% yield (Scheme 8). The ^{1}H and ^{13}C NMR spectra were consistent with a (C^Imine$_{Me}$)AuCl molecular formula where the carbenoid carbon is found at δ 172.5. As expected, the FTIR $\nu_{C=N}$ stretching frequency at 1683 cm^{-1} suggests no chelation of the iminic arm to the metal center.

Scheme 8. Reaction of (C^Imine$_{Me}$)AgCl with Au(SMe$_2$)Cl to form complex **6a**.

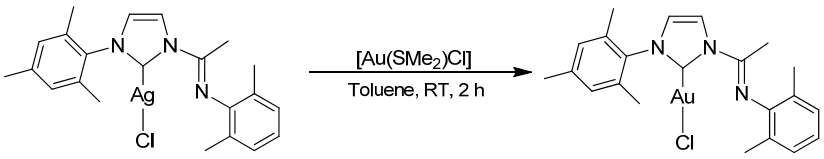

3a **6a** (C^Imine$_{Me}$)AuCl

Single crystals suitable for X-ray diffraction studies were grown at –35 °C by layering pentane onto a saturated dichloromethane solution. Compound **6a** crystallized in a monoclinic crystal system in the *P 2$_1$/c* space group. The solid-state structure of **6a** shows a coordination complex where one carbene ligand is coordinated to a gold metal center with a bound chloride (Figure 18). Au1–C1 and Au1–Cl1 bond distances are 2.014(5) and 2.2802(14) Å, respectively, with a C1–Au1–Cl1 angle of 177.83(15)°. The C4–N3

bond is 1.259(7) Å, which is consistent with the C=N stretching frequency and similar to that observed in the silver complex (**3a**). The solid-state structure of **6a** suggests that compound **6b** formed upon addition of C^Imine$_{t\text{-Bu}}$ (**2b**) to Au(SMe$_2$)Cl then rearranges upon crystallisation to form **7b**. This hypothesis is further supported by the similar chemical shifts observed from the carbenoid carbon nuclei in both compounds **6b** and **6a**, which are consistent with a (carbene)AuX-type structure. The combination of the NMR spectroscopic data for **6a** with its solid-state structure supports the hypothesis that complex **6b** is indeed initially formed upon addition of C^Imine$_{t\text{-Bu}}$ (**2b**) to Au(SMe$_2$)Cl but undergoes ligand rearrangement upon recrystallization.

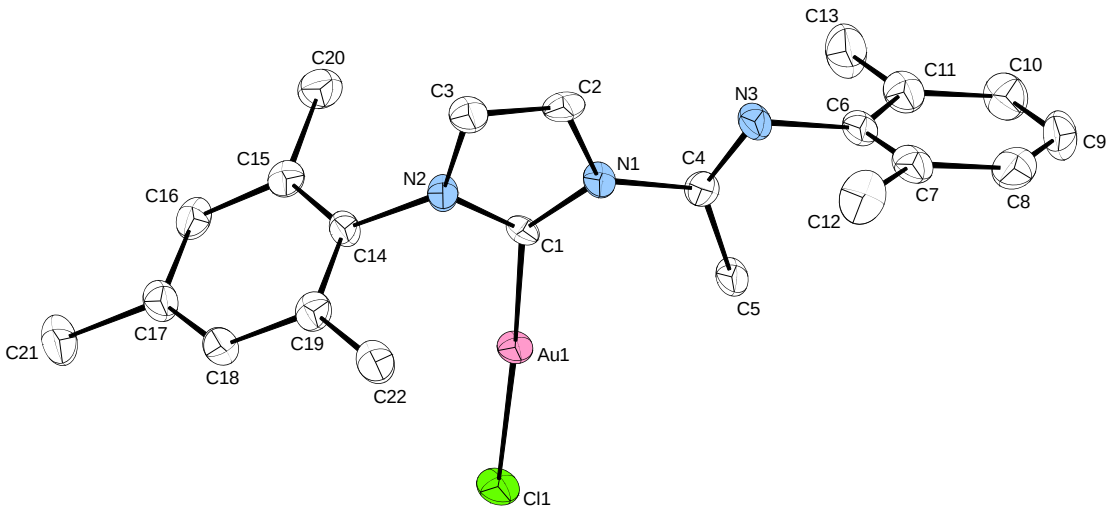

Figure 18. ORTEP plot of (C^Imine$_{Me}$)AuCl (**6a**) (50% probability level). Hydrogen atoms and a dichloromethane solvent molecule are omitted for clarity. Select bond lengths (Å) and angles (º): N1–C1 1.352(6), N2–C1 1.331(6), C2–C3 1.309(8), N1–C4 1.442(6), N3–C4 1.259(7), Au–C1 2.014(5), Au–Cl1 2.280(1), N1–C1–N2 106.9(5), N1–C1–Au1 132.1(4).

2.3 Conclusions

In summary, a series of aryl-substituted imino imidazolium salts have been synthesized and structurally characterized. The phenyl and *tert*-butyl salt derivatives necessitated activation of the imidoyl chloride by reaction with sodium tetrafluoroborate to form the corresponding nitrilium salt *in situ*. In cases where permitted, the first stable aryl-substituted imino-*N*-heterocyclic carbenes were isolated and characterized. Coordination of these ligands was explored to group 11 metals and a series of new complexes were prepared from either ligand displacement, transmetalation or reaction with a basic metal precursor. The solid-state structures of all the silver, copper and gold complexes show monodentate coordination of the ligand through the carbene leaving the iminic arm unbound.

Chapter 3. Synthesis, Characterization of Nickel(II) Complexes with Imino-*N*-Heterocyclic Carbene Ligands

Preface

A part of the research presented in this chapter has been published in a paper in which I wrote the first draft and further revisions were done by my supervisor Dr. Gino Lavoie.[57]

3.1 Introduction

Group 10 nickel and palladium halide complexes containing bulky α-diimine ligands were shown to be very effective catalysts for the polymerization of olefins.[7] These complexes, first reported in 1995, have created renewed interest in developing new coordination catalysts based on late transition metals, which are less oxophilic and more tolerant of functional groups than their early transition metal counterparts.[90,91] Interestingly, the initial α-diimine system remains one of the most effective catalysts so far developed. However, despite the early promising results, these catalysts have yet to deliver acceptable performance at elevated temperature. Reaction temperatures in excess of 50 °C and the presence of small concentration of hydrogen both have severe damaging effects on the productivity observed with these α-diimine-based catalysts, preventing their use in large-scale production plants.[13,92-94] It became a research interest to study nickel complexes containing a related hybrid bidentate ligand composed of a σ-donor/π-acceptor imine and of strong σ-donor/poor π-acceptor *N*-heterocyclic carbene (NHC). NHC's have been widely used as ancillary ligands due to the enhanced thermal stability that they impart in catalytic systems.[61,95] Although NHCs are now ubiquitous in the field

of metathesis polymerization,[96-98] their use in olefin polymerization is still very limited.[62,63,99,100] Chapter two described the synthesis of several different bis(aryl)-substituted imino-*N*-heterocyclic carbene ligands and of their corresponding group 11 transition metal complexes. This chapter describes the preparation and structural characterization of several copper and nickel complexes, including (C^Imine$_{Me}$)NiBr$_2$ and (C^Imine$_{t\text{-}Bu}$)NiBr$_2$ complexes, along with their catalytic performance in ethylene polymerization. In addition, the coordination of these ligands was explored with zinc, iron and cobalt metals.

3.2 Results and Discussion

3.2.1 Synthesis of a bis(imino-N-heterocyclic carbene)nickel complex via oxidative addition

Although the silver complex **3a** was successfully used as a transmetalating agent to isolate copper (C^Imine$_{Me}$)$_2$CuCl (**4**) and gold (C^Imine$_{Me}$)AuCl (**6a**) complexes, all attempts to prepare nickel complexes by reaction with either NiBr$_2$(DME) or NiBr$_2$(THF)$_2$ failed. Therefore a new strategy reported by Fryzuk[101] and Crabtree[102] was adopted to investigate the oxidative addition of the imidazolium salt on nickel(0) metal precursors. Reaction of one equivalent of **1a** with Ni(COD)$_2$ in THF to form (C^Imine$_{Me}$)Ni(H)(Cl) was attempted. This however resulted in the formation of Ni(C^Imine$_{Me}$)$_2$Cl$_2$ (**8**). Addition of two equivalents of **1a** also led to complex **8** as the major product in 66% yield. It is postulated that the resulting nickel dichloride complex is

generated when the partially-soluble nickel precursor oxidatively adds across the partially-soluble **1a** to form the highly reactive and basic nickel(II) hydride complex **A** (Scheme 9). Deprotonation of a second equivalent of imidazolium salt by **A** subsequently generates **8** with the release of one equivalent of molecular hydrogen. Attempts by Crabtree to prepare a palladium carbene hydride complex also led to the formation of the corresponding bis(carbene) palladium dichloride species.[102]

Scheme 9. Reaction of Imidazolium Salt **1a** with $Ni(COD)_2$.

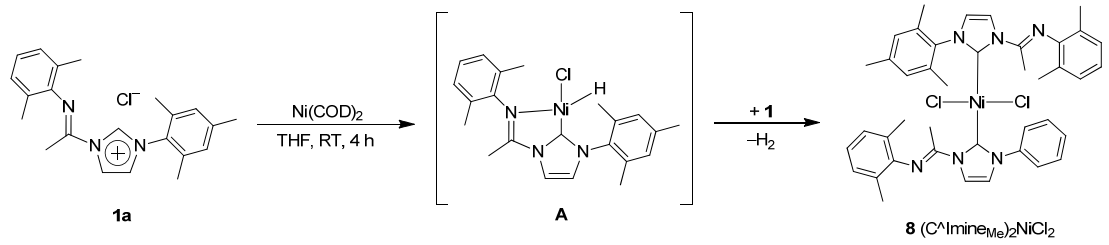

Complex **8** is diamagnetic, which is a good indication of a square-planar geometry. A highly symmetric structure is supported by the presence of only one set of resonances in its ^{1}H NMR ($CDCl_3$) spectrum. As expected, the resonance for the acidic proton in **1a** is no longer present. The two backbone (–NC*HCH*N–) protons of the carbene in **8** resonate at δ 8.02 and 6.66 compared to δ 8.51 and 7.24 for the imidazolium salt **1a**.[73] The ^{13}C NMR resonances for the backbone carbon nuclei at δ 123.0 and 120.0 differ slightly from those observed for the corresponding salt (**1a**) (δ 123.6 and 118.4). The symmetry of the structure is further supported by the presence of one single carbene resonance and one single iminic carbon resonance at δ 168.8 and 155.6, respectively. The

FTIR $\nu_{C=N}$ absorption at 1674 cm^{-1} for 15 is lower than the value reported for the imidazolium salt precursor **1a** (1691 cm^{-1}) but comparable to those for both **3a** (1682cm^{-1}) and **4** (1678 cm^{-1}), in which the ligand is bound in a monodentate fashion to the metal center exclusively through the carbenoid carbon atom.[73] Furthermore, the observed C=N stretching frequency is markedly larger than those reported for the family of early transition metal complexes (1604–1609 cm^{-1}) in which the bidentate coordination of **2b** was confirmed by X-ray crystallography.[74] This coordination mode is however unlikely for a bis(carbene) Ni(II) dichloride complex.

The solid-state structure of complex **8** was determined by X-ray diffraction analysis. Crystals were obtained by slow vapor diffusion of pentane into a concentrated solution of dichloromethane. Complex **8** crystallized in the centrosymmetric P –1 space group (Figure 19), as a slightly distorted square planar complex with both carbene ligands coordinated *trans* to each other, in agreement with the spectroscopic data. The nickel atom lies on an inversion center, which results in two sets of crystallographically-equivalent ligands and chlorine atoms, with an angle of exactly 180° for both C1–Ni1–C1a and Cl1–Ni1–Cl1a. The Ni1–C1 and Ni1–Cl1 bond lengths of 1.926(2) and 2.1822(6) Å, respectively, are within the range reported for other $(NHC)_2NiCl_2$ complexes.[103-105] The crystal structure of **8** also confirmed the monodentate coordination of the ligand through the carbenoid carbon with a N3–C4 bond length of 1.265(3) Å, statistically equivalent to that observed in **1a**. Coordination of N3 to the metal center would have led to a lengthening of the C=N bond by at least 0.02 Å.[74]

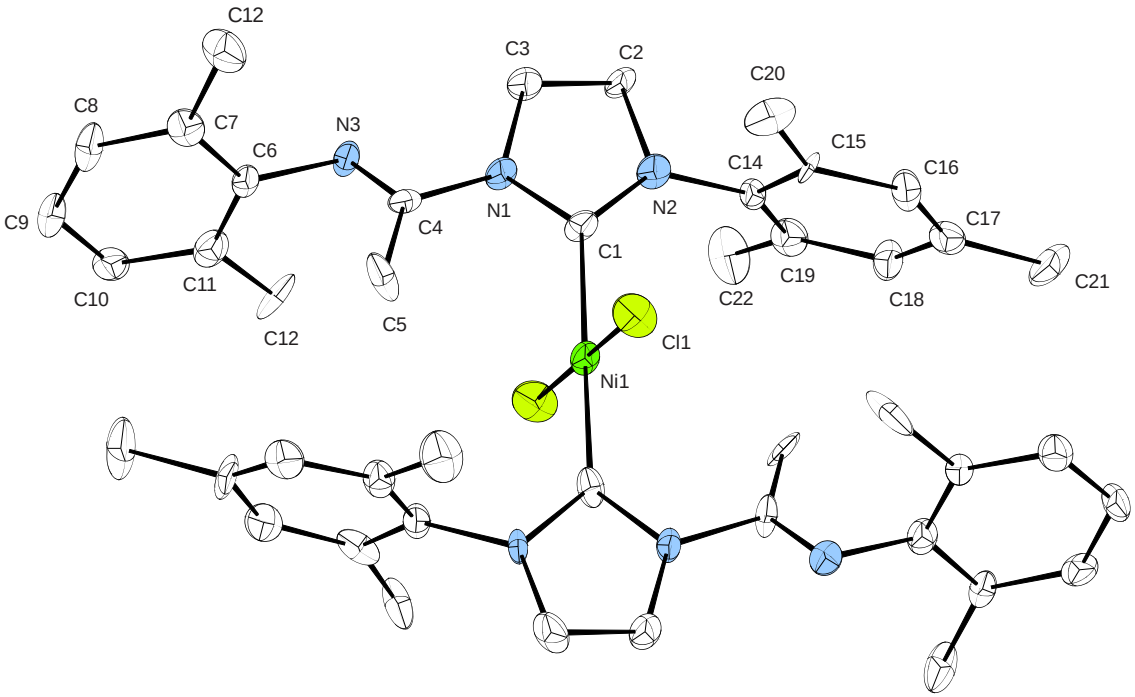

Figure 19. ORTEP plot of (C^Imine$_{Me}$)$_2$NiCl$_2$ (**8**) (50% probability level). Hydrogen atoms omitted for clarity. Selected bond lengths (Å) and angles (°): Ni1–C1 1.926(2), Ni1–Cl1 2.1822(6), N3–C4 1.265(3), C11–Ni1–C1a 180.0, C1–Ni1–Cl1 88.91(7), C1–Ni1–Cl1a 91.09(7), N1–C1–N2 103.27(17).

Considering the outcome of the oxidative addition reaction between the salt **1a** and Ni(COD)$_2$, and the inability to use either the silver adduct **3a** in transmetalation or surprisingly the free carbene **2b** in simple ligand displacement reactions with nickel(II) precursors, it was of interest to probe the efficacy of the mono-carbene copper(I) complexes (**5a** and **5b**) as transmetalating agents, as other groups have recently reported.[71,106] However, before transmetalation with copper agents was attempted, it was

first necessary to establish that the bidentate binding mode of the ligand could be observed.

3.2.2 Synthesis of chelating bis(imino-N-heterocyclic carbene) complexes of zinc, iron and cobalt

Although the preparation of nickel and palladium carbene complexes was the initial intention, efforts to prepare these target molecules were not successful and appeared more complicated than originally anticipated. Despite the successful development of synthetic protocols to prepare several group 11 complexes, the synthesis of a complex in which a bidendate coordination mode of the ligand was observed became the next research initiative.

The coordination of C^Imine$_{Me}$ **1a** to zinc was investigated since the resulting complex would be diamagnetic and the zinc metal could accommodate a bidentate ligand. Following a similar approach to prepare select copper complexes, the addition of a cooled suspension of **1a** in tetrahydrofuran to a basic zinc precursor, generated *in situ* by the reaction of zinc chloride with sodium bis(trimethylsilyl)amide, resulted in the formation of Zn(C^Imine$_{Me}$)Cl$_2$ (**9**) in 78% yield (Scheme 10).

Scheme 10. Preparation of (C^Imine$_{Me}$)ZnCl$_2$ (**9**).

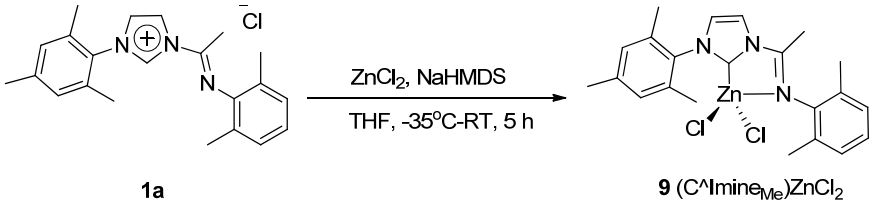

1a **9** (C^Imine$_{Me}$)ZnCl$_2$

The ^{1}H NMR ($CDCl_3$) spectrum is consistent with the formation of the carbene and coordination to zinc. The proton resonance for the central imidazolium salt (NC*H*N) is no longer present as expected. The two backbone protons of the azole ring (NC*HCH*N$_{mesityl}$) now resonate more upfield (7.79 and 7.12 ppm) compared with that of the imidazolium salt **1a** (8.51 and 7.24 ppm). In the ^{13}C NMR spectrum, the iminic carbon (*C*=N) resonance appears at 157.3 ppm and the central imidazolium carbon (N*C*N) appears at 178.5 ppm compared to 150.1 ppm and 140.2 ppm for **1a**, respectively. The relatively low FTIR $\nu_{C=N}$ absorption of complex **9** for the imine group (1657 cm^{-1}) and the higher frequency resonance for the iminic carbon at 157.3 ppm when compared to structurally-characterized monodentate-NHC complexes (**3a, 4** and **6a**) (1683-1674 cm^{-1}) suggest a chelating coordination mode of the ligand to the metal center.

Complex **9** was also characterized by X-ray diffraction methods and crystallized in the centrosymmetric P*cab* space group (Figure 20). The crystal structure of **9** shows a distorted tetrahedral complex where the ligand binds in a bidentate fashion through the carbene center and iminic nitrogen atom. The bite angle of the chelate (C1–Zn1–N3) is 79.49(16)° which is in the range of other reported chelating imine-NHC complexes (78.53-81.6°).[57,107] The Zn1–C1 bond length is 2.030(4) Å. The 2,6-dimethylphenyl and

the 2,4,6-trimethylphenyl rings are twisted 87.81° and 70.54°, respectively, from the metallocycle (Zn1–C1–N1–C4–N3). Upon coordination, the imine bond length (N3–C4) has lengthened to 1.281(5) Å compared to that of the starting imidazolium salt **1a** (1.262(4) Å).

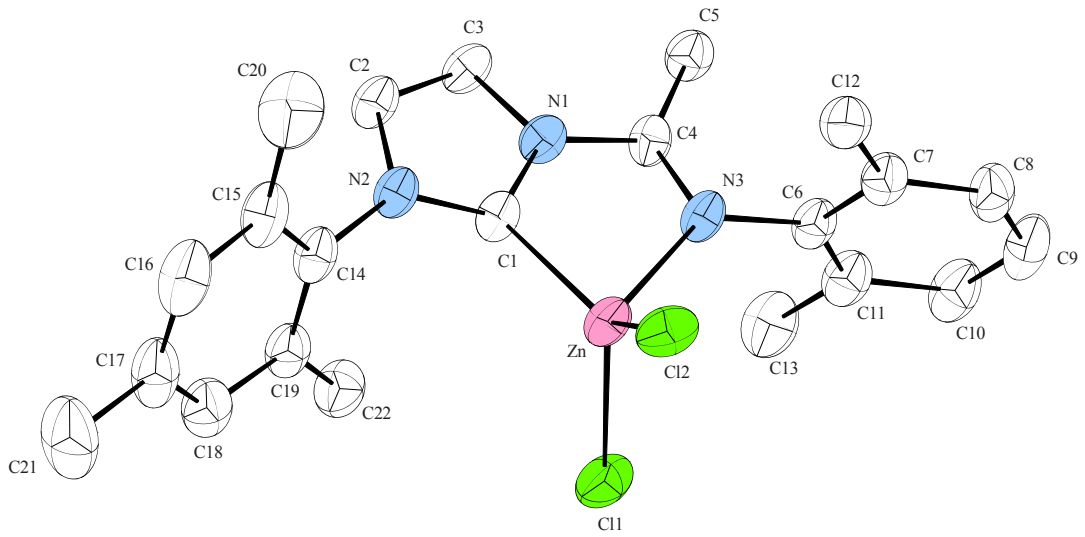

Figure 20. ORTEP plot of Zn(C^Imine$_{Me}$)Cl$_2$ (**9**) (50% probability level). Hydrogen atoms and a molecule of dichloromethane omitted for clarity. Select bond lengths (Å) and angles (deg): Zn1–C1 2.030(4), Zn1–N3 2.164(4), Zn1–Cl1 2.2339(14), Zn1–Cl2 2.2201(12), C4–N3 1.281(5), C1–Zn1–N3 79.49(16).

Interested to see if the same methology used to prepare the zinc complex could be extended to other metals, this approached was tested with the appropriate nickel and palladium precursors without any success but proved successful for iron and cobalt. Complexes Fe(C^Imine$_{Me}$)Cl$_2$ (**10**) and Co(C^Imine$_{Me}$)Cl$_2$ (**11**) were generated in 70%

and 68% yield, respectively, following a similar protocol used for the preparation of the zinc and copper complexes (Scheme 11). The FTIR $\nu_{C=N}$ absorption for **10** and **11** were observed to be 1650 cm^{-1} and 1652 cm^{-1} respectively. These values are shifted to much lower wave numbers compared to the imidazolium salt **1a** (1691 cm^{-1}), indicating a bidentate binding motif for the ligand. Due to the paramagnetic nature of complexes **10** and **11,** characterization was achieved by elemental analysis and in the case of **10**, also by structural analysis.

Scheme 11. Preparation of Fe(II)and Co(II) imino-NHC complexes (**10**) and (**11**).

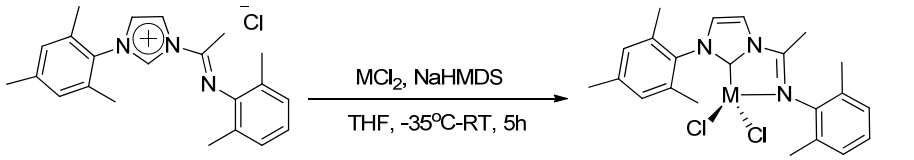

1a

10:M = Fe, (C^Imine$_{Me}$)FeCl$_2$
11: M = Co, (C^Imine$_{Me}$)CoCl$_2$

Complex **10** was characterized by X-ray diffraction and crystallized in space group P21/a with two independent molecules in the asymmetric unit cell (Figure 21). The crystal structure of **10** shows a distorted tetrahedral complex where the ligand binds in a bidentate fashion through the central carbon and the iminic nitrogen atom. The bite angle of the chelate (C1–Fe–N3) is found in the range of 75.4(2)-76.8(3)°. The Fe–C1 bond length range is 2.067(7)–2.096(7) Å. The 2,6-dimethylphenyl and the 2,4,6-trimethylphenyl rings are twisted 86.91-88.91° and 83.43-82.09°, respectively, from the metallocycle (Fe–C1–N1–C4–N3).

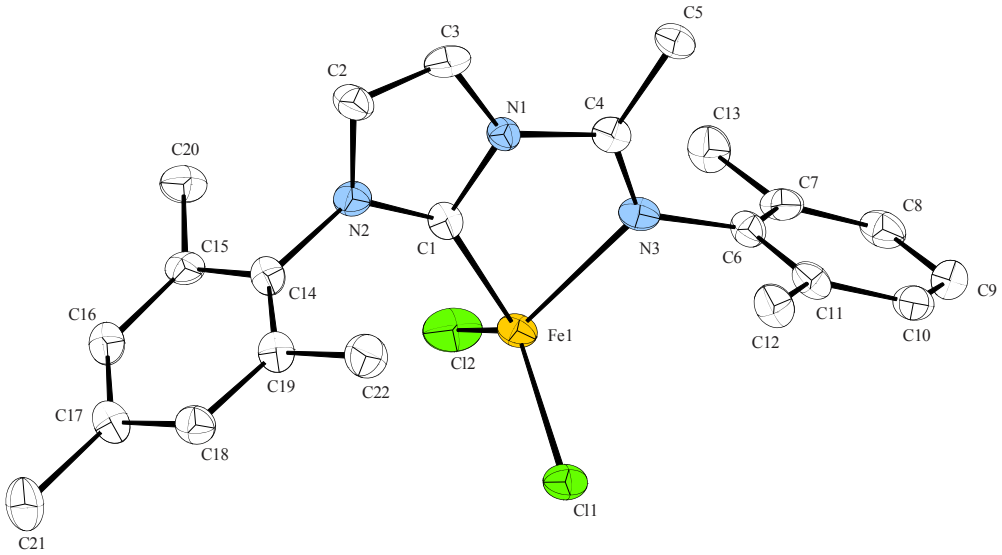

Figure 21. ORTEP plot of Fe(C^Imine$_{Me}$)Cl$_2$ (**10**) (30% probability level). Hydrogen atoms and three molecules of dichloromethane omitted for clarity and only one of two symmetrically independant molecules in the asymmetric unit cell is shown. Select bond lengths (Å) and angles (deg): Fe–C1 2.067(7)/2.096(7), Fe–N3 2.195(6)/2.176(6), Fe–Cl1 2.2339(14)/2.231(3), Fe–Cl2 2.46(2)/2.236(2), C4–N3 1.267(9)/1.270(9), C1–Fe–N3 75.4(2)/76.8(3).

3.2.3 Synthesis of chelating imino-N-heterocyclic carbene complexes of nickel

Having demonstrated the imino-*N*-heterocyclic carbenes can bind to a metal centre in a bidendate fashion, the research focus was directed back to the preparation of palladium and nickel structures. The transmetalating potential of complexes 5a and 5b was explored and successfully demonstrated. Addition of half an equivalent of the dimeric copper complex to $NiBr_2$(DME) gave the targeted paramagnetic nickel complexes 12a and 12b in 58% and 94% yield, respectively (Scheme 12).

Scheme 12. Synthesis of (C^Imine)$NiBr_2$ (**12a**, **12b**) and (C^Imine)$_2NiBr_2$ (**13**).

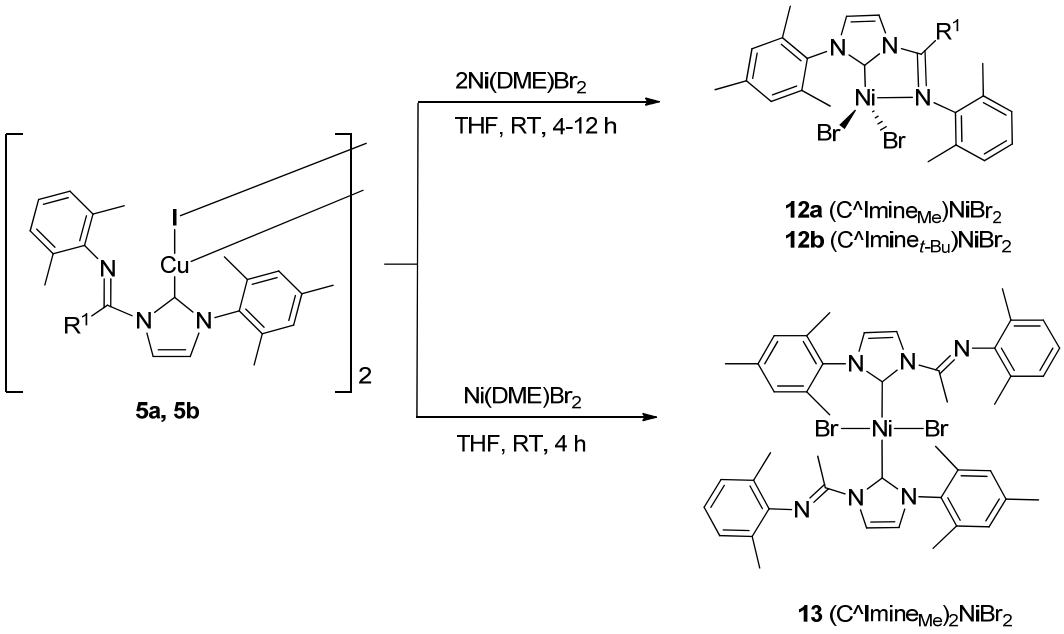

Thus, in contrast to the square planar complex **8**, these new (C^Imine)$NiBr_2$ complexes seemingly adopt the tetrahedral geometry with a chelating carbene ligand. The

bidentate coordination mode of the ligand is further supported by the C=N bond stretching frequency at 1646 and 1616 cm^{-1}, significantly lower than that observed in the corresponding imidazolium salts (**1a** and **1b**).[73,74]

In both cases, crystals suitable for X-ray diffraction studies were obtained by slow vapor diffusion of pentane into a concentrated solution of dichloromethane. Complex **12a** crystallized in the centrosymmetric $P2_1/m$ space group, with a crystallographic plane dissecting the molecule and passing through the azole ring (Figure 22). As a result, both the mesityl ring and the 2,6-dimethylphenyl ring are perfectly orthogonal to the metallacycle. The crystal structure of **12a** confirms the expected tetrahedral complex with the ligand coordinated to the metal center in a bidentate fashion. The bite angle of the chelate (C1–Ni1–N3) is 81.1(3)°, comparable to that reported for an analogous picoline-functionalized imidazole-2-ylidene nickel(II) bromide complex (81.4(3)°)[108] and within the range (78.5–81.6°) of other reported similar palladium(II) complexes.[72,109,110] The Ni1–C1 bond length measures 1.954(8) Å, somewhat elongated compared to that observed in **8** (1.926(2) Å), but in agreement with that reported by Danopoulos.[108] The iminic N3–C4 bond, at 1.290(11) Å, is also longer from that observed in the complexes **5a, 5b** and **8** (1.259(4)–1.265(7)°), in which the ligand is monodentate, but within the range (1.280(3)–1.38(2) Å) observed with related early transition metal complexes.[74] The low stretching frequency observed in the FTIR at 1646 cm^{-1} is consistent with the C=N bond length.

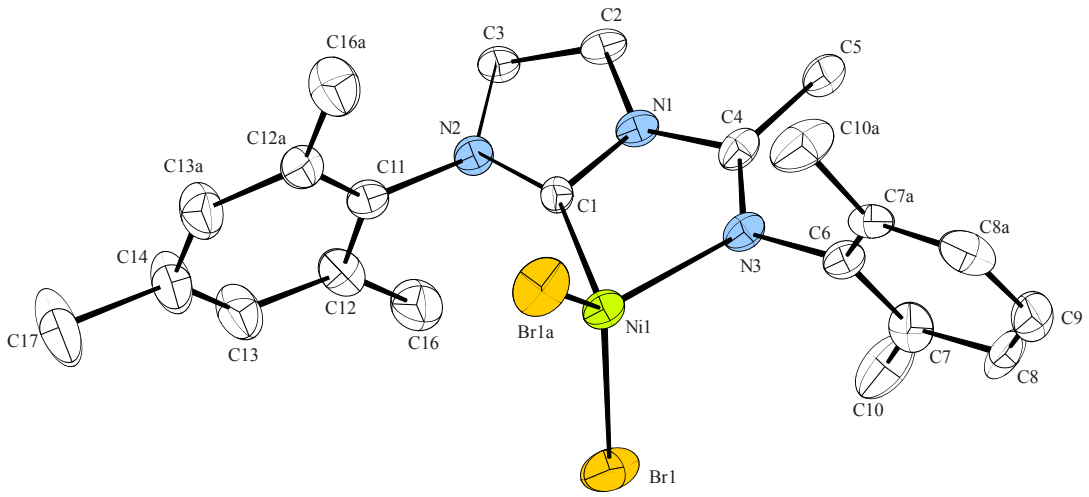

Figure 22. ORTEP plot of (C^Imine$_{Me}$)NiCl$_2$ **(12a)** (50% probability level). Hydrogen atoms omitted for clarity. Selected bond lengths (Å) and angles (°): Ni1–C1 1.954(8), Ni1–N3 2.058(7), Ni1–Br1 2.3714(8), Ni1–Br1a 2.3714(8), C4–N3 1.290(11), C1–Ni1–N3 81.1(3), Ni1–N3–C6 127.6(5).

Complex **12b** crystallized in the centrosymmetric P –1 space group (Figure 23). The asymmetric unit cell contains two molecules with similar data. The crystal structure shows a distorted tetrahedral complex with the bulky *tert*-butyl group leading to an average chelate (C1–Ni1–N3) bite angle for both independent complexes of 80.17°, slightly more acute than for the methyl analogue **12a**. The 2,6-dimethylphenyl and the mesityl rings are twisted off, on average, by 87.50° and 86.98° with respect to the metallacycle. The iminic bond length is within the expected range for a chelated ligand, at 1.282 Å, comparable to that observed in **12a** and in line with the measure C=N

stretching frequency (1616 cm^{-1}). The nature of the alkyl group attached to C4 also has a marked impact on the position of the 2,6-dimethylphenyl ring. The increased bulk of the *tert*-butyl group leads to a less open coordination sphere, with the ring significantly more tilted towards the bromide ligands. The average Ni1–N3–C6 bond angle (116.2°) in **12b** is in fact considerably lower than that observed in **12a** (127.7(5)°). This also manifests itself by a closer Ni1–C6 distance of 2.99 Å, compared to 3.15 Å in **12a**. This ability to control the steric environment about the metal center by varying the substituents on the aryl rings and on the iminic carbon is an interesting feature of this ligand. Considering the impact that some subtle changes have on catalyst activities, this feature may prove critical in harvesting the full potential of this ligand family and establishing structure-property relationships.

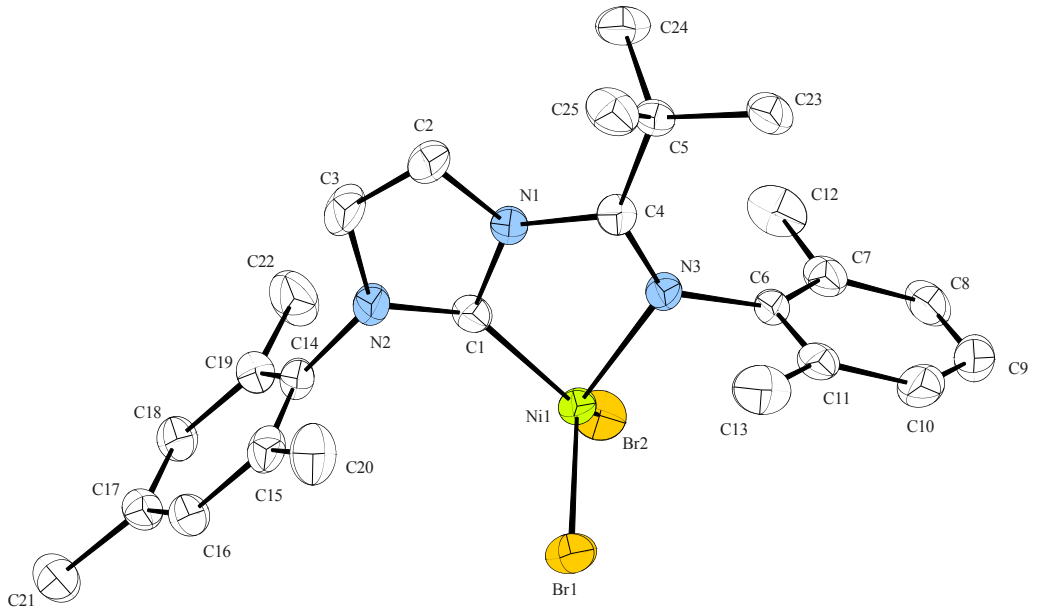

Figure 23. ORTEP plot of (C^Imine$_{t\text{-Bu}}$)NiCl$_2$ **(12b)** for one of the two molecules present in the asymmetric unit cell (50% probability level). Hydrogen atoms omitted for clarity and only one of two symmetrically independant molecules in the asymmetric unit cell is shown. Selected averaged bond lengths (Å) and angles (°): Ni1–C1 1.939, Ni1–N3 2.0475, Ni–Br1 2.36095, Ni1–Br2 2.3765, N3–C4 1.282, C1–Ni1–N3 80.17, Ni1–N3–C6 116.2.

Having demonstrated that copper complexes were efficient transmetalating agents in the formation of (C^Imine$_R$)NiBr$_2$, it was of interest to determine whether two equivalents of the carbene could actually be transferred to NiBr$_2$(DME) to synthesize the dibromide analogue of **8**. (C^Imine$_{Me}$)$_2$NiBr$_2$ (**13**) was successfully isolated in 70% yield, by reacting one equivalent of **5a** with Ni(DME)Br$_2$ (Scheme 12). Similar to that observed for complex **8**, the ^{1}H and ^{13}C NMR (CDCl$_3$) spectra of **13** consist of only one set of

resonances, indicative of a symmetric structure that was corroborated by the X-ray diffraction analysis (Figure 24). Bond lengths and angles of **13** are nearly identical to those of **8**, as expected, with the exception of the metal-halide bond length, for which the 0.16 Å- difference is in agreement with the difference in the halogen respective covalent radii.[84]

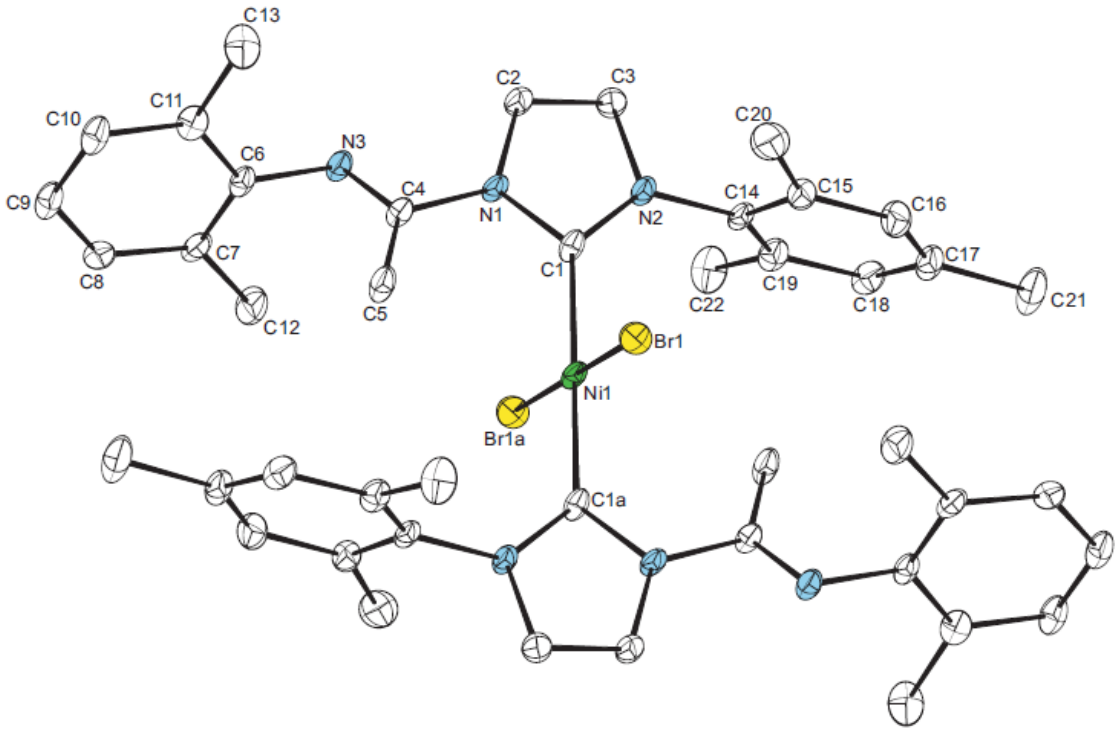

Figure 24. ORTEP plot of (C^Imine$_{Me}$)NiBr$_2$ **(13)** (50% probability level). Hydrogen atoms omitted for clarity. Selected bond lengths (Å) and angles (°): C1–Ni1 1.925(3), Ni1–Br1 2.3388(9), N3–C4 1.270(4), C1–Ni1–C1a 180.0, C1–Ni1–Br1 91.26(10), C1–Ni1–Br1a 88.74(10).

Complex **13** crystallized in the centrosymmetric P –1 space group (Figure 24). The crystal structure of **13** shows a slightly distorted square planar complex where the two carbenes are *trans* to each other. The nickel atom lies on an inversion center, resulting in a Br1–Ni–Br1a bond angle of exactly 180°. The Ni1–Br1 bond length is 2.3387(10) Å and the Ni–C1 bond length of 1.925(3) Å are within the range reported for other $(NHC)_2NiBr_2$ complexes.[108] In the final stages of refining structure **13**, additional electron density was observed close to the nickel metal center. Upon further investigation, this electron density was attributed to a small contamination (approximately 4%) of iodine bound to nickel, presumably from $[(C\text{^}Imine_{Me})CuI]_2$ used as transmetalating agent. The Ni1–I1 bond length of 2.633(12) Å is within the expected range. The FTIR $\nu_{C=N}$ absorption at 1676 cm^{-1} for **13** is lower than the values reported for the imidazolium salt precursor **1a** (1691 cm^{-1}), and nearly identical to **8** (1674 cm^{-1}). The crystal structure of **13** further confirms the ligand binds in a monodentate fashion solely through the carbene center. The N3–C4 bond length (1.270(4) Å) of the resulting uncoordinated imine fragment is within the expected values based on the previous group 11 complexes reported (**3–5**). [73]

A nickel(0) NHC complex (**14**) was prepared by the addition of **2b** to $Ni(COD)_2$ (Scheme 13). The ^1H NMR ($CDCl_3$) spectrum is consistent with the formation of the carbene and coordination to nickel with one molecule of bound 1,5-cyclooctadiene . The two backbone protons of the azole ring ($NCHCHN_{mesityl}$) resonate at 6.34 and 7.28 ppm. In the ^{13}C NMR spectrum, the iminic carbon (*C*=N) resonance appears at 150.8 ppm and the central imidazolium carbon (N*C*N) appears at 202.1 ppm. The relatively low FTIR

$\nu_{C=N}$ absorption of complex **14** for the imine group (1652 cm^{-1}) suggest a chelating coordination mode of the ligand to the metal center as has been observed for the related nickel, palladium, zinc and iron complexes (1616–1654 cm^{-1}).

Scheme 13. Preparation of a Ni(0) imino-NHC complex (**14**).

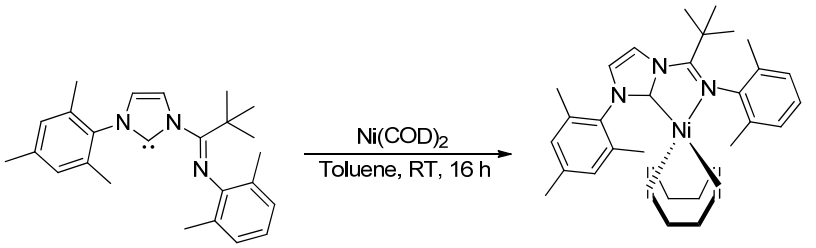

X-ray quality crystals of **14** were grown at −35°C from a concentrated solution of pentane. Compound **14** crystallized in a monoclinic crystal system in the *P* $2_1/c$ space group. The geometry around the nickel center is distorted tetrahedral with the ligand bound in a bidentate fashion along with one 1,5-cyclooctadiene molecule (Figure 25). There are few reports in literature of structurally characterized nickel(0) complexes.[48,111-113] The only other nickel(0) structure to contain carbene and COD ligands was reported by Radius and is found as a dimer in the solid state with one molecule of COD bridging between two nickel atoms.[114]

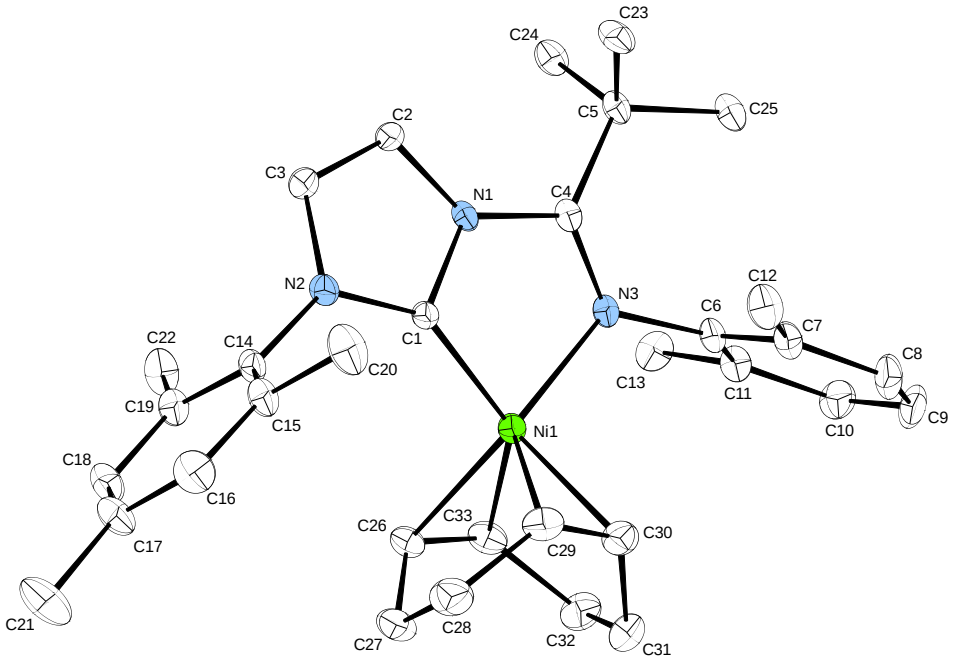

Figure 25. ORTEP plot of (C^Imine$_{t\text{-Bu}}$)Ni(COD) (**14**) (40% probability level). Hydrogen atoms and one solvent molecule of pentane are omitted for clarity. Select bond lengths (Å) and angles (deg): Ni1–C1 1.854(5), Ni1–N3 2.007(4), Ni1–C26 2.044(5), Ni1–C29 2.087(5), Ni1–C30 2.0849, Ni1–C33 2.075(5), C1–Ni1-N3 80.80(18).

The catalytic activities of all five nickel complexes **8** and **12a**–**14** towards ethylene polymerization were studied in toluene at atmospheric pressure and room temperature in the presence of 1000 equivalents methylaluminoxane as cocatalyst. Unfortunately, no ethylene uptake was observed over any extended periods of time. Chapter four will aim at understanding the poor performance of this class of complexes through the synthesis, characterization and reactivity study of the palladium analogues.

3.3 Conclusions

In summary, zinc(II), iron(II), cobalt(II), nickel(0) and nickel(II) complexes coordinated with an aryl-substituted imino-*N*-heterocyclic carbene have been synthesized, isolated and characterized. The effect of the iminic carbon substituent was studied by preparing the methyl and *tert*-butyl nickel(II) homologues. The size of the iminic carbon substituent was found to have a large impact on the bond angles and bond lengths about the metal center. The oxidative addition of an imidazolium salt precursor with $Ni(COD)_2$ led to a square planar bis(carbene)$NiCl_2$ complex. In exploring the reactivity of the **5a** and **5b**, it was further demonstrated that NHC copper(I) complexes are indeed good carbene transfer agents, and are an excellent alternative way to making NHC metal complexes. Preliminary studies using nickel complexes coordinated by one (**12a, 12b, 14**) and two (**8**, **13**) of these ligands unfortunately showed no activity in ethylene polymerization.

Chapter 4. Reactivity Study of Imino-*N*-Heterocyclic Carbene Palladium(II) Methyl Complexes

Preface

A part of the research presented in this chapter has been published in a paper in which I wrote the first draft and further revisions were done by my supervisor Dr. Gino Lavoie.[115]

4.1 Introduction

The reactivity of the metal–carbon bond plays a critical role in the stoichiometric and catalytic synthesis of organic compounds.[116-122] While carbon monoxide has historically played an important role as substrate due to its role in hydroformylation,[123,124] the related isocyanide has received relatively far less attention.[125,126] Isocyanides are of special interest due to the addition of a biologically-important nitrogen atom, and due to the presence of a new iminic reactive site for subsequent reaction on the molecule. Palladium methyl complexes of chelating nitrogen[10,127-130] and phosphine[131-135] ligands have proven capable of inserting not only one but multiple equivalents of aryl and alkyl isocyanides.[130] In many cases, the use of excess isocyanide however leads to dissociation of the ancillary ligand used, such as monodentate phosphine,[135] and chelating P–P[131] and N–N[10,131] ligands. This results in poor control over the reactivity of the transition metal complex.

Coordination of strong σ-donors such as N-heterocyclic carbenes (NHCs) may mitigate or eliminate this undesired dissociation of the ancillary ligand. To my knowledge, only one NHC palladium methyl complex has been shown to insert one equivalent of isocyanide, even when the substrate was used in excess.[63] Interestingly, in

the absence of an alkyl migratory group, isocyanide has also been found to insert into the palladium–carbene bond in palladium iodide dimers coordinated with remote N-heterocyclic carbenes.[136]

Chapter three described the synthesis and coordination of aryl-substituted imino-*N*-heterocyclic carbenes to nickel, unfortunately, the nickel complexes were found to be inactive for ethylene polymerization.[57] Therefore, considering the importance of palladium catalysts in cross-coupling reactions[61,137,138] and their ability to polymerize functionalized olefins,[8,32,94,139,140] it was decided to extend the study to diamagnetic palladium–methyl complexes to gain insight into their thermal stability and into their insertion chemistry. The synthesis and structural characterization of Pd(II) allyl and methyl complexes of C^Imine$_R$ (R = Me, Ph, *t*Bu) is presented in this chapter. In addition, the thermal stability and reactivity of both neutral and cationic Pd(II) methyl complexes of C^Imine$_R$ ligands towards ethylene, isocyanides and carbon monoxide is also described in this chapter.

4.2 Results and Discussion

4.2.1 Synthesis and Characterization of Allylic Palladium(II) Imino-NHC Complexes

Addition of two equivalents of the free carbene (**2b**) to the cationic palladium allyl complex, prepared *in situ* from reacting the palladium allyl chloride dimer with two equivalents of silver tetrafluoroborate, resulted in the formation of the cationic palladium complex **15b** (Scheme 14).

Scheme 14. Preparation of [Pd(C^Imine$_{t\text{-}Bu}$)(η^3-C_3H_5)Me]BF_4 (**15a**) and (**15b**).

15a
15b

In the ^{1}H NMR spectrum of **25b** the central allylic proton ($CH_2C\mathit{H}CH_2$) appears as a multiplet at 5.24 ppm. The *tert*-butyl resonance appears at a sharp singlet at 1.45 ppm. In the ^{13}C-NMR spectrum, the iminic carbon (*C*=N) resonance appears at 184.7 ppm and the central imidazolium carbon (N*C*N) appears at 169.2 ppm. The methyl analogue, complex **15a,** was prepared by the addition of one equivalent of the silver complex (**3a**) to the cationic palladium allyl complex (Scheme 14). Proton and carbon assignments are similar to that of **15b.**

Complex **15b** was further characterized by X-ray diffraction and crystallized in space group $P2_1/c$ (Figure 26) along with selected bond lengths and bond angles. The geometry around the palladium centre is distorted square-planar with the ligand bound to the metal through the central carbon and the nitrogen atom of the imine group. The Pd1–C1 bond length is 1.9898(1) Å and the Pd1-N3 bond length is 2.1380 Å. The Pd1–C26 bond length is 2.0906 Å while the Pd1-C28 bond length is slightly longer, measuring 2.1566(1) Å. The 2,6-dimethylphenyl and the 2,4,6-trimethylphenyl rings are twisted 86.38° and 89.68° to the metallocycle (Pd1–C1–N2–C13–N3). Having successfully demonstrated

the coordination of the ligand to palladium in a bidentate fashion, efforts were then directed to prepare more suitable palladium precatalysts.

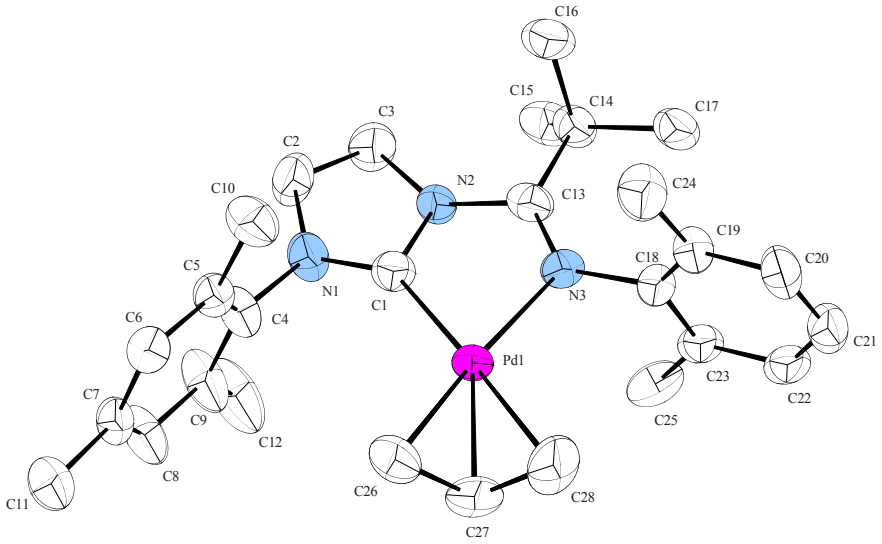

Figure 26. ORTEP plot of of [Pd(C^Imine$_{t\text{-}Bu}$)(η^3-C_3H_5)Me]BF_4 **(15a)** showing the major species (30% probability level). Hydrogen atoms and a counter anion molecule of sodium tetrafluoroborate omitted for clarity. Select bond lengths (Å) and angles (deg): Pd1–C1 1.9898(1), Pd1–N3 2.38(0), Pd1–C26 2.090(6), Pd1–C28 2.1566(1), C4–N3 1.2751, C1–Pd1–N3 76.83, C26–Pd1–C28 105.69.

4.2.1 Synthesis and Characterization of Palladium(II) Imino-NHC Methyl Complexes

The neutral palladium complexes were prepared in good yields, 80–98%, either from copper(I) transmetalation (for **16a**) or ligand displacement (for **16b** and **16c**) (Scheme 15). In contrast to the corresponding (C^Imine$_R$)$NiBr_2$ complexes,[57] these complexes are diamagnetic, indicating a square planar geometry. Their ^{1}H NMR spectra

showed one set of resonances, consistent with the formation of only one isomer, with the methyl group attached to the metal center resonating at δ 0.23–0.42 in $CDCl_3$. The conformation of all complexes was determined by 1D-NOESY NMR experiments. Selective excitation on the methyl group bound to palladium resulted in a nuclear Overhauser effect (NOE) for the mesityl ring directly attached to the azole ring, consistent with the methyl group *trans* to the imine nitrogen and the chloride *trans* to the carbene.

Scheme 15. Synthesis of Neutral (**16a**–**c**) and Cationic (**17a**–**c**) Palladium Complexes.

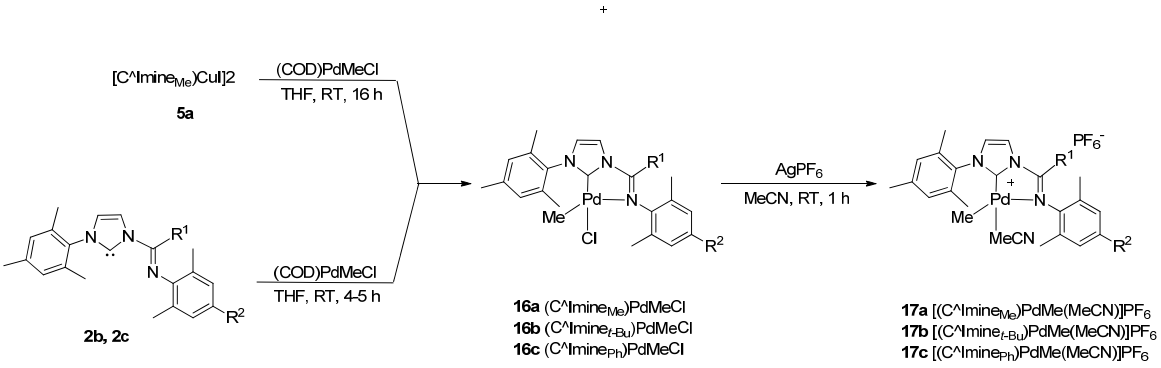

The palladium methyl carbon and the central imidazolium (N*C*N) carbon nuclei resonate at approximately δ 9 and 177, respectively, for complexes **16a**–**c**. While the resonance of the iminic carbon for both **16a** and **16c** appear at δ 156, that of the *tert*-butyl derivative **16b** is found downfield at δ 161.2. The decrease in the FTIR $\nu_{C=N}$ absorption for **16a**–**c** (1626–1652 cm^{-1}) from the corresponding imidazolium salt strongly suggests

coordination of the ligand through both the carbenoid carbon and the iminic nitrogen atoms.

The crystal structures for all three palladium complexes **16a**–**c** were obtained and selected bond angles and bond lengths are provided in Table 1 . Complexes **16a** (Figure 27) and **16c** (Figure 29) both crystallized in the space group *P* $2_1/n$, while complex **16b** crystallized in the space group *P* $2_12_12_1$ (Figure 28). All three complexes show a slightly distorted square planar structure where the chloride is *trans* to the carbene, in agreement with the assignment based on solution NMR spectroscopy. The palladium–methyl bond lengths are observed in the range 1.939(5)–1.969(4) Å, similar to those reported for related complexes of NHC^pyridine bidentate ligands.[65,67,141] The palladium–chloride bond lengths are in the range of 2.3237(9)–2.3612(12) Å. In all three complexes **16a**–**c**, the C1–Pd1–N3 bite angles are comparable, with values ranging from 77.22(17)° to 78.54(13)°. In contrast, the nature of the substituent has a marked impact on the Pd1–N3–C_{ipso} angles, with the large *tert*-butyl group pushing the xylyl ring towards the metal and resulting in the smallest angle of 117.1(3)°. The smaller methyl group yields a larger angle of 127.8(2)°, which is only slightly further reduced to 126.0(2)° upon substituting the iminic carbon with a phenyl ring. The Pd1–N3 bond length is the smallest for the *tert*-butyl (**16b**, 2.165(4) Å) and the phenyl (**16c**, 2.170(3) Å) derivatives, and the largest (2.184(3) Å) for the methyl derivative (**16a**). The Pd–C1 bond length in **16a** and **16c** are statistically equivalent, and longer at 1.969 Å compared to **16b** (1.939(5) Å). Similarly, the Pd–N–C_{ipso} bond angle in **16a** and **61c** are both significantly larger (127.8(2) and 126.0(2)°, respectively) than that in **16b** (117.1°). These greatly impact the coordination

sphere around the metal, possibly resulting in differences in reactivity towards various substrates. Finally, the solid-state structures clearly show the axial positions of the square planar structures well protected by the ortho-methyl substituents of both aryl rings, which are tilted by 85.8° and 74.0° (**16a**), 87.2° and 84.6°(**16b**), and 79.0° and 69.8° (**16c**), with respect to the mean plane formed by the metallacycle.

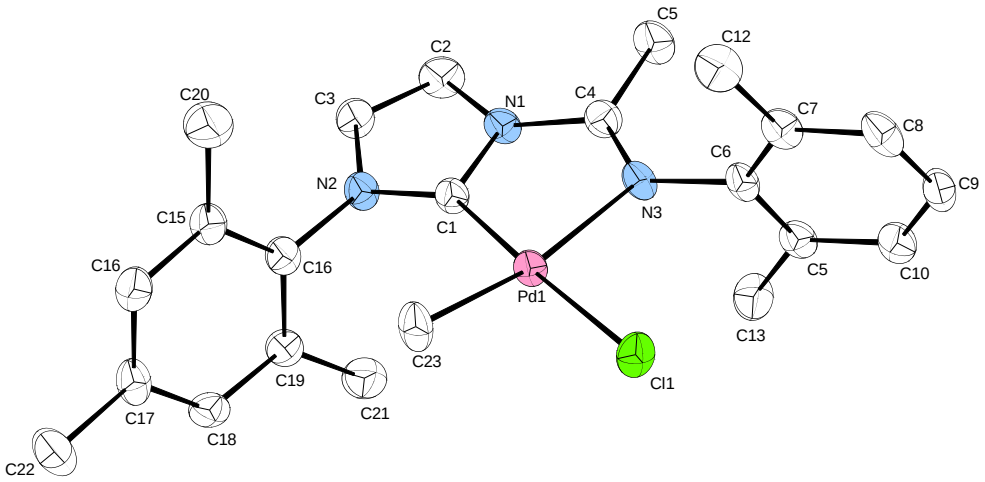

Figure 27. ORTEP plot of (C^Imine$_{Me}$)PdMeCl (**16a**) (50% probability level). Hydrogen atoms and a solvent molecule of chloroform omitted for clarity.

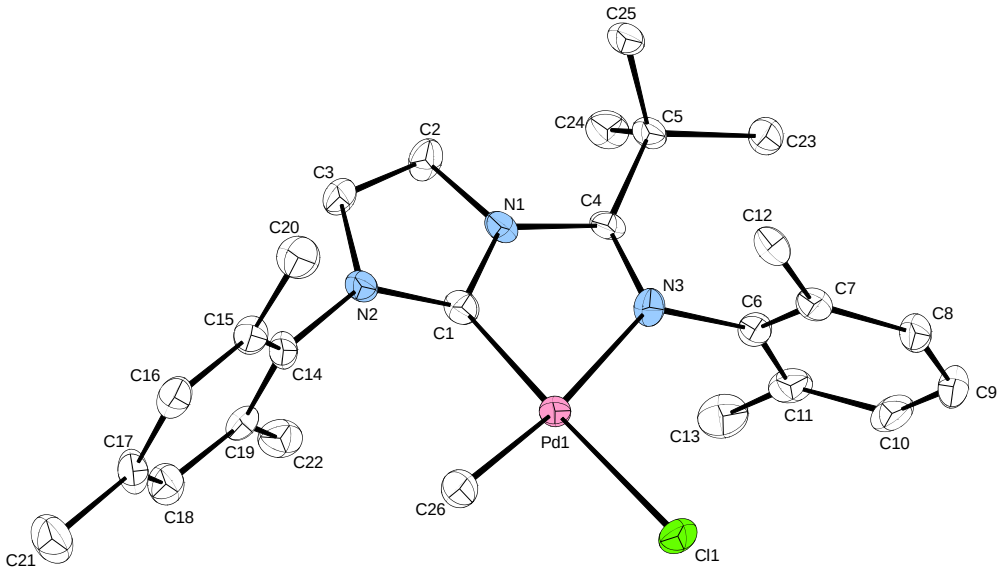

Figure 28. ORTEP plot of (C^Imine$_{t\text{-Bu}}$)PdMeCl (**16b**) (50% probability level). Hydrogen atoms and a solvent molecule of chloroform omitted for clarity.

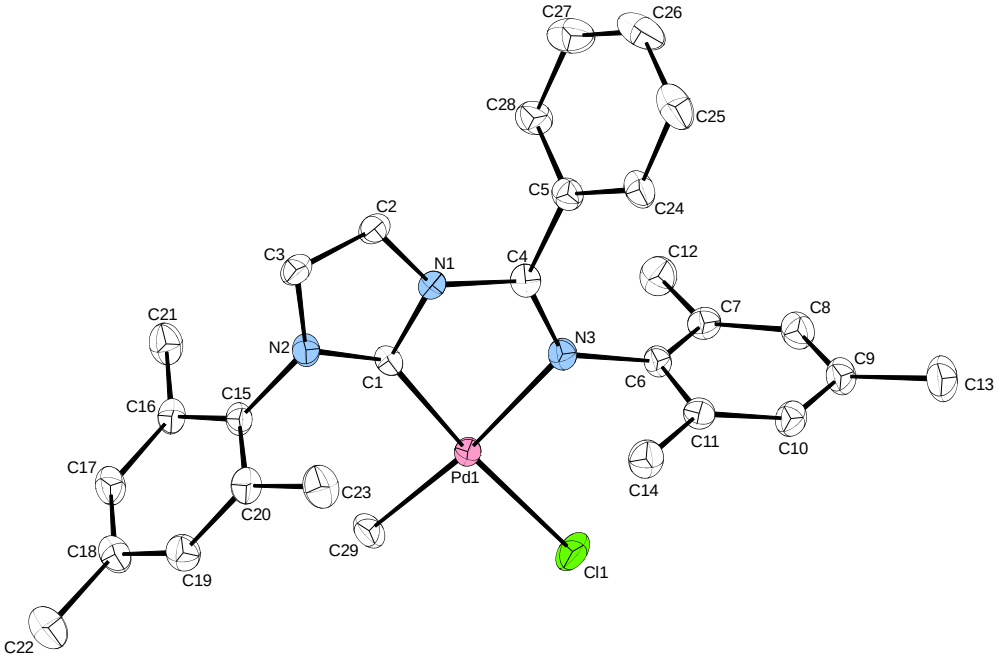

Figure 29. ORTEP plot of (C^Imine$_{Ph}$)PdMeCl (**16c**) (50% probability level). Hydrogen atoms omitted for clarity.

Table 1. Selected bond distances (Å) and angles (deg) for complexes **16a**–**16c** and **17b**.

	16a	**16b**	**16c**	**17b**
Bond Lengths				
Pd1–C1	1.969(4)	1.939(5)	1.969(3)	1.949(3)
Pd1–N3	2.184(3)	2.165(4)	2.170(3)	2.146(2)
Pd1–Cl1	2.3605(10)	2.3612(12)	2.3237(9)	—
Pd1–C_{Me}	2.033(4)	2.036(5)	2.040(4)	2.039(3)
C4–N3	1.273(5)	1.295(6)	1.295(4)	1.278(3)
Bond Angles				
C1–Pd1–N3	77.93(14)	77.22(17)	78.54(13)	77.47(10)
C1–Pd1–Cl1	174.97(12)	172.75(16)	174.26(18)	—
Pd1–N3–C_{ipso}	127.8(2)	117.1(3)	126.0(2)	116.27(16)

The related cationic methyl complexes were also prepared as model compounds for the cationic hydrocarbyl propagating species that are present in the catalytic cycle of olefin polymerization. Addition of one equivalent of silver hexafluorophosphate to compounds **16a**–**c** in acetonitrile resulted in the formation of the cationic complexes **17a**–**c** in excellent yields (Scheme 15). Similar to the neutral complexes, all cationic complexes showed only one set of resonances in the proton NMR spectra, consistent with the presence of only one isomer. 1D-NOESY NMR spectra are consistent with the methyl group *trans* to the imine nitrogen, with an acetonitrile molecule *trans* to the carbene.

The palladium-bound methyl protons in **17a**–**c** resonate at lower frequencies to those of the neutral analogues **16a**–**c**, with chemical shifts in chloroform-*d* ranging from δ –0.10 to 0.10. The acetronitrile protons appears at approximately δ 1.6 for all three cationic complexes, consistent with its coordination to the metal center. The carbenoid carbon (N*C*N) nucleus of compounds **17a**–**c** resonates at approximately δ 172, and upfield shift from that of **16a**–**c**. The lower electron density on the cationic metal center of compounds **17a**–**c** led to a decrease in π-backdonation, as evidenced by the FTIR $\nu_{C=N}$ stretching frequencies (1635–1660 cm^{-1}) that are 5–9 cm^{-1} larger than those observed in **16a**–**c**. The values of these stretching frequencies are also consistent with bidentate coordination of the ligand through the carbenoid carbon and the imine nitrogen.

X-ray quality crystals of **17b** were successfully grown at room temperature by slow vapor diffusion of diethyl ether into a saturated dichloromethane solution. Compound **17b** crystallized in a monoclinic crystal system in the *P* 2_1/n space group. The complex adopts a distorted square planar geometry, with the acetonitrile bound *trans* to the carbene, as predicted from NMR spectroscopy experiments (Figure 30). Abstraction of the chloride ion and its replacement with a molecule of acetonitrile caused a decrease in both the Pd1–N3 and C4–N3 bond lengths from 2.165(4) Å in **16b** to 2.146(2) Å in **17b**, and from 1.295(6) Å in **16b** to 1.278(3) Å in **17b**, respectively, with very little change to the Pd1–C1 bond length. This substitution also resulted in the Pd1–N3–C_{ipso} bond angle decreasing from 117.1(3) to 116.27(16)°, with little change to the C1–Pd1–N3 bite angle (77.47(10)° in **17b** compared to 77.22(17)° in **16b**).

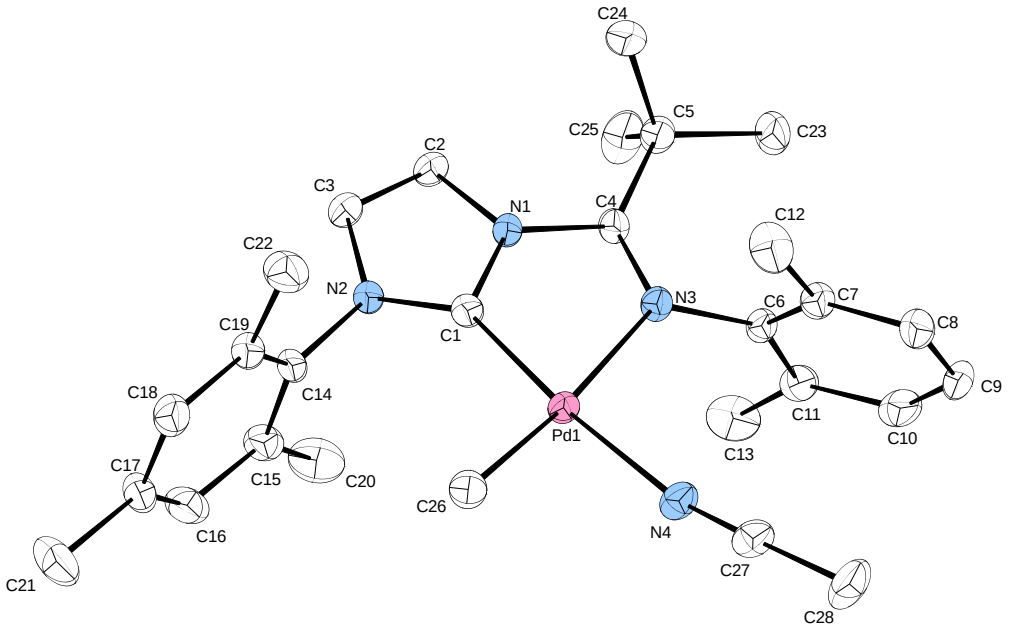

Figure 30. ORTEP plot of [(C^Imine$_{t\text{-Bu}}$)PdMe(MeCN)]PF_6 (**17b**) (50% probability level). Counteranion (PF_6^-) and hydrogen atoms omitted for clarity.

4.2.2 Reactivity Studies of Palladium Complexes

The activity of the compounds **16a–c** in the polymerization of ethylene was tested at atmospheric pressure and room temperature using 1000 equivalents methylaluminoxane (MAO) as cocatalyst. Palladium black readily formed and no ethylene uptake was noted in any of the trials. Reactions with **17a–c** also did not produce polyethylene, with and without MAO added. Considering reports of reductive elimination in other NHC palladium alkyl complexes,[51,142] thermal studies of complexes **16–17c** were undertaken to determine whether these complexes also suffered from this

undesired side-reaction, limiting their utility in catalysis involving migratory insertion of an alkyl group.

All complexes were heated to 60 °C in $CDCl_3$ and monitored overtime for any sign of decomposition. The nature of the substituent on the iminic carbon impacted the thermal stability of the neutral complexes **16a**–**c**. In the case of the *tert*-butyl derivative **16b**, *N*-(2,6-dimethylphenyl)pivalimidoyl chloride and 1-mesityl-2-methyl-1H-imidazole[143] were produced as the major species after 30 min, with complete decomposition of **16b** within 24 h (Scheme 16). In contrast, both the methyl (**16a**) and phenyl (**16c**) derivatives and the cationic complexes (**17a**–**c**) showed no evidence of decomposition when heated to 60 °C in $CDCl_3$. This is in stark contrast to other palladium alkyl systems for which the cationic species undergo reduction elimination more readily than their neutral analogues.[50,142]

Two mechanisms accounting for the formation of *N*-(2,6-dimethylphenyl)pivalimidoyl chloride and 1-mesityl-2-methyl-1H-imidazole from **16b** are proposed in Scheme 16. In path a, complex **16b** undergoes reductive elimination to generate Pd(0) and the 2-methylimidazolium salt (**4.A**), which could react with the chloride anion to produce the observed products. While chloride is a very poor nucleophile, similar cleavage of the imidazole–imine bond has been observed in other related systems.[55,58] In path b, the chloride first dissociates from **16b** to form complex **4.B**. Coordination of the imine to the cationic metal center would enhance the electrophilicity of the carbon atom, making it more susceptible to nucleophilic attack of the chloride to generate the observed imidoyl chloride. The resulting highly reactive two-coordinate (imidazolyl)(methyl)palladium

complex **C** could subsequently undergo reductive elimination to give the substituted imidazole.

Scheme 16. Proposed Mechanisms for the Thermal Decomposition of Neutral **16b**.

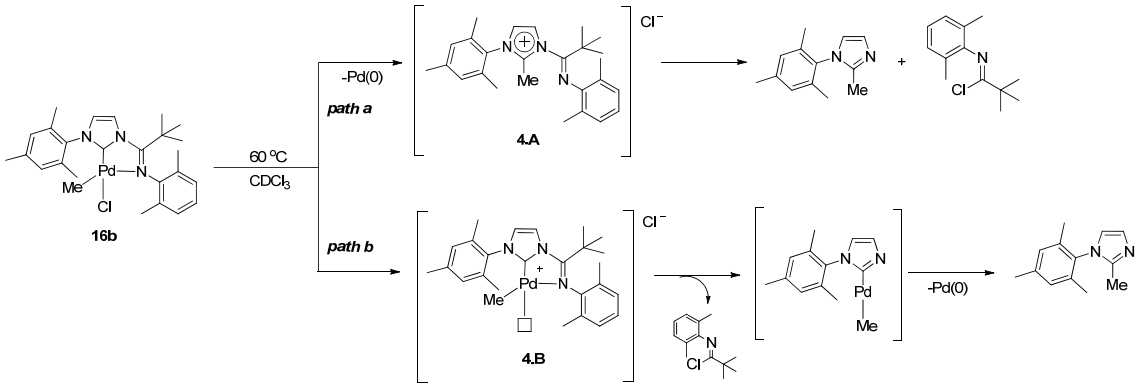

To get a better understanding of the decomposition mechanism, the imidazolium tetrafluoroborate salt **1c**, and both the neutral (**16b**) and cationic (**17b**) palladium methyl complexes were treated with chloride ions. Addition of tetrabutylammonium chloride to **1c** gave no reaction, even at elevated temperature, ruling out the formation of compound **4.A**, and consequently of path a. Compound **1c** however rapidly decomposed to *N*-mesitylimidazole and to the imidoyl chloride upon addition of HCl in diethyl ether at room temperature, probably due to protonation of the imine nitrogen, effectively activating the imine carbon for nucleophilic attack by the chloride.

While palladium complex **16b** remains intact at room temperature when exposed to Bu_4NCl, formation of *N*-(2,6-dimethylphenyl)pivalimidoyl chloride and 1-mesityl-2-methyl-1H-imidazole was observed upon heating the reaction mixture to 60 °C. The lower rate of decomposition to that observed in the absence of additional chloride ions is

in agreement with the cationic metal complex **4.B** being a key intermediate in the decomposition of **16b**. These results, coupled with the rapid decomposition of the cationic complex **17b** induced by the addition of Bu_4NCl, support the mechanism proposed in path b (Scheme 16). While dissociation of the chloride in **16a** and **16c** may also occur, the stronger imidazole–imine bond in these two complexes, indicated by their short C4–N1 bond lengths (1.406(5) and 1.412(4) Å, respectively, compared to 1.449(6) in **16b**), may prevent further decomposition to compound **C**, resulting in the reversible coordination of the chloride anion to regenerate the stable four-coordinate neutral palladium complex.

The stability of all three *cationic* complexes **17a–c** at 60 °C however suggested that the inability of these complexes to catalyze the polymerization of ethylene was not due to decomposition of a *cationic* metal alkyl propagating species but possibly arose from their inability to undergo migratory insertion. To get further insight into the ability of the palladium methyl group to insert into electrophiles, reaction of complexes **16a**–**17c** towards isocyanides was investigated. Interestingly, despite using similar experimental conditions, reaction of the palladium neutral complexes with *tert*-butyl isocyanide in toluene all led to different reaction products, further, highlighting the important role of the substituent on the imine carbon (Scheme 17).

Scheme 17. Reactivity of Neutral Complexes **16a–c** with *tert*-Butyl Isocyanides.

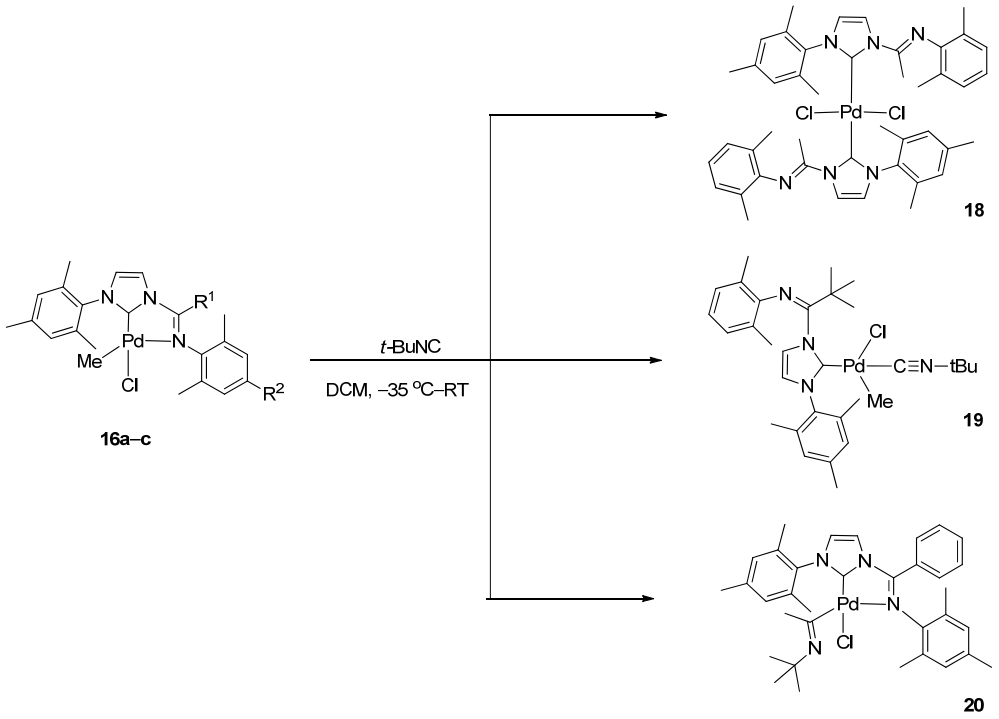

Addition of one equivalent of *tert*-butyl isocyanide to (C^Imine$_{Me}$)PdMeCl (**16a**) in toluene at –35 °C, with subsequent warming to room temperature and standard work-up resulted a yellow solid. The ^{1}H NMR spectrum was surprisingly simple, with only resonances assigned to the coordinated C^Imine$_{Me}$ ligand present, with no other proton coming from either the palladium methyl group or the isocyanide. The FTIR $\nu_{C=N}$ stretching frequency at 1674 cm^{-1} strongly suggests coordination of the C^Imine$_{Me}$ ligand exclusively through the carbenoid carbon atom. X-ray quality crystals of the isolated product were successfully obtained by slow vapor diffusion of pentane into a concentrated solution of dichloromethane.

The compound crystallized in the centrosymmetric P –1 space group, with the solid-state structure consistent with the spectroscopic data, in which two C^Imine$_{Me}$ ligands are bound to the metal center through the carbene, with the iminic arm remaining uncoordinated (Figure 31), similar to that observed in (C^Imine$_{Me}$)$_2$NiCl$_2$. Compound **18** adopts a slightly distorted square planar geometry, with both carbene ligands coordinated *trans* to each other. The palladium atom lies on an inversion center, which results in two sets of crystallographically-equivalent ligand sets and chlorine atoms. Other angles around the metal range from 89.7 (2)° to 90.3 (2)°. The Pd1–C1 bond length is of 2.027(4) Å, within the range reported for other (NHC)$_2$PdCl$_2$ complexes.[144-148] The N3–C4 bond length measures 1.252(5) Å, statistically equivalent to that observed in **1a**.[73]

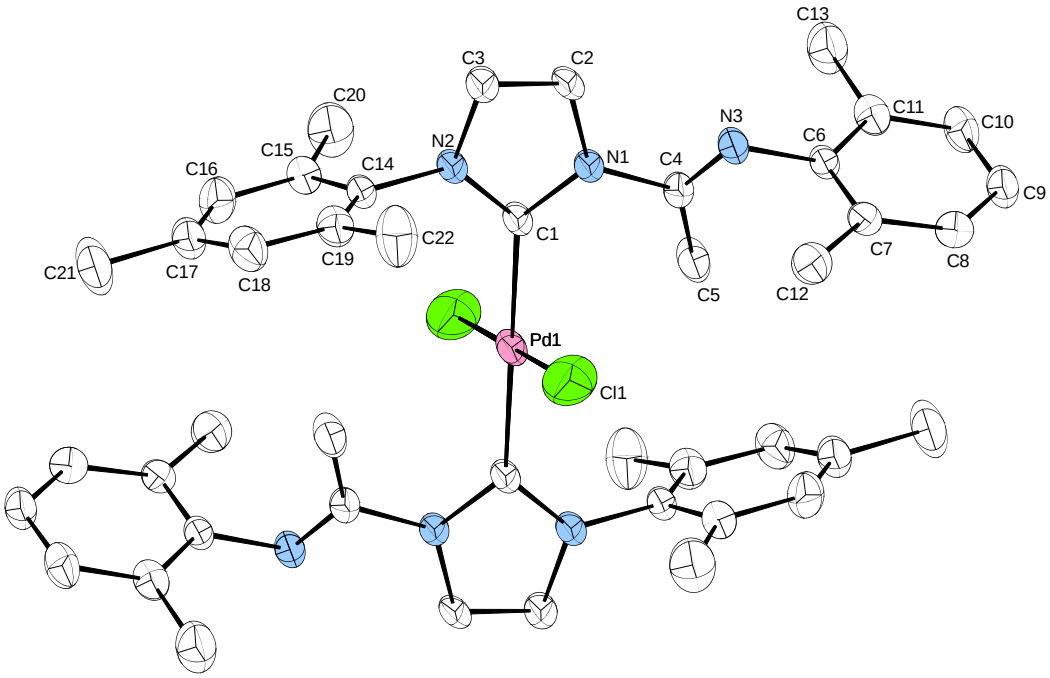

Figure 31. ORTEP plot of (C^Imine$_{Me}$)$_2$PdCl$_2$ (**18**) (50% probability level). Hydrogen atoms omitted for clarity. Selected bond distances (Å) and angles (deg): Pd1–C1 2.027(4), Pd1–Cl1 2.413(10), C4–N1 1.445(5), C4–N3 1.254(5), C1–Pd1–Cl1 89.7(2).

Under similar conditions, when *tert*-butyl isocyanide was added to (C^Imine$_{t\text{-}Bu}$)PdMeCl (**16b**) in toluene at –35 °C and allowed to warm up to room temperature, a gradual color change from tan to yellow was observed, with the final product identified as the coordinated isocyanide adduct (C^Imine$_{t\text{-}Bu}$)PdMe(*t*-BuNC)Cl (**19**) (Scheme 17). The ^{1}H NMR spectrum (C_6D_6) of compound **19** is consistent with coordination of the isocyanide with no insertion, as evidenced by a new resonance at δ 0.70 attributed to the protons of the coordinated isocyanide, and the palladium methyl protons remaining upfield at δ –0.50. Migratory insertion would have resulted in the latter resonating at a

higher frequency (δ 1.6–2.3), characteristic of the iminoacyl complex.[131] In the ^{13}C NMR spectrum, the isocyanide carbon atom that is directly attached to the metal center is observed at δ 119.6, consistent with simple coordination.[129,149,150] The IR spectrum shows a strong band at 2189 cm^{-1}, assigned to the coordinated isocyanide. Heating the reaction mixture to 70 °C to enforce migratory insertion of the methyl group into the coordinated isocyanide led to the formation of palladium black and unidentified products presumably through decomposition.

In contrast, reaction of *tert*-butyl isocyanide with (C^Imine$_{Ph}$)PdMeCl (**16c**) at room temperature yielded the insertion product **20**, as a light orange solid (Scheme 17). The ^{1}H NMR spectrum (C_6D_6) of **20** is consistent with the structure, as evidenced by a new resonance at δ 2.49 for the iminoacyl methyl protons, and the disappearance of the initial Pd–Me resonance at δ –0.50. The imine bond stretching frequency at 1638 cm^{-1} furthermore indicates that C^Imine$_{Ph}$ remains coordinated in a bidentate fashion to satisfy the preferred electronics and tetracoordinate nature of palladium(II).

Replacing the *tert*-butyl group of the isocyanide by an aryl ring has a profound effect on the chemistry displayed by complex **16a**. Reaction with an excess of 2,6-dimethylphenyl isocyanide gave spectroscopic evidence of several products of multiple insertions (Scheme 18).

Scheme 18. Reactivity of Complex **16a** with 2,6-Dimethylphenyl Isocyanide.

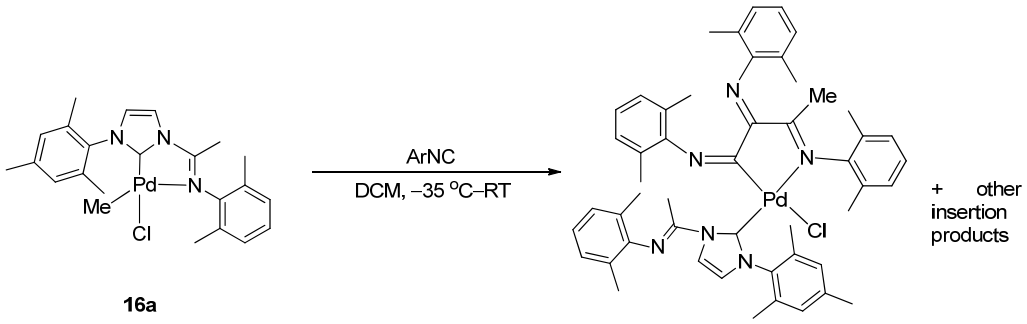

16a **21**

X-ray quality crystals were successfully isolated from the reaction mixture with **16a**. Compound **21** selectively crystallized in a monoclinic crystal system in the *P* 2_1/c space group. The palladium center adopts a distorted square planar geometry with three molecules of isocyanide inserted into the Pd–Me bond, and forming a new five-membered metallacycle, effectively breaking the chelate formed by C^Imine$_{Me}$ in **16a** (Figure 32). This demonstrates the hemilability of the imine fragment, easily dissociating from the metal center to accommodate the steric and electronic properties of the other ligands. This feature may prove invaluable in catalytic transformations when reactive coordinatively- and electronically-unsaturated intermediates are produced. These intermediates could effectively be stabilized through coordination of the imine nitrogen atom before re-entering the catalytic cycle upon associative displacement of the nitrogen donor by an incoming substrate. Complex **21** resulted from three consecutive insertions of 2,6-dimethylphenyl isocyanide into the palladium–methyl bond, as previously observed and structurally-characterized by other groups.[130,131,135] Formation of a five-membered metallacycle through coordination of the isocyanide nitrogen atom N4 is

preferred over coordination of N3 from C^Imine$_{Me,}$ generating a more favourable metal bite angle of 79.71(12)°, compared to the more acute 77.93(14)° in **16a**.

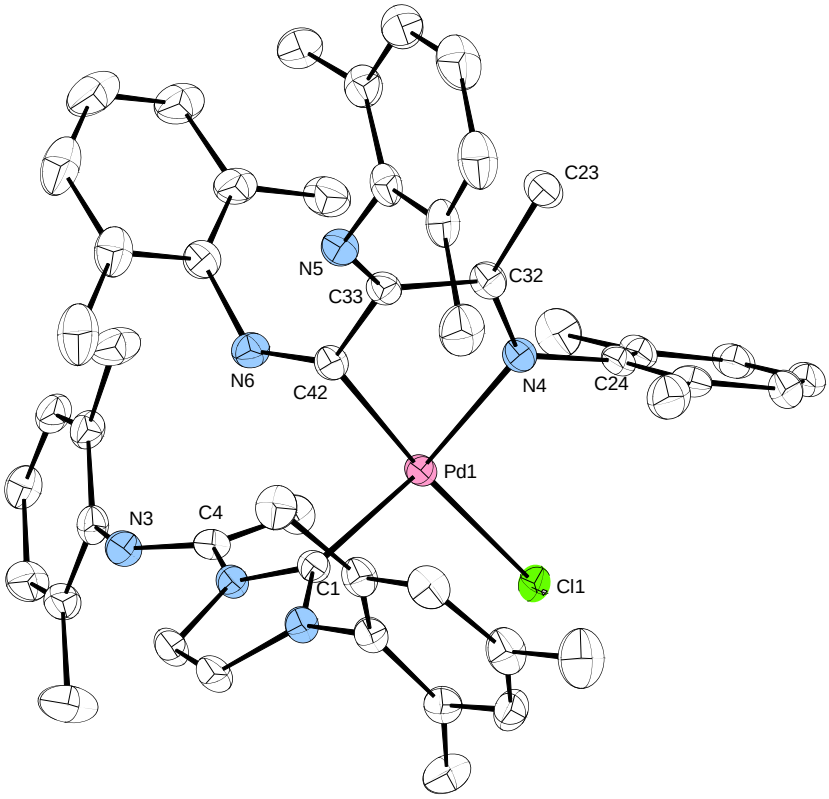

Figure 32. ORTEP plot of (C^Imine$_{Me}$)(1,2-bis[(2,6-dimethylphenyl)imino]-3-[(2,6-dimethylphenyl)imino-κ-*N*]butyl-κ-*C*]palladium(II) chloride (**21**) (50% probability level). Hydrogen atoms and one solvent molecule of chloroform omitted for clarity.

Considering the better thermal stability of the palladium complexes **17a–c** and the importance of cationic complexes in olefin polymerization catalysis, the reactivity of these complexes in isocyanide insertion was also explored. Addition of one equivalent of

either *tert*-butyl or 2,6-dimethylphenyl isocyanide to the palladium complex produced the isocyanide adduct in good yield (83–96%) (Scheme 19). The ^{1}H NMR spectra of the *tert*-butyl isocyanide reaction products (**22a**–**c**) showed sharp upfield resonances (δ 0.01 to –0.10) integrating to three protons, characteristic of the palladium methyl group. The FTIR $\nu_{C=N}$ absorption of the coordinated isocyanide were observed as a strong sharp band at 2208–2211 cm^{-1}, approximately 74 cm^{-1} higher than that of free isocyanide.[128] The ^{1}H NMR spectra for complexes **23a**–**c** are also consistent with isocyanide coordination with no evidence of migratory insertion of the methyl group, as indicated by the corresponding FTIR $\nu_{C=N}$ absorption at 2181–2184 cm^{-1}. The C=N stretching frequency for the C^Imine$_R$ ligand in **22a**–**23c** ranged from 1626 to 1656 cm^{-1}, indicating bidentate coordination.

Scheme 19. Reactivity of Cationic Complexes **17a**–**c** with Isocyanides.

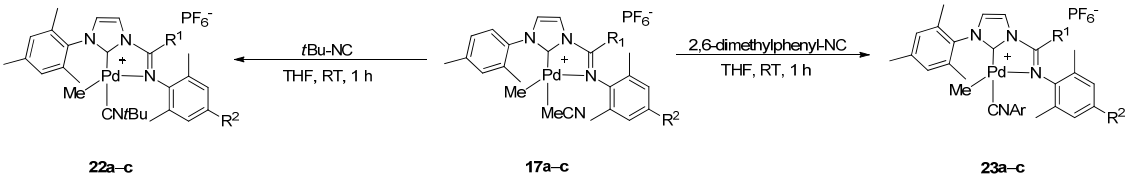

22a–c **17a–c** **23a–c**

Addition of two to five equivalents of *tert*-butyl or 2,6-dimethylphenyl isocyanide to **17a**–**c** resulted in multiple products. While unable to isolate each individual component, mass spectrometry on the reaction mixture shows signals corresponding to the isocyanide adduct of the palladium methyl complex **16b** and of palladium *N*-(2,6-

dimethylphenyl)iminoacyl insertion products, which are a result of single and multiple insertion of the methyl group into the isocyanide.

Considering the ability of isocyanide to insert multiple times into a metal-carbon bond made and the challenge in isolating and characterizing the reaction mixture, it was of interest to explore the reactivity of complexes **16a**–**17c** towards CO, which does not undergo multiple insertions. The *tert*-butyl derivative **16b** reacts with CO within a few minutes to form the acyl complex **24** in 77% yield (Scheme 20). The low energy FTIR $\nu_{C=N}$ stretching frequency of complex **24** (1631 cm^{-1}) indicates chelation of the iminic nitrogen atom. The $\nu_{C=O}$ absorption at 1689 cm^{-1} is consistent with a related NHC palladium acyl complex reported by Jordan.[63] In contrast, neutral complexes **16a** and **16c**, and all cationic **17a–c** remained intact upon exposure to one atmosphere of carbon monoxide, with no evidence of CO coordination, insertion or reductive elimination as observed by Elsevier in a related system.[151]

Scheme 20. Reactivity of Complexes **16b** with CO.

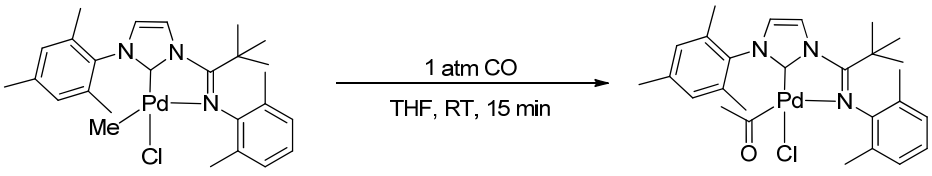

16b **24**

X-ray quality crystals of **24** were grown at room temperature by slow vapor diffusion of pentane in a saturated dichloromethane solution. Compound **24** crystallized

in a monoclinic crystal system in the *P* 2_1/n space group. The palladium center adopts a distorted square planar geometry with one equivalent of CO inserted into the Pd–Me bond (Figure 33). The acyl group (C27–O1–C26) is approximately orthogonal (85.2°) to the mean plane formed by C1, N3, Pd1 and C27. The chelate angle of 77.45(14)° remained practically unchanged from that of the staring *tert*-butyl derivative complex **16b** (77.22(17)°.

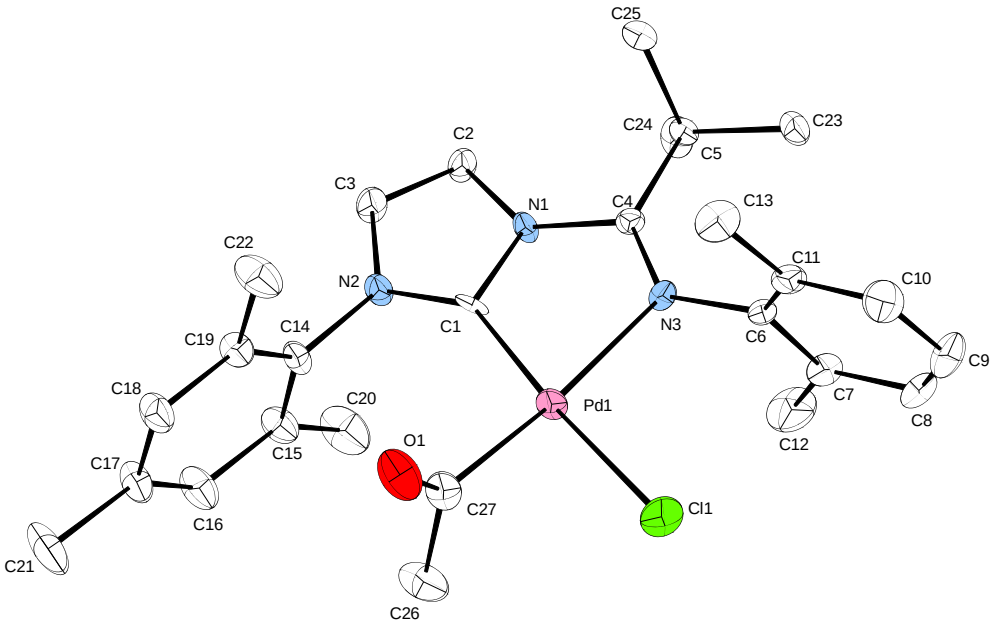

Figure 33.ORTEP plot of (C^Imine$_{Me}$)Pd(COMe)Cl (**24**) (50% probability level). Hydrogen atoms omitted for clarity. Selected bond distances (Å) and angles (deg): Pd1–C1 1.977(4), Pd1–N3 2.191(3), Pd–C27 1.972(5), C4–N3 1.282(5), C27–O1 1.205(6), C1–Pd1-N3 77.45(14), Pd–N3–C6 117.0(2).

4.3 Conclusions

Several *neutral* and *cationic* palladium complexes with an aryl-substituted acyclic imino-*N*-heterocyclic carbene were prepared, isolated and characterized to get insight into the inactivity of related nickel complexes in ethylene polymerization.[57] None of the new palladium complexes gave polyethylene at 1 atm C_2H_4 and room temperature. All three cationic palladium methyl complexes **17a-c**, model compounds for active olefin polymerization catalysts, and both neutral complexes **16a** and **16c** were found to be stable at elevated temperatures. In contrast, the *tert*-butyl derivative **16b** rapidly decomposed under similar conditions, possibly through dissociation of the chloride followed by a series of nucleophilic attack and reductive elimination to yield palladium black, 1-mesityl-2-methyl-1H-imidazole and the corresponding imidoyl chloride. Addition of MAO to **17a–c** at room temperature also caused formation of palladium black. The significant role of the substituent on the imine carbon on the reactivity of **16a–16c** with isocyanides and carbon monoxide was demonstrated. Compounds **16a–16c** indeed reacted with these electrophiles to give a variety of products, including simple adducts and multiple insertion products.

Chapter 5 – Experimental

5.1 General Comments

All manipulations were performed under a dinitrogen atmosphere in a drybox or using standard Schlenk techniques. Solvents used in the preparation of air and/or moisture sensitive compounds were dried by refluxing and then distilling from sodium (pentane and THF) or CaH_2 (dichloromethane) under a positive pressure of dinitrogen. Deuterated solvents were degassed using three freeze-pump-thaw cycles. C_6D_6 and $CDCl_3$ were vacuum distilled from sodium and CaH_2, respectively, and stored under dinitrogen. DMSO-d_6 was dried over activated 4Å molecular sieves. NMR spectra were recorded on a Bruker DRX 600 (^{1}H at 600 MHz, ^{13}C at 150.9 MHz), Bruker AV 400 (^{1}H at 400 MHz, ^{13}C at 100 MHz) or Bruker AV 300 (^{1}H at 300 MHz, ^{13}C at 75.5 MHz) spectrometer and are at room temperature unless otherwise stated. The spectra were referenced internally relative to the residual protio-solvent (^{1}H) and solvent (^{13}C) resonances and chemical shifts were reported with respect to $\delta = 0$ for tetramethylsilane. FTIR spectra were recorded a Thermo Scientific Nicolet 6700 FTIR spectrometer. Exact masses were determined by AIMS Laboratory of the Department of Chemistry, University of Toronto. Elemental composition was determined by ANALEST of the Department of Chemistry, University of Toronto or Guelph Chemical Laboratories Incorporated.

5.2 Materials

1-(2,4,6-Trimethylphenyl)imidazole, 1-(2,6-diisopropylphenyl)imidazole,[152] *N*-(2,6-dimethylphenyl)acetimidoyl chloride, *N*-(2,6-diisopropylphenyl)acetimidoyl chloride, *N*-(2,6-dimethylphenyl)pivalimidoyl chloride, *N*-(2,4,6-trimethylphenyl)benzimidoyl chloride[153] and $RuCl_2(PCy_3)_2(CHPh)$[154] were prepared according to published procedures. *N*-(2,6-Dimethylphenyl)acetamide was purchased from Sigma-Aldrich or Alfa Aesar and used without further purification. Silver carbonate and copper(I) iodide were purchased from BDH and Riedel-de Haën respectively, and were dried overnight in a vacuum oven at 80 °C. Sodium bis(trimethylsilyl)amide, nickel(II) bromide ethylene glycol dimethyl ether complex, zinc(II) chloride, iron(II) chloride, cobalt(II) chloride and bis(1,5-cycloocatadiene) nicke(0) were purchased from Sigma-Aldrich and used without further purification. Palladium(II) chloride, allyl palladium chloride dimer and (1,5-cyclooctadiene)methyl palladium(II) chloride were purchased from Strem and used without further purification. Silver hexafluorophosphate was purchased from Alfa Aesar and used as received. *tert*-Butyl isocyanide, 2,6-dimethylphenyl isocyanide, sodium bis(trimethylsilyl)amide were purchased from Sigma-Alrich and used as received. Methylaluminoxane was donated by Albermarle Corp. Deuterated NMR solvents were purchased from Cambridge Isotope Laboratories.

5.3 Preparations

Compound 1a, C^Imine$_{Me}$·HCl: *N*-(2,6-Dimethylphenyl)acetimidoyl chloride (2.32 g, 12.7 mmol) was dissolved in a minimal amount of THF and added to a THF (50 mL) solution of 1-(2,4,6-trimethylphenyl)imidazole (2.38 g, 12.8 mmol) at room temperature. A white precipitate formed within minutes. The reaction mixture was left to stir for a total of 3.5 h and filtered. The white solid was washed with THF (30 mL) and dried under vacuum (3.42 g, 9.27 mmol, 73 %). Crystals suitable for X-ray diffraction study were grown at room temperature under nitrogen by slow diffusion of pentane into a saturated dichloromethane solution using a diffusion bridge. ^{1}H NMR (400 MHz, $CDCl_3$) *E-isomer (major)*: δ 11.98 (br t, 1H, NC*H*N$_{(mesityl)}$), 8.51 (br t, ^{3}J = 1.7 Hz, 1H, NC*H*CN$_{(mesityl)}$), 7.24 (br t, ^{3}J = 1.6 Hz, 1H, NCC*H*N$_{(mesityl)}$), 7.10 (d, ^{3}J = 7.5 Hz, 2H, *m*-C*H*$_{(2,6\text{-xylyl})}$), 7.01–7.03 (m, 3H, *p*-C*H*$_{(2,6\text{-xylyl})}$ + *m*-C*H*$_{(mesityl)}$), 2.76 (s, 3H, C*H*$_{3(imine)}$), 2.32 (s, 3H, *p*-C*H*$_{3(mesityl)}$), 2.25 (s, 6H, *o*-C*H*$_{3(mesityl)}$), 2.08 (s, 6H, *o*-C*H*$_{3(2,6\text{-xylyl})}$); *Z-isomer (minor)*: δ 7.97 (s, 1H, NCCN$_{(mesityl)}$), 7.46 (s, 1H, NCCN$_{(mesityl)}$), 7.05 (s, 3H, C*H*$_{(2,6\text{-xylyl})}$), 7.02 (2H, *m*-C*H*$_{(mesityl)}$, unobserved because of overlap with resonance from major isomer but predicted from correlation observed in ^{1}H-^{13}C HSQC spectra), 2.35 (s, 3H, *p*-C*H*$_{3(mesityl)}$), 2.22 (s, 3H, C*H*$_{3(imine)}$), 2.21(s, 3H, CH$_{3(mesityl)}$), 2.06 (s, 3H, CH$_{3(mesityl)}$), 1.99 (s, 6H, *o*-C*H*$_{3(2,6\text{-xylyl})}$). ^{13}C{^{1}H} NMR (100 MHz, $CDCl_3$) *E-isomer (major)*: δ 150.1 (*C*=N), 143.3 (*C*$_{(2,6\text{-xylyl})}$), 141.6 (*p*-*C*$_{(mesityl)}$), 140.2 (N*C*N), 134.3 (*C*$_{(mesityl)}$), 130.8 (*o*-*C*$_{(mesityl)}$), 130.1 (*m*-*C*H$_{(mesityl)}$), 128.5 (*m*-*C*H$_{(2,6\text{-xylyl})}$), 126.5 (*o*-*C*$_{(2,6\text{-xylyl})}$), 125.0 (*p*-*C*H$_{(2,6\text{-xylyl})}$), 123.6 (NC*C*N$_{(mesityl)}$), 118.4 (N*C*CN$_{(mesityl)}$), 21.2 (*p*-*C*H$_{3(mesityl)}$), 18.3 (*o*-*C*H$_{3(2,6\text{-xylyl})}$), 18.2 (*o*-

$CH_{3(mesityl)}$), 17.6 ($CH_{3(imine)}$); *Z-isomer (minor)*: δ 168.8 (*C*=N), 141.4 (*p*-$C_{(mesityl)}$), 135.8 (*o*-$C_{(mesityl)}$), 130.0 (*o*-$C_{(2,6\text{-xylyl})}$), 129.9 ($C_{(2,6\text{-xylyl})}$), 128.73 ($CH_{(2,6\text{-xylyl})}$), 128.4 ($CH_{3(mesityl)}$), 128.3 ($CH_{(2,6\text{-xylyl})}$), 127.9 (*m*-$CH_{(mesityl)}$), 124.3 ($NCCN_{(mesityl)}$), 23.4 ($CH_{3(mesityl)}$), 21.2 ($CH_{3(mesityl)}$), 18.6 ($CH_{3(imine)}$), 17.6 ($CH_{3(mesityl)}$), 17.41 ($CH_{3(2,6\text{-xylyl})}$). FTIR (KBr) $\nu_{C=N}$ 1691 cm^{-1}. Anal. Calcd. for $C_{22}H_{26}ClN_3$ (%): C, 71.82; H, 7.12 ; N, 11.42; Found (%): C, 71.38; H,7.66; N, 11.63. HRMS (ESI^+, Dichloromethane) Calculated for $C_{22}H_{26}N_3Cl$, m/z = 332.2121 $[M - Cl]^+$; Found: 332.2121 $[M - Cl]^+$.

Compound 1a', C^Imine$_{Me}$··HCl: *N*-(2,6-Diisopropylphenyl)acetimidoyl chloride (2.72 g, 11.4 mmol) was dissolved in a minimal amount of toluene and added to a toluene (35 mL) solution of 1-(2,4,6-trimethylphenyl)imidazole (2.13 g, 11.4 mmol) at room temperature. A white precipitate formed within minutes. The reaction mixture was left to stir for a total of 19 h and filtered. The white solid was washed with THF (30 mL) and dried under vacuum (3.28 g, 7.75 mmol, 68 %).^{1}H NMR (400 MHz, $CDCl_3$) : δ 12.20 (s, 1H, NC*H*$N_{(mesityl)}$), 8.51 (s, 1H, NC*H*$CN_{(mesityl)}$), 7.27 (s, 1H, NCC*H*$N_{(mesityl)}$), 7.20 (br s, 3H, *p*-C*H*$_{(DIPP)}$ + *m*-C*H*$_{(DIPP)}$), 7.04 (s, 2H, *m*-C*H*$_{(mesityl)}$), 2.79 (s, 3H, C*H*$_{3(imine)}$), 2.67 (m, ^3J = 6.8 Hz, 2H, *o*-C*H*$_{(DIPP)}$), 2.34 (s, 3H, *p*-C*H*$_{3(mesityl)}$), 2.26 (s, 6H, *o*-C*H*$_{3(mesityl)}$), 1.20 (d, ^3J = 6.8 Hz, 6H, *o*-C*H*$_{3(DIPP1)}$), 1.14 (d, ^3J = 6.9 Hz, 6H, *o*-C*H*$_{3(DIPP2)}$). $^{13}C\{^1H\}$ NMR (100 MHz, $CDCl_3$): δ 149.8 (*C*=N), 141.7 (*p*-$C_{(mesityl)}$), 140.7 ($C_{(DIPP)}$), 140.3 (N*C*N), 136.7 (*o*-$C_{(DIPP)}$), 134.2 (*o*-$C_{(mesityl)}$), 130.74 ($C_{(mesityl)}$), 130.2 (*m*-$CH_{(mesityl)}$), 125.8 (*p*-$CH_{(DIPP)}$), 123.9 (NC*C*$N_{(mesityl)}$), 123.7 (*m*-$CH_{(DIPP)}$), 118.3 (N*C*$CN_{(mesityl)}$), 28.7 (*o*-$CH_{(dipp)}$), 23.5 (*o*-$CH_{3(dipp2)}$), 23.0 (*o*-$CH_{3(DIPP1)}$), 21.3 (*p*-$CH_{3(mesityl)}$), 18.3 (*o*-$CH_{3(mesityl)}$),

17.4 ($CH_{3(imine)}$). FTIR (cast-$CDCl_3$) $\upsilon_{C=N}$ 1698 cm^{-1}. Anal. Calcd. for $C_{26}H_{34}ClN_3$ (%): C, 73.65; H, 8.08 ; N, 9.91; Found (%): C, 73.38; H,8.18; N, 10.17.

Compound 1a", C^Imine$_{Me"}$·HCl: *N*-(2,6-Dimethylphenyl)acetimidoyl chloride (119.9 mg, 0.660 mmol) was dissolved in a minimal amount of THF and added to a THF (10 mL) solution of 1-(2,6-diisopropylphenyl)imidazole (150.7 g, 0.660 mmol) at room temperature. The reaction mixture was left to stir for a total of 4 h and filtered. The white solid was washed with pentane (15 mL) and dried under vacuum to give a white solid (206 mg, 0.502 mmol, 76 %). ^{1}H NMR (400 MHz, $CDCl_3$) *E* isomer δ 11.75 (s, 1H, NC*H*N$_{(mesityl)}$), 8.78 (s, 1H, NC*H*CN$_{(DIPP)}$), 7.53 (t, ^3J = 7.9 Hz, 1H, *p*-C*H*$_{(DIPP)}$), 7.33 (d, ^3J = 7.9 Hz, 2H, *m*-C*H*$_{(DIPP)}$), 7.32 (s, 1H, NCC*H*N$_{(DIPP)}$), 7.09 (d, ^3J = 7.5 Hz, 2H, *m*-C*H*$_{(xylyl)}$), 7.09 (t, ^3J = 7.5 Hz, 1H, *p*-C*H*$_{(xylyl)}$), 2.80 (s, 3H, C*H*$_{3(imine)}$), 2.45 (m, ^3J = 6.6 Hz, 2H, *o*-C*H*$_{(DIPP)}$), 2.09 (s, 6H, *o*-C*H*$_{3(xylyl)}$), 1.33 (s, ^3J = 6.6 Hz, 6H, *o*-C*H*$_{3(DIPP)}$), 1.17 (s, ^3J = 6.6 Hz, 6H, *o*-C*H*$_{3(DIPP)}$). ^{13}C{^{1}H} NMR (100 MHz, $CDCl_3$): δ 150.2 (*C*=N), 145.2 (*o*-*C*$_{(DIPP)}$), 145.1 (*C*$_{(xylyl)}$), 139.4 (N*C*N), 132.3 (*p*-*C*H$_{(DIPP)}$), 130.3 (*C*$_{(DIPP)}$), 128.5 (*m*-*C*H$_{(xylyl)}$), 126.4 (*o*-*C*$_{(xylyl)}$), 125.1 (*p*-*C*H$_{(xylyl)}$), 125.0 (NC*C*N$_{(DIPP)}$), 124.9 (*m*-*C*H$_{(DIPP)}$), 119.2 (N*C*CN$_{(xylyl)}$), 29.0 (*o*-*C*H$_{(DIPP)}$), 24.6 (*o*-*C*H$_{3(DIPP)}$), 24.3 (*o*-*C*H$_{3(DIPP)}$), 18.4 (*o*-*C*H$_{3(xylyl)}$), 17.8 (*C*H$_{3(imine)}$). Anal. Calcd. for $C_{25}H_{32}ClN_3$ (%): C, 73.24; H, 7.87 ; N, 10.25; Found (%): C, 73.37; H,8.12; N, 10.10.

Compound 1b, C^Imine$_{t\text{-}Bu}$·HBF$_4$: Solid $NaBF_4$ (1.78 g, 16.2 mmol) was added to a solution of *N*-(2,6-dimethylphenyl)pivalimidoyl chloride (3.63 g, 16.2 mmol) in

acetonitrile (70 mL). The turbid solution was allowed to stir for 48 h at ambient temperature. Solid 1-(2,4,6-trimethylphenyl)imidazole (3.03 g, 16.3 mmol) was added to the solution and the brown solution was allowed to stir for an additional 24 h. Volatiles were removed in vacuo and the product was redissolved in CH_2Cl_2 (25 mL), filtered and the product was precipitated with pentane (60 mL). The white solid was filtered and washed with pentane to give a light brown product (5.38 g, 11.7 mmol, 72%). ^{1}H NMR (400 MHz, $CDCl_3$) *(Major Isomer E)*: 8.39 (s, 1H, NC*H*N$_{(mesityl)}$), 7.70 (s, 1H, NC*H*CN$_{(mesityl)}$), 7.25 (s, 1H, NCC*H*N$_{(mesityl)}$), 6.93–6.85 (m, 3H, *m*-C*H*$_{(2,6\text{-xylyl})}$ + *p*-C*H*$_{(2,6\text{-xylyl})}$), 6.91 (s, 2H, *m*-C*H*$_{(mesityl)}$), 2.28 (s, 3H, *p*-C*H*$_{3(mesityl)}$), 2.09 (s, 6H, *o*-C*H*$_{3(2,6\text{-xylyl})}$), 1.65 (s, 6H, *o*-C*H*$_{3(mesityl)}$), 1.53 (s, 9H, C(C*H*$_3$)$_{3(imine)}$). ^{13}C{^{1}H} NMR (100 MHz, $CDCl_3$) *(Major Isomer)*: 154.6 (*C*=N), 143.1 (*C*$_{(2,6\text{-xylyl})}$), 141.7 (*p*-*C*$_{(mesityl)}$), 134.8 (N*C*N$_{(mesityl)}$), 134.2 (*o*-*C*$_{(mesityl)}$), 129.9 (*C*$_{(mesityl)}$), 129.8 (*m*-*C*H$_{(mesityl)}$), 128.6 (*m*-*C*H$_{(2,6\text{-xylyl})}$), 125.7 (*o*-*C*$_{(2,6\text{-xylyl})}$), 125.2 (*p*-*C*H$_{(2,6\text{-xylyl})}$), 124.2 (NC*C*N$_{(mesityl)}$), 122.5 (N*C*CN$_{(mesityl)}$), 40.5 (*C*(CH$_3$)$_{3(imine)}$), 28.3 (C(*C*H$_3$)$_{3(imine)}$), 21.2 (*p*-*C*H$_{3(mesityl)}$), 18.1 (*o*-*C*H$_{3(2,6\text{-xylyl})}$), 16.7 (*o*-*C*H$_{3(mesityl)}$). FTIR (cast film) $\nu_{C=N}$ 1696 cm^{-1}, 1673 cm^{-1}. Anal. Calcd. for $C_{25}H_{32}BF_4N_3$ (%): C, 65.09; H, 6.99 ; N, 9.11; Found (%):C, 65.22; H, 7.10 ; N, 8.86.

Compound 1c, C^Imine$_{Ph}$·HBF$_4$: *N*-(2,4,6-Dimethylphenyl)benzimidoyl chloride (3.10 g, 12.0 mmol) was dissolved in a minimal amount of acetonitrile and added to a suspension of acetonitrile (60 mL) solution of $NaBF_4$ (1.32 g, 12.0 mmol) at room temperature and stirred for 36 h. 2,4,6-Trimethylphenylimidazole (2.24 g, 12.04 mmol)

was subsequently added and the reaction mixture was stirred for an additional 12 h. Volatiles were then removed under vacuum and the resulting brown solid was dissolved in a minimal amount of dichloromethane. The solution was filtered and pentane was added to the filtrate to precipitate the product. The solid was further washed with pentane and dried under vacuum, giving the product as a light brown solid (4.83 g, 9.75 mmol, 81%). ^{1}H NMR (400 MHz, $CDCl_3$): δ 8.81 (s, 1H, NC*H*N$_{(azole)}$), 8.09 (s, 1H, NC*H*CN$_{(azole\text{-}mesityl)}$), 7.52 (s, 1H, NCC*H*N$_{(azole\text{-}mesityl)}$), 7.37 (m, 5H, C*H*$_{(phenyl)}$), 7.01 (s, 2H, *m*-C*H*$_{(azole\text{-}mesityl)}$), 6.74 (s, 2H, *m*-C*H*$_{(N\text{-}mesityl)}$), 2.33 (s, 3H, *p*-C*H*$_{3(azole\text{-}mesityl)}$), 2.20 (s, 3H, *p*-C*H*$_{3(N\text{-}mesityl)}$), 2.17 (s, 6H, *o*-C*H*$_{3(N\text{-}mesityl)}$), 2.02 (s, 6H, *o*-C*H*$_{3(azole\text{-}mesityl)}$).^{13}C{^{1}H} NMR (100 MHz, $CDCl_3$): δ 148.1 (*C*=N), 141.8 (*p*-*C*$_{(azole\text{-}mesityl)}$), 140.7 (*C*$_{ipso(N\text{-}mesityl)}$), 134.5 (*C*$_{(phenyl)}$), 134.4 (*o*-*C*$_{(azole\text{-}mesityl)}$), 132.6 (*C*$_{(phenyl)}$), 130.7 (*C*$_{ipso(azole\text{-}mesityl)}$), 130.1 (*m*-*C*H$_{(azole\text{-}mesityl)}$), 130.0 (*p*-*C*$_{(N\text{-}mesityl)}$), 129.5 (*C*$_{(phenyl)}$), 129.0 (*m*-*C*H$_{(N\text{-}mesityl)}$), 128.0 (*C*$_{(phenyl)}$), 126.6 (*o*-*C*$_{(N\text{-}mesityl)}$), 124.9 (NC*C*N$_{(azole\text{-}mesityl)}$), 121.9 (N*C*CN$_{(azole\text{-}mesityl)}$), 21.2 (*p*-*C*H$_{3(azole\text{-}mesityl)}$), 20.8 (*p*-*C*H$_{3(N\text{-}mesityl)}$), 18.4 (*o*-*C*H$_{3(N\text{-}mesityl)}$), 17.6 (*o*-*C*H$_{3(azole\text{-}mesityl)}$). FTIR (cast-$CDCl_3$) $\nu_{C=N}$ 1675 cm^{-1}. Anal. Calcd for $C_{28}H_{30}N_3BF_4$ (%): C, 67.89; H, 6.10; N, 8.48. Found (%): C, 68.13; H, 5.86; N, 8.33.

Compound 2b, C^Imine$_{t\text{-}Bu}$: A cooled solution of $NaN[Si(CH_3)_3]_2$ (439 mg, 2.20 mmol) in THF (15 mL) was added slowly to a THF (15 mL) solution of C^Imine·HBF_4 (**1b**) (953 mg, 2.07 mmol) at –78 °C. The light brown solution was allowed to stir at –78 °C for 30 min before the flask was removed from the bath and allowed to stir at room temperature for an additional 1.5 h. Volatiles were removed under reduced pressure and

the light brown product was redissolved in pentane, filtered, and dried in vacuo to yield the tan-coloured product (455 mg, 1.22 mmol, 59%). Crystals suitable for X-ray diffraction studies were grown from a saturated pentane solution at –35 °C. ^{1}H NMR (400 MHz, C_6D_6) 6.88 (d, ^{3}J = 7.2 Hz, 2H, *m*-C*H*$_{(2,6\text{-xylyl})}$), 6.81 (t, ^{3}J = 7.4 Hz, 1H, *p*-C*H*$_{(2,6\text{-xylyl})}$), 6.70 (s, 2H, *m*-C*H*$_{(mesityl)}$), 6.40 (s, 1H, NC*H*CN$_{(mesityl)}$), 5.98 (s, 1H, NCC*H*N$_{(mesityl)}$), 2.21 (s, 6H, *o*-C*H*$_{3(2,6\text{-xylyl})}$), 2.09 (s, 3H, *p*-C*H*$_{3(mesityl)}$), 1.87 (s, 6H, *o*-C*H*$_{3(mesityl)}$), 1.63 (s, 9H, C(C*H*$_3$)$_{3(imine)}$). ^{13}C{^{1}H} NMR (100 MHz, C_6D_6) 218.3 (N*C*N$_{(mesityl)}$), 162.5 (*C*=N), 146.7 (*C*$_{(2,6\text{-xylyl})}$), 138.5 (*C*$_{(mesityl)}$), 137.5 (*p*-*C*$_{(mesityl)}$), 135.3 (*o*-*C*$_{(mesityl)}$), 129.0 (*m*-*C*H$_{(mesityl)}$), 127.9 (*m*-*C*H$_{(2,6\text{-xylyl})}$), 126.5 (*o*-*C*$_{(2,6\text{-xylyl})}$), 123.3 (*p*-*C*H$_{(2,6\text{-xylyl})}$), 119.0 (NC*C*N$_{(mesityl)}$), 118.9 (N*C*CN$_{(mesityl)}$), 41.0 (*C*(CH$_3$)$_{3(imine)}$), 29.3 (C(*C*H$_3$)$_{3(imine)}$), 21.0 (*p*-*C*H$_{3(mesityl)}$), 18.8 (*o*-*C*H$_{3(2,6\text{-xylyl})}$), 17.7 (*o*-*C*H$_{3(mesityl)}$). FTIR (cast film) $\nu_{C=N}$ 1662 cm^{-1}.

Compound 2c, C^Imine$_{Ph}$: A suspension of C^Imine$_{Ph}$·HBF$_4$ **1c** (96.7 mg, 0.195 mmol) and KN[Si(CH$_3$)$_3$]$_2$ (39.1 mg, 0.196 mmol) in toluene (15 mL) was cooled to –78 °C and stirred at this temperature for 30 min. The flask was then removed from the bath and stirred at room temperature for an additional 1.5 h. Volatiles were removed under reduced pressure and pentane (20 mL) was added to extract the product. The pentane solution was filtered and the filtrated was dried under reduced pressure to give a yellow solid (57.2 mg, 0.140 mmol, 72%). ^{1}H NMR (400 MHz, C_6D_6): δ 7.51 (d, ^{3}J = 7.5 Hz, 2H, *p*-C*H*$_{(phenyl)}$), 7.32 (s, 1H, NC*H*CN$_{(azole\text{-}mesityl)}$), 6.94–6.89 (m, 3H, *m*-C*H*$_{(phenyl)}$ + *o*-C*H*$_{(phenyl)}$), 6.65 (s, 2H, *m*-C*H*$_{(azole\text{-}mesityl)}$), 6.48 (s, 1H, NCC*H*N$_{(azole\text{-}mesityl)}$), 6.48 (s, 2H,

m-C*H*$_{(N\text{-mesityl})}$), 2.07 (s, 6H, *o*-C*H*$_{3(\text{azole-mesityl})}$), 1.97 (s, 3H, *p*-C*H*$_{3(\text{azole-mesityl})}$), 1.94 (s, 3H, *p*-C*H*$_{3(\text{azole-mesityl})}$), 1.80 (s, 6H, *o*-C*H*$_{3(N\text{-mesityl})}$). $^{13}C\{^1H\}$ NMR (100 MHz, C_6D_6): δ 158.2 (*C*=N), 146.0 (*C*$_{\text{ipso(N-mesityl)}}$), 137.9 (*p*-*C*$_{(\text{azole-mesityl})}$), 136.8 (*C*$_{\text{ipso(azole-mesityl)}}$), 135.3 (*o*-*C*$_{(\text{azole-mesityl})}$), 131.8 (*p*-*C*$_{(N\text{-mesityl})}$), 130.1 (N*C*CN$_{(\text{azole-mesityl})}$), 129.7 (*o*-*C*$_{(\text{phenyl})}$), 129.3 (*p*-*C*$_{(\text{phenyl})}$), 129.1 (*C*$_{\text{ipso(phenyl)}}$), 128.9 (NC*C*N$_{(\text{azole-mesityl})}$), 128.8 (*m*-*C*H$_{(\text{azole-mesityl})}$), 127.6 (*m*-*C*$_{(\text{phenyl})}$), 125.0 (*o*-*C*$_{(N\text{-mesityl})}$), 123.7 (*m*-*C*H$_{(\text{N-mesityl})}$), 21.0 (*p*-*C*H$_{3(\text{azole-mesityl})}$), 20.7 (*p*-*C*H$_{3(N\text{-mesityl})}$), 18.4 (*o*-*C*H$_{3(N\text{-mesityl})}$), 18.0 (*o*-*C*H$_{3(\text{azole-mesityl})}$); resonance for N*C*N was not observed. FTIR (cast-solvent) $\nu_{C=N}$ 1652 cm^{-1}. Anal. Calcd for $C_{28}H_{29}N_3$ (%): C, 82.52; H, 7.17; N, 10.31. Found (%): C, 82.26; H, 6.90; N, 10.58.

Compound 3a, Ag(C^Imine$_{Me}$)Cl: To a solution of C^imine·HCl **1a** (1.04 g, 2.82 mmol) in acetonitrile (70 mL) was added activated powdered 4Å molecular sieves and silver carbonate (0.807 g, 2.93 mmol) at room temperature. The reaction mixture was *stirred* with *exclusion of light* for 64 h and then filtered. The filtrate was evaporated to dryness and dissolved in the minimum amount of dichloromethane, pentane was added dropwise to precipitate the product. The solid was filtered, washed with pentane and dried in vacuo to yield the product as a light brown solid (1.02 g, 2.17 mmol, 77%). Crystals suitable for X-ray diffraction study were grown at –35 ºC under nitrogen by layering pentane onto a saturated dichloromethane solution. ^1H NMR (400 MHz, $CDCl_3$): 8.32 (d, ^3J = 1.5 Hz, 1H, NC*H*CN$_{(\text{mesityl})}$), 7.10 (d, ^3J = 7.4 Hz, 2H, *m*-C*H*$_{(2,6\text{-xylyl})}$), 7.06 (d, ^3J = 1.5 Hz, 1H, NCC*H*N$_{(\text{mesityl})}$), 6.98–7.03 (m, 3H, *p*-C*H*$_{(2,6\text{-xyly})}$ + *m*-C*H*$_{(\text{mesityl})}$), 2.59 (s, 3H, C*H*$_{3(\text{imine})}$), 2.35 (s, 3H, *p*-C*H*$_{3(\text{mesityl})}$), 2.10 (s, 6H,*o*-

C*H*$_{3(2,6\text{-xylyl})}$), 2.08 (s, 6H, *o*-C*H*$_{3(\text{mesityl})}$). ^{13}C{^{1}H} NMR (100 MHz, $CDCl_3$): 152.2 (*C*=N), 144.5 (*C*$_{(2,6\text{-xylyl})}$), 140.3 (*p*-*C*$_{(\text{mesityl})}$), 135.7 (*o*-*C*$_{(\text{mesityl})}$), 134.6 (*C*$_{(\text{mesityl})}$), 129.9 (*m*-*C*H$_{(\text{mesityl})}$)), 128.5 (*m*-*C*H$_{(2,6\text{-xylyl})}$), 126.4 (*o*-*C*$_{(2,6\text{-xylyl})}$), 124.4 (*p*-*C*H$_{(2,6\text{-xylyl})}$), 123.0 (NC*C*N$_{(\text{mesityl})}$), 119.5 (N*C*CN$_{(\text{mesityl})}$), 21.3 (*p*-*C*H$_{3(\text{mesityl})}$), 18.3 (*C*H$_{3(\text{imine})}$ and *o*-*C*H$_{3(2,6\text{-xylyl})}$), 18.1 (*o*-*C*H$_{3(\text{mesityl})}$). FTIR (KBr) $\nu_{C=N}$ 1682 cm^{-1}. Anal. Calcd. for $C_{22}H_{25}AgClN_3 \cdot 0.5\ CH_2Cl_2$ (%): C, 52.25; H, 5.07; N, 8.12; Found (%): C, 51.02; H, 4.97; N, 8.85. HRMS (ESI$^+$, Dichloromethane) Calculated for $C_{22}H_{25}AgN_3Cl$, m/z = 438.1099 [M – Cl]$^+$; Found: 438.1074 [M – Cl]$^+$.

Compound 3a', Ag(C^Imine$_{Me'}$)Cl: To a solution of C^Imine$_{Me'}$·HCl **1a'** (1.25 g, 0.00295 mol) in acetonitrile (40 mL) was added activated powdered 4Å molecular sieves and silver carbonate (0.813 g, 0.00295 mmol) at room temperature. The reaction mixture was *stirred* with *exclusion of light* for 64 h and then filtered. The filtrate was evaporated to dryness and dissolved in the minimum amount of dichloromethane, pentane was added dropwise to precipitate the product. The solid was filtered, washed with pentane and dried in vacuo to yield the product as a light brown solid (156 mg, 0.000295 mmol, 10%). ^{1}H NMR (400 MHz, $CDCl_3$) : δ 8.34 (s, 1H, NC*H*CN$_{(\text{mesityl})}$), 7.21-7.17 (m, 3H, *p*-C*H*$_{(\text{DIPP})}$ + *m*-C*H*$_{(\text{DIPP})}$), 7.07 (s, 1H, NCC*H*N$_{(\text{mesityl})}$), 7.02 (s, 2H, *m*-C*H*$_{(\text{mesityl})}$), 2.73(m, ^{3}J = 6.8 Hz, 2H, *o*-C*H*$_{(\text{DIPP})}$), 2.62 (s, 3H, C*H*$_{3(\text{imine})}$), 2.36 (s, 3H, *p*-C*H*$_{3(\text{mesityl})}$), 2.10 (s, 6H, *o*-C*H*$_{3(\text{mesityl})}$), 1.21 (d, ^{3}J = 6.8 Hz, 6H, *o*-C*H*$_{3(\text{DIPP1})}$), 1.18 (d, ^{3}J = 6.9 Hz, 6H, *o*-C*H*$_{3(\text{DIPP2})}$). ^{13}C{^{1}H} NMR (100 MHz, $CDCl_3$): δ 182.5 (d, $^{1}J_{13C\text{-}107Ag}$ = 924 Hz, d, $^{1}J_{13C\text{-}109Ag}$ = 1068 Hz), 153.3 (*C*=N), 142.0 (*C*$_{(\text{DIPP})}$), 140.3 (*p*-*C*$_{(\text{mesityl})}$), 136.7 (*o*-*C*$_{(\text{DIPP})}$),

135.7($C_{(mesityl)}$), 134.6 (o-$C_{(mesityl)}$), 129.9 (m-$CH_{(mesityl)}$), 125.1 (p-$CH_{(DIPP)}$), 123.6 (m-$CH_{(DIPP)}$), 123.1 (d, $^3J_{Ag\text{-}C}$ = 24 Hz, NCCN$_{(mesityl)}$), 119.3 (d, $^3J_{Ag\text{-}C}$ = 20 Hz, NCCN$_{(mesityl)}$), 28.7 (o-$CH_{(DIPP)}$), 23.5 (o-$CH_{3(DIPP2)}$), 23.0 (o-$CH_{3(DIPP1)}$), 21.3 (p-$CH_{3(mesityl)}$), 18.8 ($CH_{3(imine)}$), 18.1 (o-$CH_{3(mesityl)}$). Anal. Calcd. for $C_{26}H_{33}AgClN_3$: C, 58.82; H, 6.27; N, 7.92; Found (%): C, 58.40; H, 6.01; N, 7.60.

Compound 3a", Ag(C^Imine$_{Me"}$)Cl: To a solution of C^Imine$_{Me"}$·HCl **1a"** (76.9 mg, 0.188 mmol) in acetonitrile (10 mL) was added activated powdered 4Å molecular sieves and silver carbonate (51.7 mg, 0.187 mmol) at room temperature. The reaction mixture was *stirred* with *exclusion of light* for 64 h and then filtered. The filtrate was evaporated to dryness and dissolved in the minimum amount of dichloromethane, pentane was added dropwise to precipitate the product. The solid was filtered, washed with pentane and dried in vacuo to yield the product as a light brown solid (76.6 mg, 0.148 mmol, 79%).^{1}H NMR (400 MHz, $CDCl_3$) δ 8.34 (s, 1H, NCHCN$_{(DIPP)}$), 7.52 (t, ^3J = 7.8 Hz, 1H, p-C$H_{(DIPP)}$), 7.31 (d, ^3J = 7.8 Hz, 2H, m-C$H_{(DIPP)}$), 7.13 (s, 1H, NCCHN$_{(DIPP)}$), 7.11 (s, 2H, m-C$H_{(xylyl)}$), 7.02 (t, ^3J = 7.7 Hz, 1H, p-C$H_{(xylyl)}$), 2.61 (s, 3H, C$H_{3(imine)}$), 2.47 (m, ^3J = 6.8 Hz, 2H, o-C$H_{(DIPP)}$), 2.13 (s, 6H, o-C$H_{3(xylyl)}$), 1.30 (s, ^3J = 6.8 Hz, 6H, o-C$H_{3(DIPP)}$), 1.17 (s, ^3J = 6.8 Hz, 6H, o-C$H_{3(DIPP)}$). ^{13}C{^{1}H} NMR (100 MHz, $CDCl_3$): δ 182.8 (NCN), 152.2 (C=N), 145.5 (o-$C_{(DIPP)}$), 144.3 ($C_{(xylyl)}$), 134.9 ($C_{(DIPP)}$), 131.1 (p-$CH_{(DIPP)}$), 128.4 (m-$CH_{(xylyl)}$), 126.3 (o-$C_{(xylyl)}$), 124.6 (m-$CH_{(DIPP)}$), 124.4 (p-$CH_{(xylyl)}$), 124.0 (NCCN$_{(DIPP)}$), 119.1 (NCCN$_{(xylyl)}$), 28.4 (o-$CH_{(DIPP)}$), 24.6 (o-$CH_{3(DIPP)}$), 24.5 (o-

*C*H$_{3(DIPP)}$), 18.3 (*o*-*C*H$_{3(xylyl)}$ + *C*H$_{3(imine)}$). Anal. Calcd. for $C_{25}H_{31}AgClN_3$ (%): C, 58.10; H, 6.05 ; N, 8.13; Found (%): C, 57.88; H,5.84; N, 7.91.

Compound 4, Cu(C^Imine$_{Me}$)$_2$Cl: A solution of Ag(C^Imine$_{Me}$)Cl (**3a**) (321 mg, 0.677 mmol) dissolved in dichloromethane (5 mL) and was added to solid copper(I) iodide (128 mg, 0.674 mmol). The reaction mixture was stirred in the dark for 18 h. The solution was then filtered and volatiles were removed from the filtrate. The resulting solid was dissolved in a minimal amount of dichloromethane and pentane was added to crash out the product. The isolated solid was further purified by a pentane wash to give a cream-coloured solid. (178 mg, 0.465 mmol, 69% yield). Crystals suitable for X-ray diffraction study were grown at –35 ºC under nitrogen by layering pentane onto a saturated dichloromethane solution. ^{1}H NMR (400 MHz, $CDCl_3$): 8.26 (d, ^3J = 1.8 Hz, 1H, NC*H*CN$_{(mesityl)}$), 7.10 (d, ^3J = 7.4 Hz, 2H, *m*-C*H*$_{(2,6\text{-}xylyl)}$), 6.99–7.02 (m, 3H, *m*-C*H*$_{(mesityl)}$ + *p*-C*H*$_{(2,6\text{-}xylyl)}$), 6.98 (d, ^3J = 1.9 Hz, 1H, NCC*H*N$_{(mesityl)}$), 2.69 (s, 3H, C*H*$_{3(imine)}$), 2.35 (s, 3H, *p*-C*H*$_{3(mesityl)}$), 2.11 (s, 6H, *o*-C*H*$_{3(mesityl)}$), 2.10 (s, 6H, *o*-C*H*$_{3(2,6\text{-}xylyl)}$). ^{13}C{^{1}H} NMR (100 MHz, $CDCl_3$): 178.6 (*C*-Cu), 152.1 (*C*=N), 144.3 (*C*$_{(2,6\text{-}xylyl)}$), 139.8 (*p*-*C*$_{(mesityl)}$), 135.2 (*o*-*C*$_{(mesityl)}$), 134.3 (*C*$_{(mesityl)}$), 129.6 (*m*-CH$_{(mesityl)}$), 128.2 (*m*-*C*H$_{(2,6\text{-}xylyl)}$), 126.2 (*o*-*C*$_{(2,6\text{-}xylyl)}$), 124.1 (*p*-*C*H$_{(2,6\text{-}xylyl)}$), 122.5 (NC*C*N$_{(mesityl)}$), 118.3 (N*C*CN$_{(mesityl)}$), 21.0 (*p*-*C*H$_{3(mesityl)}$), 18.5 (*C*H$_{3(imine)}$ 18.0 (*o*-*C*H$_{3(2,6\text{-}xylyl)}$), 17.9 (*o*-*C*H$_{3(mesityl)}$). FTIR (KBr) $\nu_{C=N}$ 1678 cm^{-1}. HRMS (ESI$^+$, Methanol) Calculated for $C_{44}H_{50}CuN_6Cl$, m/z = 725.3393 [M – Cl]$^+$; Found: 725.3344 [M – Cl]$^+$.

Compound 5a, [Cu(C^Imine$_{Me}$)I]$_2$: Sodium bis(trimethylsilyl)amide (1.16 g, 6.34 mmol) was dissolved in THF (5 mL) and added dropwise to a THF (5 mL) suspension of copper(I) iodide (1.21 g, 6.34 mmol) at a –35 °C. The reaction mixture was gradually warmed to room temperature and subsequently stirred for an additional hour. To this reaction mixture was then added dropwise a THF (5 mL) suspension of **1a** (2.33 g, 6.34 mmol) at –35 °C. The reaction mixture was gradually warmed to room temperature and stirred for an additional 4 h. The mixture was filtered and the filtrate was concentrated to about 5 mL. Pentane was added to precipitate a yellow solid. The solid was collected by filtration and further washed with pentane to give the desired product as a yellow solid. Yield: 2.67 g, 5.14 mmol, 81%. Crystals suitable for X-ray diffraction studies were grown at –35 °C under nitrogen by layering pentane onto a saturated dichloromethane solution. ^{1}H NMR (400 MHz, $CDCl_3$): δ 8.19 (s, 1H, NC*H*CN$_{(mesityl)}$), 7.09 (d, ^3J = 7.5 Hz, 2H, *m*-C*H*$_{(2,6\text{-}xylyl)}$), 6.98 (t, ^3J = 7.5 Hz, 1H, *p*-C*H*$_{(2,6\text{-}xyly)}$), 6.87 (s, 2H, *m*-C*H*$_{(mesityl)}$), 6.83 (s, 1H, NCC*H*N$_{(mesityl)}$), 2.46 (br s, 3H, C*H*$_{3(imine)}$), 2.15 (s, 3H, *p*-C*H*$_{3(mesityl)}$), 2.10 (s, 6H, *o*-C*H*$_{3(mesityl)}$), 2.07 (s, 6H, *o*-C*H*$_{3(2,6\text{-}xylyl)}$). ^{13}C{^{1}H} NMR (100 MHz, $CDCl_3$): 186.0 (N*C*N), 153.6 (*C*=N), 145.2 (*C*$_{(2,6\text{-}xylyl)}$), 139.4 (*p*-*C*$_{(mesityl)}$), 135.8 (*C*$_{(mesityl)}$), 135.2 (*o*-*C*$_{(mesityl)}$), 129.4 (*m*-*C*H$_{(mesityl)}$), 128.2 (*m*-*C*H$_{(2,6\text{-}xylyl)}$), 126.8 (*o*-*C*$_{(2,6\text{-}xylyl)}$), 123.9 (*p*-*C*H$_{(2,6\text{-}xylyl)}$), 122.0 (NC*C*N$_{(mesityl)}$), 117.8 (N*C*CN$_{(mesityl)}$), 21.0 (*p*-*C*H$_{3(mesityl)}$), 18.5 (*o*-*C*H$_{3(2,6\text{-}xylyl)}$), 18.5 (*o*-*C*H$_{3(mesityl)}$), 18.5 (*C*H$_{3(imine)}$ unobserved because of overlap with other carbon resonances but predicted from correlation observed in ^{1}H-^{13}C HSQC spectra). FTIR (cast film): $\nu_{C=N}$ 1678 cm^{-1}. Anal. Calcd for $C_{22}H_{25}N_3CuI$ (%): C, 50.63; H, 4.83; N, 8.05. Found (%): C, 50.38; H, 4.90; N, 7.76.

Compound 5b, [Cu(C^Imine$_{t\text{-Bu}}$)I]$_2$: C^Imine$_{t\text{-Bu}}$ (**1b**) (79.6 mg, 0.213 mmol) was dissolved in THF (1.5 mL) and added to a suspension of copper(I) iodide (40.6 mg, 0.213 mmol) in THF (1.5 mL). The reaction mixture was stirred for 4 h. The solution was then filtered and volatiles were removed under vacuum. The resulting solid was washed with pentane to give the desired product as a beige solid. Yield: 114 mg, 0.202 mmol, 95%. Crystals suitable for X-ray diffraction studies were grown at –35 °C under nitrogen by layering pentane onto a saturated dichloromethane solution. ^{1}H NMR (400 MHz, $CDCl_3$): δ 6.90 (s, 2H, *m*-C*H*$_{(mesityl)}$), 6.89 (s, 1H, NC*H*CN$_{(mesityl)}$), 6.87 (s, 2H, *m*-C*H*$_{(2,6\text{-xylyl})}$), 6.81 (m, 1H, *p*-C*H*$_{(2,6\text{-xylyl})}$), 6.69 (d, ^3J = 1.8 Hz, 1H, NCC*H*N$_{(mesityl)}$), 2.29 (s, 3H, *p*-C*H*$_{3(mesityl)}$), 2.28 (s, 6H, *o*-C*H*$_{3(2,6\text{-xylyl})}$), 1.75 (s, 6H, *o*-C*H*$_{3(mesityl)}$), 1.58 (s, 9H, C(C*H*$_3$)$_{3(imine)}$). ^{13}C{^{1}H} NMR (100 MHz, $CDCl_3$): δ 178.8 (N*C*N$_{(mesityl)}$), 159.9 (*C*=N), 144.5 (*C*$_{(2,6\text{-xylyl})}$), 139.8 (*p*-*C*$_{(mesityl)}$), 134.6 (*o*-*C*$_{(mesityl)}$), 134.5 (*C*$_{(mesityl)}$), 129.5 (*m*-*C*H$_{(mesityl)}$), 128.0 (*m*-*C*H$_{(2,6\text{-xylyl})}$), 125.5 (*o*-*C*$_{(2,6\text{-xylyl})}$), 124.1 (*p*-*C*H$_{(2,6\text{-xylyl})}$), 120.7 (NC*C*N$_{(mesityl)}$), 119.7 (N*C*CN$_{(mesityl)}$), 40.6 (*C*(CH$_3$)$_{3(imine)}$), 29.7 (C(*C*H$_3$)$_{3(imine)}$), 21.3 (*p*-*C*H$_{3(mesityl)}$), 20.0 (*o*-*C*H$_{3(2,6\text{-xylyl})}$), 17.5 (*o*-*C*H$_{3(mesityl)}$). FTIR (cast film): $\nu_{C=N}$ 1664 cm^{-1}. Anal. Calcd for $C_{25}H_{31}N_3CuI$ (%): C, 53.24; H, 5.54; N, 7.45. Found (%): C, 52.55; H, 5.56; N, 7.35. HRMS (ESI$^+$, CH_2Cl_2) Calculated for $C_{50}H_{62}Cu_2I_2N_6$, *m/z* = 1126.1717 [M]$^+$; Found: 1126.1685 [M]$^+$.

Compound 6a, Au(C^Imine$_{Me}$)Cl: A solution of (C^Imine$_{Me}$)AgCl (**3a**) (177 mg, 0.374 mmol) in dichloromethane (3 mL) was added to a solution of Au(SMe$_2$)Cl (110 mg, 0.374 mmol) in dichloromethane (5 mL). The resulting mixture was stirred for 30 min,

and subsequently filtered through Celite. The filtrate was evaporated to dryness under reduced pressure and taken up in a minimum amount of THF. The product was isolated as a beige solid by pentane-induced precipitation (179 mg, 0.318 mmol, 85%). ^{1}H NMR (400 MHz, $CDCl_3$): δ = 8.26 (d, ^{3}J = 1.8 Hz, 1 H, NC*H*CN$_{(mesityl)}$), 7.10 (d, ^{3}J = 7.6 Hz, 2 H, *m*-C*H*$_{(2,6\text{-xylyl})}$), 7.03–6.99 (m, 4 H, *p*-C*H*$_{(2,6\text{-xylyl})}$ + *m*-C*H*$_{(mesityl)}$ + NCC*H*N$_{(mesityl)}$), 2.82 (s, 3 H, C*H*$_{3(imine)}$), 2.35 (s, 3 H, *p*-C*H*$_{3(mesityl)}$), 2.10 ppm (s, 12 H, *o*-C*H*$_{3(2,6\text{-xylyl})}$ + *o*-C*H*$_{3(mesityl)}$); ^{13}C NMR (100 MHz, $CDCl_3$): δ = 172.5 (N*C*N), 153.1 (*C*=N), 144.5 (*C*$_{ipso(2,6\text{-xylyl})}$), 140.2 (*p*-*C*$_{(mesityl)}$), 135.3 (*C*$_{ipso(mesityl)}$), 134.7 (*o*-*C*$_{(mesityl)}$), 129.8 (*m*-*C*H$_{(mesityl)}$)), 128.5 (*m*-*C*H$_{(2,6\text{-xylyl})}$), 126.3 (*o*-*C*$_{(2,6\text{-xylyl})}$), 124.5 (*p*-*C*H$_{(2,6\text{-xylyl})}$), 122.3 (NC*C*N$_{(mesityl)}$), 119.5 (N*C*CN$_{(mesityl)}$), 21.3 (*p*-*C*H3$_{(mesityl)}$), 19.9 (*C*H3$_{(imine)}$), 18.3 (*o*-*C*H3$_{(2,6\text{-xylyl})}$), 18.2 ppm (*o*-*C*H3$_{(mesityl)}$); FTIR (cast film) $\nu_{C=N}$ 1683 cm^{-1}; Anal. Calcd for for $C_{22}H_{25}AuClN_3$ (%): C 46.86, H 4.47, N 7.45; Found (%): C 47.12, H 4.50, N 7.19.

Compound 6b, Au(C^Imine$_{t\text{-Bu}}$)Cl: C^Imine$_{t\text{-Bu}}$ (**1b**) (122 mg, 0.326 mmol) was dissolved in toluene (6 mL), and solid dimethylsulfidegold(I) chloride (96.1 mg, 0.326 mmol) was added in small portions. The reaction mixture was stirred for 2 h at room temperature. Excess solvent was removed under vacuum. The sample was then dissolved in a minimal amount of THF, filtered through a plug of Celite and pentane was added to the filtrate to precipitate the product. The product was isolated by filtration and washed with pentane to give **6** as an off-white solid (156 mg, 0.258 mmol, 79%). Crystals suitable for X-ray diffraction studies were grown at room temperature under nitrogen by layering pentane onto a saturated THF solution. ^{1}H NMR (400 MHz, C_6D_6): δ = 6.79 (s +

br, 2 H, *m*-C*H*$_{(2,6\text{-xylyl})}$), 6.73 (t, ^{3}J = 6.8 Hz, 1 H, *p*-C*H*$_{(2,6\text{-xylyl})}$), 6.51 (s, 2 H, *m*-C*H*$_{(\text{mesityl})}$), 6.18 (d, ^{3}J = 1.8 Hz, 1 H, NC*H*CN$_{(\text{mesityl})}$), 5.68 (d, ^{3}J = 1.8 Hz, 1 H, NCC*H*N$_{(\text{mesityl})}$), 2.74 (s + br, 3 H, *o*-C*H*$_{3(\text{mesityl})}$), 1.96 (s, 3 H, *p*-C*H*$_{3(\text{mesityl})}$), 1.77 (s + br, 6 H, *o*-C*H*$_{3(2,6\text{-xylyl})}$), 1.38 (s, 9 H, C(C*H*$_3$)$_{3(\text{imine})}$), 1.33 ppm (s + br, 3 H, *o*-C*H*$_{3(\text{mesityl})}$); ^{13}C NMR (100 MHz, C_6D_6): δ = 172.7 (N*C*N), 158.9 (*C*=N), 144.6 (*C*$_{(2,6\text{-xylyl})}$), 139.7 (*p*-*C*$_{(\text{mesityl})}$), 134.8 (*o*-*C*$_{(\text{mesityl})}$), 134.9 (*C*$_{(\text{mesityl})}$), 129.5 (*m*-*C*H$_{(\text{mesityl})}$), 128.9 (*m*-*C*H$_{(2,6\text{-xylyl})}$), 127.7 (*m*-*C*H$_{(2,6\text{-xylyl})}$), 124.2 (*p*-*C*H$_{(2,6\text{-xylyl})}$), 120.0 (NC*C*N$_{(\text{mesityl})}$), 119.4 (N*C*CN$_{(\text{mesityl})}$), 41.1 (*C*(CH$_3$)$_3$), 29.7 (C(*C*H$_3$)$_3$), 21.2 (*p*-*C*H$_{3(\text{mesityl})}$ + *o*-*C*H$_{3(\text{mesityl})}$), 18.5 (*o*-*C*H$_{3(2,6\text{-xylyl})}$), 17.5 (*o*-*C*H$_{3(2,6\text{-xylyl})}$), 17.0 ppm (*o*-*C*H$_{3(\text{mesityl})}$); FTIR (cast film): $\nu_{C=N}$ 1664 cm^{-1}; Anal. Calcd for $C_{50}H_{62}N_6Au_2Cl_2$ (%): C 49.55, H 5.16, N 6.93; Found (%): C 49.7, H 4.93, N 6.68.

Compound 8, Ni(C^Imine$_{Me}$)$_2$Cl$_2$: A THF (12 mL) suspension of 1-(1-(2,6-dimethylphenylimino)ethyl)-3-(2,4,6-trimethylphenyl)imidazolium chloride (**1a**) (246 mg, 0.669 mmol) was added dropwise to a THF (4 mL) suspension of Ni(COD)$_2$ (91.6 mg, 0.333 mmol). The reaction mixture was stirred for 4 h, resulting in a color change from a milky yellow to deep red. The mixture was filtered through a plug of Celite and the solution was dried under vacuum to give an orange-red solid. Further purification was achieved by recrystallization by dissolving the solid in a minimal amount of dichloromethane and adding a layer of pentane. The solution was stored at –35 °C for overnight, resulting in the formation of reddish orange crystals. The mother liquor was decanted off, the solid was washed with pentane (2 × 6 mL). The crystals were crushed

into a fine powder and the sample was dried under reduced pressure to give a reddish orange solid. Yield: 174.5 mg, 0.220 mmol, 66%. Crystals suitable for X-ray diffraction studies were grown at room temperature under nitrogen by slow vapor diffusion of pentane into a saturated dichloromethane solution. ^{1}H NMR (400 MHz, $CDCl_3$): δ 8.02 (s, 1H, NC*H*CN$_{(mesityl)}$), 7.23 (s, 2H, *m*-C*H*$_{(2,6\text{-xylyl})}$), 7.13 (t, ^{3}J = 7.1 Hz, 1H, *p*-C*H*$_{(2,6\text{-xyly})}$), 7.03 (s, 2H, *m*-C*H*$_{(mesityl)}$), 6.66 (s, 1H, NCC*H*N$_{(mesityl)}$), 3.70 (s, 3H, C*H*$_{3(imine)}$), 2.27 (s, 6H, *o*-C*H*$_{3(mesityl)}$), 2.17 (s, 3H, *p*-C*H*$_{3(mesityl)}$), 2.16 (s, 6H,*o*-C*H*$_{3(2,6\text{-xylyl})}$). ^{13}C{^{1}H} NMR (100 MHz, $CDCl_3$): 168.8 (N*C*N), 155.6 (*C*=N), 145.8 (*C*$_{(2,6\text{-xylyl})}$), 139.7 (*p*-*C*$_{(mesityl)}$), 137.5 (*o*-*C*$_{(mesityl)}$), 136.3 (*C*$_{(mesityl)}$), 129.4 (*m*-*C*H$_{(mesityl)}$), 128.1 (*m*-*C*H$_{(2,6\text{-xylyl})}$), 127.0 (*o*-*C*$_{(2,6\text{-xylyl})}$), 123.7 (*p*-*C*H$_{(2,6\text{-xylyl})}$), 123.0 (NC*C*N$_{(mesityl)}$), 120.0 (N*C*CN$_{(mesityl)}$), 20.9 (*p*-*C*H$_{3(mesityl)}$), 20.6 (*C*H$_{3(imine)}$), 19.10 (*o*-*C*H$_{3(mesityl)}$), 18.3 (*o*-*C*H$_{3(2,6\text{-xylyl})}$). FTIR (cast film): $\nu_{C=N}$ 1674 cm^{-1}. Anal. Calcd for $C_{44}H_{50}Cl_2N_6Ni$ (%): C, 66.68; H, 6.36; N, 10.60. Found (%): C, 66.40; H, 6.17; N, 10.42.

Compound 9, Zn(C^Imine$_{Me}$)Cl$_2$: Sodium bis(trimethylsilyl)amide (1.16 g, 6.34 mmol) was dissolved in THF (5 mL) and added dropwise to a THF (5 mL) suspension of zinc(II) chloride (1.21 g, 6.34 mmol) at a temperature of -35 °C. The reaction mixture was gradually warmed to room temperature and subsequently stirred for 1 h. To this reaction mixture, was then added dropwise a THF (5 mL) suspension of 1-(1-(2,6-dimethylphenylimino)ethyl)-3-(2,4,6-trimethylphenyl)-imidazolium chloride (**1a**) (2.33 g, 6.34 mmol) at –35 °C. The reaction mixture was gradually warmed to room temperature and stirred for an additional 4 h. The mixture was filtered and the filtrate was

concentrated to about 5 mL. Pentane was added to precipitate a yellow solid, which was further washed with pentane to give a white solid. Yield: 191.2 mg, 4.94 mmol, 78%. ^{1}H NMR (400 MHz, $CDCl_3$): δ 7.79 (d, ^{3}J = 1.6 Hz, 1H, NC*H*CN$_{(mesityl)}$), 7.12 (d, ^{3}J = 1.8 Hz, 1H, NCC*H*N$_{(mesityl)}$), 7.04 (m, 3H, *p*-C*H*$_{(2,6\text{-}xylyl)}$ + *m*-C*H*$_{(2,6\text{-}xylyl)}$), 6.98 (s, 2H, *m*-C*H*$_{(mesityl)}$), 2.34 (s, 3H, C*H*$_{3(imine)}$), 2.33 (s, 3H, *p*-C*H*$_{3(mesityl)}$), 2.28 (s, 6H,*o*-C*H*$_{3(2,6\text{-}xylyl)}$), 2.13 (s, 6H, *o*-C*H*$_{3(mesityl)}$). ^{13}C{^{1}H} NMR (100 MHz, $CDCl_3$): 178.5 (N*C*N), 157.3 (*C*=N), 141.4 (*C*$_{(2,6\text{-}xylyl)}$), 140.5 (*p*-*C*$_{(mesityl)}$), 134.5 (*o*-*C*$_{(mesityl)}$), 134.1 (*C*$_{(mesityl)}$), 129.7 (*m*-*C*H$_{(mesityl)}$)), 129.5 (*o*-*C*$_{(2,6\text{-}xylyl)}$), 128.8 (*m*-*C*H$_{(2,6\text{-}xylyl)}$), 126.6 (*p*-*C*H$_{(2,6\text{-}xylyl)}$), 125.8 (NC*C*N$_{(mesityl)}$), 118.4 (N*C*CN$_{(mesityl)}$), 21.2 (*p*-*C*H$_{3(mesityl)}$), 18.9 (*o*-*C*H$_{3(2,6\text{-}xylyl)}$), 18.0 (*o*-*C*H$_{3(mesityl)}$), 15.4 (*C*H$_{3(imine)}$). FTIR (cast-DCM) $\nu_{C=N}$ 1653 cm^{-1}. Anal. Calcd for $C_{22}H_{25}N_3Cl_2Zn$ (%): C, 56.49; H, 5.39; N, 8.98. Found (%): C, 56.20; H, 5.12; N, 9.25.

Compound 10, Fe(C^Imine$_{Me}$)Cl$_2$: Sodium bis(trimethylsilyl)amide (164 mg, 0.892 mmol) was dissolved in THF (4 mL) and added dropwise to a THF (4 mL) suspension of iron(II) chloride (113 mg, 0.893 mmol) at a temperature of -35 °C. The reaction mixture was gradually warmed to room temperature and subsequently stirred for 1 h. To this reaction mixture, was then added dropwise a THF (6 mL) suspension of imidazolium salt **1a** (329 mg, 0.893 mmol) at -35 °C and an additional 5 mL of THF was added. The reaction mixture was gradually warmed to room temperature and stirred for an additional 4 h. The mixture was filtered twice through Celite and the filtrate was concentrated down. Pentane was added to precipitate a yellow solid which was further washed with pentane, toluene and twice with ether, then was dried under reduced pressure. Yield: 287 mg, .624

mmol, 70%. FTIR (cast-DCM) $\nu_{C=N}$ 1650 cm^{-1}. Anal. Calcd for $C_{22}H_{25}N_3Cl_2Fe$ (%): C, 57.67; H, 5.50; N, 9.17. Found (%): C, 57.55; H, 5.34; N, 8.89. For elemental analysis, further purification of the sample was achieved by recrystallization by dissolving the solid in a minimal amount of THF and adding a layer of pentane. The solution was stored at -35° for overnight, resulting in the formation of fine needle-like yellow crystals. The mother liquor was decanted off, the solid was washed with pentane and the crystals were dried under reduced pressure to give a yellow solid.

Compound 11, Co(C^Imine$_{Me}$)Cl$_2$: Sodium bis(trimethylsilyl)amide (108 mg, 0.590 mmol) was dissolved in THF (4 mL) and added dropwise to a THF (4 mL) suspension of cobalt(II) chloride (76.5 mg, 0.589 mmol) at a temperature of –35 °C. The reaction mixture was gradually warmed to room temperature and subsequently stirred for 1 h. To this reaction mixture, was then added dropwise a THF (8 mL) suspension of imidazolium salt **1a** (217 mg, 0.589 mmol) at –35 °C. The reaction mixture was gradually warmed to room temperature and stirred for an additional 4 h. The mixture was filtered twice through Celite and the filtrate was dried under reduced pressure. Pentane was added to wash the blue solid which was then dried under reduced pressure. The solid that was recovered from the first filtration was washed with 10 mL of dichloromethane, filtered through Celite and dried under reduced pressure. The solid from the dichloromethane fraction was washed with pentane and combined with the blue solid of the THF filtrate fraction. Yield: 186 mg, .400 mmol, 68%. FTIR (cast-DCM) $\nu_{C=N}$ 1652 cm^{-1}. Anal.

Calcd for $C_{22}H_{25}N_3Cl_2Co$ (%): C, 57.28; H, 5.46; N, 9.11. Found (%): C, 57.37; H, 5.19; N, 8.95.

Compound 12a, Ni(C^Imine$_{Me}$)Br$_2$: Complex **5a** (298 mg, 0.285 mmol) was dissolved in THF (4 mL) and added dropwise to a THF (8 mL) suspension of $NiBr_2$(DME) (176 mg, 0.570 mmol). The mixture was stirred for 18 h at room temperature, filtered through a plug of Celite. The filtrate was collected and the volatiles removed in vacuo give an orange-brown solid. The solid was further purified by recrystallization from dichloromethane and pentane at –35 °C. Yield: 183.5 mg, 0.331 mmol, 58%. Crystals suitable for X-ray diffraction studies were grown at room temperature under nitrogen by slow vapor diffusion of pentane into a saturated dichloromethane solution. FTIR (cast film): $\nu_{C=N}$ 1646 cm^{-1}. Anal. Calcd for $C_{22}H_{25}Br_2N_3Ni$ (%): C, 48.05; H, 4.58; N, 7.64. Found (%): C, 47.82; H, 4.31; N, 7.50.

Compound 12b, Ni(C^Imine$_{t\text{-}Bu}$)Br$_2$: Complex **5b** (528 mg, 0.468 mmol) was dissolved in THF (10 mL) and added dropwise to a THF (10 mL) suspension of $NiBr_2$(DME) (288 mg, 0.933 mmol). The mixture was allowed to stir at room temperature for 27 h, filtered and the solution was concentrated to 4 mL and pentane was added to precipitate the product. The solid was further washed with pentane (3 × 6 mL) and dried under reduced pressure to give a brown solid. Yield: 522 mg, 0.877 mmol, 94%. Crystals suitable for X-ray diffraction studies were grown at room temperature under nitrogen by slow vapor diffusion of pentane into a saturated dichloromethane solution. FTIR (cast film): $\nu_{C=N}$

1616 cm^{-1}. Anal. Calcd for $C_{25}H_{31}Br_2N_3Ni$ (%): C, 50.72; H, 5.28; N, 7.10. Found (%): C, 50.45; H, 4.99; N, 6.87.

Compound 13, Ni(C^Imine$_{Me}$)$_2$Br$_2$: A solution of [(C^Imine$_{Me}$)CuI]$_2$ **5a** (44.5 mg, 0.0426 mmol) in THF (6 mL) was added dropwise to a THF (4 mL) suspension of $NiBr_2$(DME) (13.3 mg, 0.0431 mmol). The mixture was allowed to stir for 2 h at room temperature. The resulting solution was filtered through a plug of Celite. The volume of the solution was reduced to 2 mL and was pentane was added to crash out the product. The isolated solid was further purified by a pentane wash and dried under reduced pressure to give an orange solid. Yield: 26.2 mg, 0.0298 mmol, 70%. Crystals suitable for X-ray diffraction studies were grown at room temperature under nitrogen by slow vapor diffusion of pentane into a saturated tetrahydrofuran solution. ^{1}H NMR (400 MHz, C_6D_6): δ 7.87 (s, 1H, NC*H*CN$_{(mesityl)}$), 6.94-6.90 (m, 3H, *m*-C*H*$_{(2,6\text{-xylyl})}$ and *m*-C*H*$_{(2,6\text{-xylyl})}$), 6.62 (s, 2H, *m*-C*H*$_{(mesityl)}$), 5.86 (s, 1H, NCC*H*N$_{(mesityl)}$), 2.43 (s, 3H, C*H*$_{3(imine)}$), 2.06 (s, 6H, *o*-C*H*$_{3(mesityl)}$), 1.91 (s, 3H, *p*-C*H*$_{3(mesityl)}$), 1.89 (s, 6H, *o*-C*H*$_{3(2,6\text{-xylyl})}$). ^{13}C{^{1}H} NMR (100 MHz, C_6 D_6): 153.7 (*C*=N), 145.51 (*C*$_{(2,6\text{-xylyl})}$), 139.3 (*p*-*C*$_{(mesityl)}$), 135.53 (*o*-*C*$_{(mesityl)}$), 129.4 (*m*-*C*H$_{(mesityl)}$), 128.2 (*m*-*C*H$_{(2,6\text{-xylyl})}$), 127.2 (*o*-*C*$_{(2,6\text{-xylyl})}$), 123.9 (*p*-*C*H$_{(2,6\text{-xylyl})}$), 121.5 (NC*C*N$_{(mesityl)}$), 117.3 (N*C*CN$_{(mesityl)}$), 20.6 (*p*-*C*H$_{3(mesityl)}$), 17.9 (*o*-*C*H$_{3(mesityl)}$), 17.8 (*o*-*C*H$_{3(2,6\text{-xylyl})}$). 17.7 (*C*H$_{3(imine)}$). The poor solubility of the compound precluded the observation of resonances for the carbenoid and the mesityl ring ipso carbon nuclei. FTIR (cast film): $\nu_{C=N}$1676 cm^{-1}. Anal. Calcd for $C_{44}H_{50}Br_2N_6Ni$ (%): C, 59.96; H, 5.72; N, 9.53. Found (%): C, 60.04; H, 5.56; N, 9.79.

Compound 14, Ni(C^Imine$_{t\text{-Bu}}$)COD: A solution of C^Imine$_{t\text{-Bu}}$ (**2b**) (165 mg, 0.441 mmol) in toluene (6 mL) and was added to a solution of bis-(1,5-cyclooctadiene)nickel(0) (121 mg, 0.441 mmol) in toluene (6 mL). The reaction mixture was stirred at room temperature overnight. The reaction mixture was filtered through a plug of Celite and volatiles were removed under reduced pressure to give a dark purple solid. A minimal amount of pentane was added and the sample was placed in the freezer (–35°C) overnight which resulted in formation of a crystalline dark purple. Excess pentane was carefully removed and the sample was dried under vacuum (194 mg, 0.359 mmol, 81%). Crystals suitable for X-ray diffraction were grown from a concentrated pentane solution that was cooled overnight at –35°C. ^{1}H NMR (400 MHz, $CDCl_3$): δ 7.28 (s, 1H, NC*H*CN$_{(mesityl)}$), 7.03 (d, ^{3}J = 7.1 Hz, 2H, *m*-C*H*$_{(2,6\text{-xylyl})}$), 6.98 (t, ^{3}J = 7.1 Hz, 1H, *p*-C*H*$_{(2,6\text{-xylyl})}$), 6.87 (s, 2H, *m*-C*H*$_{(mesityl)}$), 6.34 (s, 1H, NCC*H*N$_{(mesityl)}$), 4.46 (m, 2H, C*H*$_{COD}$), 3.53(m, 2H, C*H*$_{COD}$), 2.20 (s, 6H, *o*-C*H*$_{3(mesityl)}$), 2.16 (s, 3H, *p*-C*H*$_{3(mesityl)}$), 2.12 (s, 6H, *o*-C*H*$_{3(2,6\text{-xylyl})}$), 2.06 (m, 4H, C*H*$_{COD}$), 1.76 (m, 4H, C*H*$_{COD}$), 1.03 (s, 9H, C(C*H*$_3$)$_{3(imine)}$). ^{13}C{^{1}H} NMR (100 MHz, $CDCl_3$): δ 202.1 (N*C*N$_{(mesityl)}$), 150.8 (*C*$_{ipso(2,6\text{-xylyl})}$), 144.9 (*C*=N), 138.8 (*C*$_{ipso(mesityl)}$), 138.1 (*p*-*C*$_{(mesityl)}$), 136.6 (*o*-*C*$_{(mesityl)}$), 129.1 (*m*-*C*H$_{(mesityl)}$), 128.8 (*o*-*C*$_{(2,6\text{-xylyl})}$), 127.8 (*m*-*C*H$_{(2,6\text{-xylyl})}$), 122.8 (*p*-*C*H$_{(2,6\text{-xylyl})}$), 122.3 (NC*C*N$_{(mesityl)}$), 114.6 (N*C*CN$_{(mesityl)}$), 81.6 (*C*H$_{COD}$), 79.3 (*C*H$_{COD}$), 39.9 (*C*(CH$_3$)$_{3(imine)}$), 31.6 (*C*H$_{COD}$), 30.9 (*C*H$_{COD}$), 28.5 (C(*C*H$_3$)$_{3(imine)}$), 22.7 (*p*-*C*H$_{3(mesityl)}$), 18.8 (*o*-*C*H$_{3(2,6\text{-xylyl})}$), 18.2 (*o*-*C*H$_{3(mesityl)}$). Anal. Calcd for $C_{33}H_{43}N_3Ni$ (%): C, 73.34; H, 8.02; N, 7.78. Found (%): C, 73.08; H, 7.74; N, 8.05.

Compound 15a, [Pd(C^Imine$_{Me}$)(η^3-C_3H_5)]BF_4: A solution of palladium allyl chloride dimer (88.6 mg, 0.242 mmol) in THF (8 mL) was added to a suspension of silver tetrafluoroborate (94.8 mg, 0.487 mmol) in THF (2 mL). Upon addition, the solution immediately became cloudy and the formation of a white precipitate was observed. The solution was left to stir for an additional 15 min and was then filtered through celite. A solution of (C^Imine$_{Me}$)AgCl (**3a**) (230 mg, 0.484 mmol) in THF (6 mL) was added dropwise to the cationic palladium precursor. The resulting reaction mixture was left to stir for 4 h. The solution was then filtered through celite, the solvent was concentrated down and pentane was added to precipitate the product. The solid was collected and further washed with pentane and dried under reduced pressure to give a pale beige/brown solid. Yield: 228 mg, 0.358 mmol, 74%. ^{1}H NMR (400 MHz, $CDCl_3$): δ 8.23 (d, ^3J = 1.7 Hz, 1H, NC*H*CN$_{(mesityl)}$), 7.15-7.11 (m, 4H, *p*-C*H*$_{(2,6\text{-xylyl})}$ + *m*-C*H*$_{(2,6\text{-xylyl})}$ + NCC*H*N$_{(mesityl)}$), 7.04 (s, 2H, *m*-C*H*$_{(mesityl)}$), 5.29-5.19 (m, 1H, allyl CH_2CHCH_2), 3.42 ppm (d + br, $^3J^{syn}_{H\text{-}H}$ = 7.7 Hz, 1H, allyl C$_{(trans\ to\ carbene)}$H$_{anti}$H$_{syn}$), 3.04 (d, $^3J^{anti}_{H\text{-}H}$ = 14.0 Hz, 1H, allyl C$_{(trans\ to\ carbene)}$H$_{anti}$H$_{syn}$), 2.76 (m, 1H, allyl C$_{(trans\ to\ imine)}$H$_{anti}$H$_{syn}$), 2.55 (s, 3H, C*H*$_{3(imine)}$), 2.38 (s, 3H, *p*-C*H*$_{3(mesityl)}$), 2.26 (s + br, 4H, *o*-C*H*$_{3(xylxyl)}$ + allyl C$_{(trans\ to\ imine)}$H$_{anti}$H$_{syn}$, splitting pattern is not observed as there is overlap from resonance from one *ortho*-C*H*$_3$ group from xylyl ring), 2.12 (s, 6H, *o*-C*H*$_{3(xylxyl)}$ + *o*-C*H*$_{3(mesityl)}$), 2.02 (s, 3H, *o*-C*H*$_{3(mesityl)}$). ^{13}C{^{1}H} NMR (100 MHz, $CDCl_3$): δ 183.3 (N*C*N), 165.5(*C*=N), 145.2 (*C*$_{(2,6\text{-xylyl})}$), 140.4 (*p*-*C*$_{(mesityl)}$), 135.4 (*C*$_{(mesityl)}$), 134.6 (*o*-*C*$_{(mesityl)}$), 134.3 (*o*-*C*$_{(mesityl)}$), 129.5 (*m*-*C*H$_{(mesityl)}$), 129.4 (*m*-*C*H$_{(mesityl)}$), 129.0 (*m*-*C*H$_{(2,6\text{-xylyl})}$), 128.9 (*m*-*C*H$_{(2,6\text{-xylyl})}$), 128.74 (*o*-*C*$_{(2,6\text{-xylyl})}$), 129.70 (*o*-*C*$_{(2,6\text{-xylyl})}$), 127.0 (*p*-*C*H$_{(2,6\text{-xylyl})}$), 124.0 (NC*C*N$_{(mesityl)}$),

120.9 (N*C*CN$_{(mesityl)}$), 119.9 (allyl CH$_2$*C*HCH$_2$), 72.6 (allyl *C*$_{(trans\ to\ carbene)}$H$_2$CHCH$_2$), 50.3 (CH$_2$CH*C*$_{(trans\ to\ imine)}$H$_2$), 21.3 (*p*-*C*H$_{3(mesityl)}$), 18.4 (*o*-*C*H$_{3(2,6\text{-}xylyl)}$), 18.0 (*o*-*C*H$_{3(mesityl)}$), 14.4 (*o*-*C*H$_{3(imine)}$). Anal. Calcd for $C_{25}H_{30}BF_4N_3Pd$ (%): C, 53.07; H, 5.34; N, 7.43. Found (%): C, 52.84; H, 5.55; N, 7.15.

Compound 15b, [Pd(C^Imine$_{t\text{-}Bu}$)(η^3-C$_3$H$_5$)]BF$_4$: A solution of palladium allyl chloride dimer (60.6 mg, 0.166 mmol) in THF (6 mL) was added to a suspension of silver tetrafluoroborate (65.0 mg, 0.334 mmol) in THF (2 mL). Upon addition, the solution immediately became cloudy and the formation of a white precipitate was observed. The solution was left to stir for an additional 15 min and was then filtered through celite. A solution of carbene **2b** (124 mg, 0.333 mmol) in THF (4 mL) was added dropwise to the cationic palladium precursor. The resulting reaction mixture was left to stir for 1.5 h. The solution was then filtered, the solvent was concentrated down to 4 mL and pentane was added to precipitate the product. The solid was collected and further washed pentane and dried under reduced pressure to give a pale beige solid. Yield: 179 mg, 0.293 mmol, 88%. ^{1}H NMR (400 MHz, $CDCl_3$): δ 8.45 (d, ^3J = 2.2 Hz, 1H, NC*H*CN$_{(mesityl)}$), 7.32 (d, ^3J = 1.9 Hz, 1H, NCC*H*N$_{(mesityl)}$),7.08-7.04 (m, 3H, *p*-C*H*$_{(2,6\text{-}xylyl)}$ + *m*-C*H*$_{(2,6\text{-}xylyl)}$), 7.01 (s, 2H, *m*-C*H*$_{(mesityl)}$), 5.29-5.18 (m, 1H, allyl CH$_2$C*H*CH$_2$), 2.98 (d, $^3J^{anti}_{H\text{-}H}$ = 14.1 Hz, 1H, allyl C$_{(trans\ to\ carbene)}$*H*$_{anti}$H$_{syn}$), 2.87 ppm (dd, $^3J^{syn}_{H\text{-}H}$ = 8.0 Hz, $^2J_{H\text{-}H}$ = 1.4 Hz, 1H, allyl C$_{(trans\ to\ carbene)}$H$_{anti}$*H*$_{syn}$), 2.48 (m, 1H, allyl C$_{(trans\ to\ imine)}$H$_{anti}$*H*$_{syn}$), 2.36 (s, 6H, *o*-C*H*$_{3(xylxyl)}$ + *p*-C*H*$_{3(mesityl)}$), 2.22 (s, 3H, *o*-C*H*$_{3(xylxyl)}$), 2.13 ppm (dd, $^2J_{H\text{-}H}$ = 2.1 Hz, 1H, allyl C$_{(trans\ to\ imine)}$*H*$_{anti}$H$_{syn}$, splitting pattern is not completely observed as there is partial overlap from

resonance from one *ortho*-CH_3 group from mesityl ring at 2.12 ppm), 2.12 (s, 3H, *o*-C$H_{3(\text{mesityl})}$), 2.01 (s, 3H, *o*-C$H_{3(\text{mesityl})}$), 1.45 (s, 9H, C(CH_3)$_{3(\text{imine})}$). $^{13}C\{^1H\}$ NMR (100 MHz, $CDCl_3$): δ 184.7 (N*C*N), 169.2(*C*=N), 148.4 (*C*$_{(2,6\text{-xylyl})}$), 140.4 (*p*-*C*$_{(\text{mesityl})}$), 135.7 (*C*$_{(\text{mesityl})}$), 134.5 (*o*-*C*$_{(\text{mesityl})}$), 134.1 (*o*-*C*$_{(\text{mesityl})}$), 129.5 (*m*-*C*H$_{(\text{mesityl})}$), 129.4 (*m*-*C*H$_{(\text{mesityl})}$), 128.4 (*m*-*C*H$_{(2,6\text{-xylyl})}$), 128.3 (*m*-*C*H$_{(2,6\text{-xylyl})}$), 126.9 (*o*-*C*$_{(2,6\text{-xylyl})}$), 129.7 (*o*-*C*$_{(2,6\text{-xylyl})}$), 126.3 (*p*-*C*H$_{(2,6\text{-xylyl})}$), 123.8 (NC*C*N$_{(\text{mesityl})}$), 123.1 (N*C*CN$_{(\text{mesityl})}$), 121.1 (allyl CH_2*C*HCH_2), 76.2 (allyl *C*$_{(\text{trans to carbene})}H_2CHCH_2$), 48.9 ($CH_2CH$*C*$_{(\text{trans to imine})}H_2$), 40.9 (*C*(C$H_3$)$_{3(\text{imine})}$), 29.7 (C(*C*$H_3$)$_{3(\text{imine})}$), 21.3 (*p*-*C*H$_{3(\text{mesityl})}$), 19.1 (*o*-*C*H$_{3(2,6\text{-xylyl})}$), 19.0 (*o*-*C*H$_{3(2,6\text{-xylyl})}$), 17.99 (*o*-*C*H$_{3(\text{mesityl})}$), 17.96 (*o*-*C*H$_{3(\text{mesityl})}$). Anal. Calcd for $C_{28}H_{36}BF_4N_3Pd$ (%): C, 55.33; H, 5.97; N, 6.91. Found (%): C, 55.15; H, 6.13; N, 7.07.

Compound 16a, Pd(C^Imine$_{Me}$)MeCl: A solution of [Cu(C^Imine$_{Me}$)I]$_2$ (**5a**) (233 mg, 0.224 mmol) in THF (12 mL) was added to a solution of (1,5-cyclooctadiene)palladium(II) methyl chloride (118 mg, 0.447 mmol) in THF (4 mL). The resulting mixture was stirred at room temperature for 16 h then the solution was filtered through Celite. The mixture was concentrated down to 6 mL and pentane was added to precipitate the product. A beige solid was recovered and further washed with pentane (2 × 6 mL) and dried under reduced pressure (173 mg, 0.354 mmol, 80%). Crystals suitable for X-ray diffraction were grown at room temperature by slow vapor diffusion of pentane into a saturated chloroform solution. ^1H NMR (400 MHz, $CDCl_3$): δ 7.49 (d, ^3J = 1.9 Hz, 1H, NC*H*CN$_{(\text{mesityl})}$), 7.07–7.06 (m, 3H, *p*-C*H*$_{(2,6\text{-xyly})}$ + *m*-C*H*$_{(2,6\text{-xylyl})}$), 6.98 (s, 2H, *m*-C*H*$_{(\text{mesityl})}$), 6.83 (d, ^3J = 1.9 Hz, 1H, NCC*H*N$_{(\text{mesityl})}$), 2.35 (s, 3H, *p*-C$H_{3(\text{mesityl})}$), 2.22 (s,

9H, C$H_{3(\text{imine})}$ + *o*-C$H_{3(2,6\text{-xylyl})}$), 2.13 (s, 6H, *o*-C$H_{3(\text{mesityl})}$), 0.30 (s, 3H, Pd–CH_3). ^{13}C{^{1}H} NMR (100 MHz, $CDCl_3$): δ 176.0 (N*C*N), 156.2(*C*=N), 142.2 (*C*$_{\text{ipso}(2,6\text{-xylyl})}$), 140.1 (*p*-*C*$_{(\text{mesityl})}$), 134.8 (*C*$_{\text{ipso}(\text{mesityl})}$), 134.5 (*o*-*C*$_{(\text{mesityl})}$), 129.7 (*o*-*C*$_{(2,6\text{-xylyl})}$), 129.4 (*m*-*C*H$_{(\text{mesityl})}$), 128.2 (*m*-*C*H$_{(2,6\text{-xylyl})}$), 126.2 (*p*-*C*H$_{(2,6\text{-xylyl})}$), 124.2 (NC*C*N$_{(\text{mesityl})}$), 116.9 (N*C*CN$_{(\text{mesityl})}$), 21.4 (*p*-*C*H3$_{(\text{mesityl})}$), 18.9 (*o*-*C*H3$_{(2,6\text{-xylyl})}$), 18.0 (*o*-*C*H3$_{(\text{mesityl})}$), 14.8 (*C*H3$_{(\text{imine})}$), –8.9 (Pd–*C*H$_3$). FTIR (cast-DCM): $\nu_{C=N}$ 1652 cm^{-1}. Anal. Calcd for $C_{23}H_{28}N_3ClPd$ (%): C, 56.57; H, 5.78; N, 8.60. Found (%): C, 56.42; H, 6.07; N, 8.42.

Compound 16b, Pd(C^Imine$_{t\text{-Bu}}$)MeCl: A solution of C^Imine$_{t\text{-Bu}}$ (**2b**) (323 mg, 0.864 mmol) in THF (8 mL) and was added to a solution of (1,5-cyclooctadiene)palladium(II) methyl chloride (207 mg, 0.782 mmol) in THF (6 mL). The reaction mixture was stirred for 5 h. Volatiles were removed under reduced pressure and a pentane wash (2 × 8 mL) was performed to give a beige solid (415 mg, 0.766 mmol, 98%). Crystals suitable for X-ray diffraction were grown at room temperature by slow vapor diffusion of pentane into a saturated chloroform solution.^{1}H NMR (400 MHz, $CDCl_3$): δ 7.81 (d, ^3J = 2.0 Hz, 1H, NC*H*CN$_{(\text{mesityl})}$), 6.70 (m, 3H, *p*-C*H*$_{(2,6\text{-xylyl})}$ + *m*-C*H*$_{(2,6\text{-xylyl})}$), 6.97 (s, 2H, *m*-C*H*$_{(\text{mesityl})}$), 6.81 (d, ^3J = 2.2 Hz, 1H, NCC*H*N$_{(\text{mesityl})}$), 2.34 (s, 3H, *p*-C*H*$_{3(\text{mesityl})}$), 2.29 (s, 6H, *o*-C*H*$_{3(2,6\text{-xylyl})}$), 2.15 (s, 6H, *o*-C*H*$_{3(\text{mesityl})}$), 1.39 (s, 9H, C(C*H*$_3$)$_{3(\text{imine})}$), 0.23 (s, 3H, Pd–C*H*$_3$). ^{13}C{^{1}H} NMR (100 MHz, $CDCl_3$): δ 177.8 (N*C*N$_{(\text{mesityl})}$), 161.2 (*C*=N), 143.7 (*C*$_{\text{ipso}(2,6\text{-xylyl})}$), 139.9 (*p*-*C*$_{(\text{mesityl})}$), 135.1 (*C*$_{\text{ipso}(\text{mesityl})}$), 134.5 (*o*-*C*$_{(\text{mesityl})}$), 129.4 (*m*-*C*H$_{(\text{mesityl})}$), 128.8 (*o*-*C*$_{(2,6\text{-xylyl})}$), 127.3 (*m*-*C*H$_{(2,6\text{-xylyl})}$), 125.4 (*p*-*C*H$_{(2,6\text{-xylyl})}$), 122.7 (NC*C*N$_{(\text{mesityl})}$), 119.5 (N*C*CN$_{(\text{mesityl})}$), 39.9 (*C*(CH$_3$)$_{3(\text{imine})}$), 30.0 (C(*C*H$_3$)$_{3(\text{imine})}$), 21.3 (*p*-

*C*H$_{3(\text{mesityl})}$), 19.4 (*o*-*C*H$_{3(2,6\text{-xylyl})}$), 18.02 (*o*-*C*H$_{3(\text{mesityl})}$), –8.6 (Pd–*C*H$_3$). FTIR (cast-DCM): $\nu_{C=N}$ 1626 cm^{-1}. Anal. Calcd for $C_{26}H_{34}N_3ClPd$ (%): C, 58.87; H, 6.46; N, 7.92. Found (%): C, 59.10; H, 6.32; N, 8.09.

Compound 16c, Pd(C^Imine$_{Ph}$)MeCl: C^Imine$_{Ph}$ (**2c**) (259 mg, 0.635 mmol) dissolved in THF (8 mL) and was added to a solution of (1,5-cyclooctadiene)palladium(II) methyl chloride (159 mg, 0.601 mmol) in THF (8 mL). The reaction mixture was stirred for 4 h. Volatiles were removed under reduced pressure and a pentane wash was performed to give a light cream solid (307 mg, 0.544 mmol, 91%). Crystals suitable for X-ray diffraction were grown at room temperature by slow diffusion of pentane into a saturated chloroform solution. ^{1}H NMR (400 MHz, $CDCl_3$): δ 7.50 (t, ^3J = 7.5 Hz, 1H, *p*-C*H*$_{(\text{phenyl})}$), 7.42 (t, ^3J = 7.5 Hz, 2H, *m*-C*H*$_{(\text{phenyl})}$), 7.35 (d, ^3J = 7.5 Hz, 2H, *o*-C*H*$_{(\text{phenyl})}$), 7.08 (d, ^3J = 2.0 Hz, 1H, NC*H*CN$_{(\text{azole-mesityl})}$), 7.02 (s, 2H, *m*-C*H*$_{(\text{azole-mesityl})}$), 6.75 (s, ^3J = 2.0 Hz, 1H, NCC*H*N$_{(\text{azole-mesityl})}$), 6.73 (s, 2H, *m*-C*H*$_{(N\text{-mesityl})}$), 2.38 (s, 3H, *p*-C*H*$_{3(\text{azole-mesityl})}$), 2.25 (s, 6H, *o*-C*H*$_{3(N\text{-mesityl})}$), 2.21 (s, 6H, *o*-C*H*$_{3(\text{azole-mesityl})}$), 2.19 (s, 3H, *p*-C*H*$_{3(N\text{-mesityl})}$), 0.42 (s, 3H, Pd–C*H*$_3$).^{13}C{^{1}H} NMR (100 MHz, C_6D_6): δ 176.5 (NC*N*$_{(\text{azole-mesityl})}$), 156.5 (*C*=N), 140.1 (*p*-*C*$_{(\text{azole-mesityl})}$), 139.6 (*C*$_{\text{ipso(N-mesityl)}}$), 135.1 (*p*-*C*$_{(N\text{-mesityl})}$), 134.9 (*C*$_{\text{ipso(azole-mesityl)}}$), 134.5 (*o*-*C*$_{(\text{azole-mesityl})}$), 131.8 (*p*-*C*H$_{(\text{phenyl})}$), 129.4 (*m*-*C*H$_{(\text{azole-mesityl})}$), 129.0 (*m*-*C*H$_{(\text{phenyl})}$), 128.6 (*m*-*C*H$_{(\text{N-mesityl})}$), 128.3 (*o*-*C*H$_{(\text{phenyl})}$), 128.1 (*C*$_{\text{ipso(phenyl)}}$), 123.5 (NC*C*N$_{(\text{azole-mesityl})}$), 118.7 (N*C*CN$_{(\text{azole-mesityl})}$), 21.4 (*p*-*C*H$_{3(\text{azole-mesityl})}$), 21.1 (*p*-*C*H$_{3(N\text{-mesityl})}$), 19.2 (*o*-*C*H$_{3(N\text{-mesityl})}$), 18.0 (*o*-*C*H$_{3(\text{azole-mesityl})}$), –8.8 (Pd–*C*H$_3$), resonance for (*o*-

$C_{(N\text{-mesityl})}$) was not observed. FTIR (cast-DCM): $\nu_{C=N}$ 1635 cm^{-1}. Anal. Calcd for $C_{29}H_{32}N_3ClPd$ (%): C, 61.71; H, 5.71; N, 7.44. Found (%): C, 61.49; H, 5.45; N, 7.18.

Compound 17a, Pd(C^Imine$_{Me}$)(Me)(MeCN)]PF$_6$: A solution of (C^Imine$_{Me}$)PdMeCl (**16a**) (202 mg, 0.414 mmol) in MeCN (6 mL) was added to a suspension of silver hexafluorophosphate (105 mg, 0.415 mmol) in MeCN (4 mL) and stirred at room temperature for 1 h in the absence of light. The solution was filtered through a plug of Celite and the volatiles were removed under reduced pressure. The resulting tan residue was washed with pentane (2 × 4mL) and dried under reduced pressure to give a light beige solid (236 mg, 0.369 mmol, 89%). ^{1}H NMR (400 MHz, $CDCl_3$): δ 7.93 (d, ^3J = 2.0 Hz, 1H, NC*H*CN$_{(mesityl)}$), 7.13 (m, 3H, *p*-C*H*$_{(2,6\text{-xylyl})}$ + *m*-C*H*$_{(2,6\text{-xylyl})}$), 6.98 (s, 2H, *m*-C*H*$_{(mesityl)}$), 6.93 (d, ^3J = 2.0 Hz, 1H, NCC*H*N$_{(mesityl)}$), 2.43 (s, 3H, C*H*$_{3\ (imine)}$), 2.35 (s, 3H, *p*-C*H*$_{3(mesityl)}$), 2.23 (s, 6H, *o*-C*H*$_{3(2,6\text{-xylyl})}$), 2.09 (s, 6H, *o*-C*H*$_{3(mesityl)}$), 1.72 (s, 3H, *CH*$_3$CN), 0.00 (s, 3H, Pd–C*H*$_3$). ^{13}C{^{1}H} NMR (100 MHz, $CDCl_3$): δ 170.3 (N*C*N$_{(mesityl)}$), 160.1 (*C*=N), 141.1 (*C*$_{(2,6\text{-xylyl})}$), 140.4 (*p*-*C*$_{(mesityl)}$), 134.4 (*o*-*C*$_{(mesityl)}$), 134.3 (*C*$_{(mesityl)}$), 129.8 (*o*-*C*$_{(2,6\text{-xylyl})}$), 129.5 (*m*-*C*H$_{(mesityl)}$), 128.6 (*m*-*C*H$_{(2,6\text{-xylyl})}$), 126.9 (*p*-*C*H$_{(2,6\text{-xylyl})}$), 124.9 (NC*C*N$_{(mesityl)}$), 120.1 (N*C*CN$_{(mesityl)}$), 117.2 (CH$_3$*C*N), 21.3 (*p*-*C*H$_{3(mesityl)}$), 18.3 (*o*-*C*H$_{3(2,6\text{-xylyl})}$), 17.8 (*o*-*C*H$_{3(mesityl)}$), 14.7 (*C*H$_{3(imine)}$), 1.6 (*C*H$_3$CN), –9.1 (Pd–*C*H$_3$). FTIR (cast-DCM): $\nu_{C=N}$ 1662 cm^{-1}. Anal. Calcd for $C_{25}H_{31}N_4F_6PPd$ (%): C, 47.00; H, 4.89; N, 8.77. Found (%): C, 46.90; H, 5.15; N, 8.52.

Compound 17b, Pd(C^Imine$_{t\text{-Bu}}$)(Me)(MeCN)]PF$_6$: A solution of (C^Imine$_{t\text{-Bu}}$)PdMeCl (**16b**) (122 mg, 0.230 mmol) in MeCN (8 mL) was added to a suspension of silver hexafluorophosphate (60.0 mg, 0.237 mmol) in MeCN (2 mL) and stirred at room temperature for 1 h in the absence of light. The solution was filtered through a plug of Celite and the volatiles were removed under reduced pressure. The resulting brown residue was washed with pentane and dried under reduced pressure to give a champagne-colored solid (140 mg, 0.206 mmol, 89%). ^{1}H NMR (400 MHz, $CDCl_3$): δ 8.19 (d, ^3J = 2.1 Hz, 1H, NC*H*CN$_{(mesityl)}$), 7.11 (d, ^3J = 7.4 Hz, 2H, *m*-C*H*$_{(2,6\text{-xylyl})}$), 7.06 (m, 1H, *p*-C*H*$_{(2,6\text{-xylyl})}$), 7.03 (d, ^3J = 2.1 Hz, 1H, NCC*H*N$_{(mesityl)}$), 6.97 (s, 2H, *m*-C*H*$_{(mesityl)}$), 2.34 (s, 3H, *p*-C*H*$_{3(mesityl)}$), 2.30 (s, 6H, *o*-C*H*$_{3(2,6\text{-xylyl})}$), 2.10 (s, 6H, *o*-C*H*$_{3(mesityl)}$), 1.71 (s, 3H, *CH*$_3$CN), 1.43 (s, 9H, C(C*H*$_3$)$_{3(imine)}$), –0.08 (s, 3H, Pd-C*H*$_3$). ^{13}C{^{1}H} NMR (100 MHz, $CDCl_3$): δ 172.1 (N*C*N$_{(mesityl)}$), 164.5 (*C*=N), 143.6 (*C*$_{ipso(2,6\text{-xylyl})}$), 140.4 (*p*-*C*$_{(mesityl)}$), 134.5 (*C*$_{ipso(mesityl)}$), 134.2 (*o*-*C*$_{(mesityl)}$), 129.5 (*m*-*C*H$_{(mesityl)}$), 128.3 (*o*-*C*$_{(2,6\text{-xylyl})}$), 128.0 (*m*-*C*H$_{(2,6\text{-xylyl})}$), 126.0 (*p*-*C*H$_{(2,6\text{-xylyl})}$), 124.5 (NC*C*N$_{(mesityl)}$), 122.2 (N*C*CN$_{(mesityl)}$), 118.7 (CH$_3$*C*N), 40.4 (*C*(CH$_3$)$_{3(imine)}$), 29.7 (C(*C*H$_3$)$_{3(imine)}$), 21.3 (*p*-*C*H$_{3(mesityl)}$), 19.0 (*o*-*C*H$_{3(2,6\text{-xylyl})}$), 17.9 (*o*-*C*H$_{3(mesityl)}$), 1.6 (*C*H$_3$CN), –8.2 (Pd–*C*H$_3$). FTIR (cast-DCM): $\nu_{C=N}$ 1634 cm^{-1}. Anal. Calcd for $C_{28}H_{37}N_4F_6PPd$ (%): C, 49.38; H, 5.48; N, 8.23. Found (%): C, 49.09; H, 5.41; N, 8.05.

Compound 17c, Pd(C^Imine$_{Ph}$)(Me)(MeCN)]PF$_6$: A solution of (C^Imine$_{Ph}$)PdMeCl (**16c**) (125 mg, 0.221 mmol) in MeCN (10 mL) was added to a suspension of silver hexafluorophosphate (57.1 mg, 0.226 mmol) in MeCN (2 mL) and stirred at room

temperature for 1 h in the absence of light. The solution was filtered through a plug of Celite and the volatiles were removed under reduced pressure. The resulting brown residue was washed with pentane and dried under reduced pressure to give a brown solid (148 mg, 0.207 mmol, 94%). ^{1}H NMR (400 MHz, $CDCl_3$): δ 7.56 (t, ^{3}J = 7.4 Hz, 1H, *p*-C*H*$_{(phenyl)}$), 7.48 (t, ^{3}J = 7.4 Hz, 2H, *m*-C*H*$_{(phenyl)}$), 7.41 (d, ^{3}J = 7.4 Hz, 2H, *o*-C*H*$_{(phenyl)}$), 7.37 (d, ^{3}J = 2.0 Hz, 1H, NC*H*CN$_{(azole\text{-}mesityl)}$), 7.00 (s, 2H, *m*-C*H*$_{(azole\text{-}mesityl)}$), 6.98 (s, ^{3}J = 2.0 Hz, 1H, NCC*H*N$_{(azole\text{-}mesityl)}$), 6.83 (s, 2H, *m*-C*H*$_{(N\text{-}mesityl)}$), 2.36 (s, 3H, *p*-C*H*$_{3(azole\text{-}mesityl)}$), 2.22 (s, 3H, *p*-C*H*$_{3(N\text{-}mesityl)}$), 2.21 (s, 6H, *o*-C*H*$_{3(N\text{-}mesityl)}$), 2.01 (s, 6H, *o*-C*H*$_{3(azole\text{-}mesityl)}$), 1.75 (s, 3H, *CH*$_3$CN), -0.10 (s, 3H, Pd–C*H*$_3$). ^{13}C{^{1}H} NMR (100 MHz, $CDCl_3$): δ 171.3 (N*C*N$_{(mesityl)}$), 158.8 (*C*=N), 140.5 (*p*-*C*$_{(azole\text{-}mesityl)}$), 138.9 (*C*$_{ipso(N\text{-}mesityl)}$), 136.4 (*p*-*C*$_{(N\text{-}mesityl)}$), 134.4 (*o*-*C*$_{(azole\text{-}mesityl)}$), 133.0 (*p*-*C*H$_{(phenyl)}$), 129.8 (*o*-*C*$_{(N\text{-}mesityl)}$), 129.6 (*m*-*C*H$_{(azole\text{-}mesityl)}$), 129.5 (*m*-*C*H$_{(phenyl)}$ + *C*$_{ipso(azole\text{-}mesityl)}$), 129.1 (*m*-*C*$_{(N\text{-}mesityl)}$), 128.5 (*o*-*C*H$_{(phenyl)}$), 126.2 (*C*$_{ipso(phenyl)}$), 125.0 (NC*C*N$_{(azole\text{-}mesityl)}$), 121.1 (N*C*CN$_{(azole\text{-}mesityl)}$), 119.5 (CH$_3$*C*N), 21.3 (*p*-*C*H$_{3(azole\text{-}mesityl)}$), 20.8 (*p*-*C*H$_{3(N\text{-}mesityl)}$), 18.7 (*o*-*C*H$_{3(N\text{-}mesityl)}$), 17.9 (*o*-*C*H$_{3(azole\text{-}mesityl)}$), 1.6 (*C*H$_3$CN), –8.9 (Pd–*C*H$_3$). FTIR (cast-DCM): $\nu_{C=N}$ 1640 cm^{-1}. Anal. Calcd for $C_{31}H_{35}N_4F_6PPd$ (%): C, 52.07; H, 4.93; N, 7.84. Found (%): C, 51.86; H, 4.70; N, 8.01.

Compound 18, Pd(C^Imine$_{Me}$)$_2$Cl$_2$: *tert*-Butyl isocyanide (6.0 μL, 0.053 mmol) was syringed into a cooled (–35 °C) solution of **16a** (26.0 mg, 0.053 mmol) in toluene (4 mL) and stirred at room temperature for 16 h. Volatiles were removed under reduced pressure and a pentane wash was performed to give a yellow-cream-colored solid. Sample was

further purified by slow vapor diffusion of pentane onto a saturated dichloromethane solution over a period of several days to provide small yellow crystals (14.2 mg, 0.0169 mmol, 32 %). ^{1}H NMR (400 MHz, $CDCl_3$): δ 7.97 (s, 1H, NC*H*CN$_{(mesityl)}$), 7.16 (d, ^{3}J = 7.4 Hz, 2H, *m*-C*H*$_{(2,6\text{-xylyl})}$), 7.07 (m, 1H, *p*-C*H*$_{(2,6\text{-xyly})}$), 6.97 (s, 2H, *m*-C*H*$_{(mesityl)}$), 6.67 (s, 1H, NCC*H*N$_{(mesityl)}$), 3.61 (s, 3H, C*H*$_{3(imine)}$), 2.19 (s, 6H, *o*-C*H*$_{3(mesityl)}$), 2.10 (s, 3H, *p*-C*H*$_{3(mesityl)}$), 2.07 (s, 6H, *o*-C*H*$_{3(2,6\text{-xylyl})}$). ^{13}C{^{1}H} NMR (100 MHz, $CDCl_3$): δ 168.2 (N*C*N), 155.1 (*C*=N), 145.2 (*C*$_{ipso(2,6\text{-xylyl})}$), 139.3 (*p*-*C*$_{(mesityl)}$), 137.0 (*o*-*C*$_{(mesityl)}$), 135.7 (*C*$_{ipso(mesityl)}$), 128.9 (*m*-*C*H$_{(mesityl)}$), 127.6 (*m*-*C*H$_{(2,6\text{-xylyl})}$), 126.5 (*o*-*C*$_{(2,6\text{-xylyl})}$), 123.2 (*p*-*C*H$_{(2,6\text{-xylyl})}$), 122.6 (NC*C*N$_{(mesityl)}$), 119.5 (N*C*CN$_{(mesityl)}$), 20.4 (*p*-*C*H$_{3(mesityl)}$), 20.1 (*C*H$_{3(imine)}$), 18.6 (*o*-*C*H$_{3(mesityl)}$), 18.9 (*o*-*C*H$_{3(2,6\text{-xylyl})}$). FTIR (cast-DCM): $\nu_{C=N}$ 1700 cm^{-1}. Anal. Calcd for $C_{44}H_{50}N_6Cl_2Pd$ (%): C, 62.90; H, 6.00; N, 10.00. Found (%): C, 62.67; H, 5.74; N, 10.17.

Compound 19, Pd(C^Imine$_{t\text{-Bu}}$)Me(*tert*-BuNC)Cl: *tert*-Butyl isocyanide (30.0 μL, 0.265 mmol) was syringed into a cooled (–35 °C) solution of **16b** (67.5 mg, 0.127 mmol) in toluene (6 mL) and stirred at room temperature for 16 h. Volatiles were removed under reduced pressure and a pentane wash was performed to give a cream-colored solid (60.0 mg, 0.0978 mmol, 77%). ^{1}H NMR (400 MHz, C_6D_6): δ 7.09 (s + br, 1H, *p*-C*H*$_{(2,6\text{-xylyl})}$), 6.91 (d, ^{3}J = 7.2 Hz, 2H, *m*-C*H*$_{(2,6\text{-xylyl})}$), 6.62 (s, 1H, *m*-C*H*$_{(mesityl)}$), 6.61 (d, ^{3}J = 1.6 Hz, 1H, NC*H*CN$_{(mesityl)}$), 6.58 (s, 1H, *m*-C*H*$_{(mesityl)}$), 5.98 (s, 1H, NCC*H*N$_{(mesityl)}$), 3.19 (s, 3H, *o*-C*H*$_{3(2,6\text{-xylyl})}$), 2.60 (s, 3H, *p*-C*H*$_{3(mesityl)}$), 1.96 (s, 3H, *o*-C*H*$_{3(mesityl)}$), 1.80 (s, 3H, *o*-C*H*$_{3(mesityl)}$), 1.79 (s, 9H, C(C*H*$_{3)3(imine)}$ + 3H, *o*-C*H*$_{3(2,6\text{-xylyl})}$), 0.70 (s, 9H,

CNC(CH_3)$_{3(isocyanide)}$, –0.50 (s, 3H, Pd–CH_3). $^{13}C\{^1H\}$ NMR (100 MHz, C_6D_6): δ 157.6 (*C*=N), 144.7 ($C_{ipso(2,6\text{-}xylyl)}$), 138.6 (*o*-$C_{(mesityl)}$), 137.5 (*p*-$C_{(mesityl)}$), 136.6 (*o*-$C_{(mesityl)}$), 134.3 ($C_{ipso(mesityl)}$), 130.1 (*m*-C$H_{(mesityl)}$), 129.0 (*p*-C$H_{(2,6\text{-}xylyl)}$), 128.5 (*m*-C$H_{(mesityl)}$), 128.0 (*m*-C$H_{(2,6\text{-}xylyl)}$), 124.2 (*m*-C$H_{(mesityl)}$), 123.2 (*o*-$C_{(2,6\text{-}xylyl)}$), 122.8 (*o*-$C_{(2,6\text{-}xylyl)}$), 120.5 (NC*C*N$_{(mesityl)}$), 120.2 (N*C*CN$_{(mesityl)}$), 119.6 (*C*NC(CH$_3$)$_{3(isocyanide)}$, 55.8 (CN*C*(CH$_3$)$_{3(isocyanide)}$, 41.4 (*C*(CH$_3$)$_{3(imine)}$), 30.3 (C(*C*H$_3$)$_{3(imine)}$), 29.5 (CNC(*C*H$_3$)$_{3(isocyanide)}$, 21.9(*o*-*C*H$_{3(2,6\text{-}xylyl)}$), 21.0 (*o*-*C*H$_{3(mesityl)}$), 20.0 (*p*-*C*H$_{3(mesityl)}$), 19.0 (*o*-*C*H$_{3(2,6\text{-}xylyl)}$), 18.1 (*o*-*C*H$_{3(mesityl)}$), –14.9 (Pd-*C*H$_3$); resonance for NC*C*N$_{(mesityl)}$ was not observed. FTIR (cast-DCM): $\nu_{C=N\text{-}ligand}$ 1696 and 1684 cm^{-1}, $\nu_{C=N\text{-}isocyanide}$ 2189 cm^{-1}. Anal. Calcd for $C_{31}H_{43}N_4ClPd$ (%): C, 60.68; H, 7.06; N, 9.13. Found (%): C, 60.42; H, 7.22; N, 8.85.

Compound 20, Pd(C^Imine$_{Ph}$)Me(tBuNC)Cl: *tert*-Butyl isocyanide (22 μL, 0.20 mmol) was syringed into a cooled (–35 °C) solution of **16c** (54.2 mg, 0.0960 mmol) in toluene (8 mL) and stirred at room temperature for 24 h. Volatiles were removed under reduced pressure to give an light orange solid. A minimal amount of DCM was added to dissolve the crude material that was then filtered through a plug of Celite. Pentane was added to precipitate the product as an orange solid, which was further washed with pentane. The solid was dried under reduced pressure to give the desired product was a light orange solid (42.9 mg, 0.0555 mmol, 69%). ^1H NMR (400 MHz, C_6D_6): δ 6.84 (m, 1H, *p*-C$H_{(phenyl)}$), 6.80 (m, 4H, *m*-C$H_{(phenyl)}$ + *o*-C$H_{(phenyl)}$), 6.72 (s, 1H, *m*-C$H_{(azole\text{-}mesityl)}$), 6.71 (s, 1H, *m*-C$H_{(azole\text{-}mesityl)}$), 6.62 (s, 1H, *m*-C$H_{(N\text{-}mesityl)}$), 6.54 (s, 1H, *m*-C$H_{(N\text{-}mesityl)}$),

6.31 (s, 1H, NC*H*CN$_{(azole\text{-}mesityl)}$), 5.80 (s, 1H, NCC*H*N$_{(azole\text{-}mesityl)}$), 2.48 (s, 3H, *p*-C*H*$_{3(azole\text{-}mesityl)}$), 2.19 (s, 3H, *o*-C*H*$_{3(azole\text{-}mesityl)}$), 2.18 (s, 3H, Pd-C=N(CCH$_3$)$_3$C*H*$_3$), 2.16 (s, 3H, *o*-C*H*$_{3(N\text{-}mesityl)}$), 2.07 (s, 3H, *o*-C*H*$_{3(azole\text{-}mesityl)}$), 2.03 (s, 3H, *p*-C*H*$_{3(N\text{-}mesityl)}$), 2.01 (s, 3H, *o*-C*H*$_{3(N\text{-}mesityl)}$), 1.89 (s, 9H, Pd-C=N(C*H*$_3$)$_3$CH$_3$). ^{13}C{^{1}H} NMR (100 MHz, C_6D_6): δ 156.1 (*C*=N), 140.2 (*p*-*C*$_{(N\text{-}mesityl)}$), 140.1 (*p*-*C*$_{(azole\text{-}mesityl)}$), 135.4 (*o*-*C*$_{(azole\text{-}mesityl)}$), 135.3 (*C*$_{ipso(azole\text{-}mesityl)}$), 134.8 (*o*-*C*$_{(N\text{-}mesityl)}$), 134.2 (*o*-*C*$_{(N\text{-}mesityl)}$), 131.4 (*C*H$_{(phenyl)}$), 131.3 (*C*H$_{(phenyl)}$), 129.9 (*m*-*C*H$_{(N\text{-}mesityl)}$), 129.6 (*m*-*C*H$_{(azole\text{-}mesityl)}$), 129.1 (*m*-*C*H$_{(azole\text{-}mesityl)}$), 129.0 (*m*-*C*H$_{(N\text{-}mesityl)}$), 128.8 (*C*H$_{(phenyl)}$), 128.5 (*C*H$_{(phenyl)}$), 123.0 (NC*C*N$_{(azole\text{-}mesityl)}$), 118.8 (N*C*CN$_{(azole\text{-}mesityl)}$), 55.5 (Pd–C=N(*C*CH$_3$)$_3CH_3$), 32.7 (Pd–C=N(CCH$_3$)$_3$*C*H$_3$), 32.5 (Pd–C=N(C*C*H$_3$)$_3CH_3$), 21.0 (*p*-*C*H$_{3(N\text{-}mesityl)}$ + 19.2 *o*-*C*H$_{3(N\text{-}mesityl)}$), 19.8 (*p*-*C*H$_{3(azole\text{-}mesityl)}$), 18.9 (*o*-*C*H$_{3\ (azole\text{-}mesityl)}$ + *o*-*C*H$_{3(N\text{-}mesityl)}$), 18.3 (*o*-*C*H$_{3(azole\text{-}mesityl)}$); resonances for NCN$_{(azole\text{-}mesityl)}$, ipso-*C*$_{(phenyl)}$, and Pd–*C*=N(CCH$_3$)$_3CH_3$ were not observed. FTIR (cast-DCM): $\nu_{C=N}$ 1638 cm^{-1}. Anal. Calcd for $C_{34}H_{41}N_4ClPd$ (%): C, 63.06; H, 6.38; N, 8.65. Found (%): C, 62.86; H, 6.32; N, 8.49.

Compound 21, [(C^Imine$_{Ph}$)][(1,2-bis[(2,6-dimethylphenyl)imino]-3-[(2,6-dimethylphenyl)imino-κ-*N*]butyl-κ-*C*}palladium chloride: A cooled solution (–35 °C) solution of 2,6-dimethylphenyl isocyanide (13.3 mg, 0.101 mmol) in THF (4 mL) was added to a cooled (–35 °C) partially-soluble solution of **11a** (24.5 mg, 0.0502 mmol) in THF (2 mL). The mixture was dried in vacuo and washed with pentane to give the product as an orange-pink solid (mass recovered 32.4 mg). Crystals suitable for X-ray diffraction were grown at room temperature by slow vapor diffusion of pentane into a

saturated chloroform solution. ^{1}H NMR (400 MHz, $CDCl_3$): major isomer (80%) δ 8.35 (d, ^{3}J = 1.3 Hz, 1H, NC*H*CHN$_{(mesityl)}$), 7.04 (s + br; accidental overlap with minor isomer), 6.98 (m; accidental overlap with minor isomer), 6.88 (m; accidental overlap with minor isomer), 6.78 (m; accidental overlap with minor isomer), 3.35 (s, 3H, C*H*$_{3(C^Imine)}$), 2.37 (s, 3H), 2.33 (s, 3H), 2.25 (s, 3H), 2.10 (s, 3H), 2.08 (s, 3H), 1.97 (s, 6H), 1.91 (s, 3H), 1.77 (s, 3H), 1.58 (s, 3H), 1.41 (s, 3H), 1.15 (s, 3H), ; minor isomer (20%) δ 8.40 (s, 1H, NC*H*CHN$_{(mesityl)}$), 7.04 (s + br, 3H; accidental overlap with major isomer), 6.98 (m; accidental overlap with major isomer), 6.88 (m; accidental overlap with major isomer), 6.78 (m; accidental overlap with major isomer), 3.32 (s, 3H, C*H*$_{3(C^Imine)}$), 2.37 (s, 3H; accidental overlap with major isomer), 2.35 (s, 3H), 2.29 (s, 3H), 2.06 (s, 3H), 2.01 (s, 3H), 1.91 (s, 3H; accidental overlap with major isomer), 1.77 (s, 3H; accidental overlap with major isomer), 1.58 (s, 3H; accidental overlap with major isomer), 1.41 (s, 6H; accidental overlap with major isomer), 1.15 (s, 6H; accidental overlap with major isomer), . ^{13}C{^{1}H} NMR (100 MHz, $CDCl_3$; only resonances for the *major* isomer are reported) δ 180.5, 170.9, 164.6, 154.3, 150.3, 146.8, 145.3, 143.0, 138.9, 137.7, 136.5, 135.2, 129.9, 129.5, 128.7, 128.5, 128.4, 128.1, 128.0, 127.9, 127.8, 127.7, 126.9, 124.0, 123.5, 122.3, 122.1, 120.4 (N*C*CN), 59.7 (Pd–(C(=NXyl))$_3$*C*H$_3$), 21.2 (*C*H$_{3(C^Imine)}$), 19.7, 19.5, 19.0, 18.6, 18.4, , 17.5, 16.8. Anal. Calcd for $C_{50}H_{55}N_6ClPd$ (%): C, 68.10; H, 6.29; N, 9.53. Found (%): C, 67.89; H, 6.24; N, 9.35.

Compound 22a, [Pd(C^Imine$_{Me}$)(Me)(*t*-BuNC)]PF$_6$: *tert*-Butyl isocyanide (8.0 μL, 0.071 mmol) was syringed into a solution of **17a** (45.5 mg, 0.0712 mmol) in THF (6 mL)

and stirred at room temperature for 1 h. Volatiles were removed under reduced pressure and a pentane wash was performed to give a brown solid (46.1 mg, 0.0677 mmol, 96%). ^{1}H NMR (400 MHz, $CDCl_3$): δ 7.95 (d, ^{3}J = 1.8 Hz, 1H, NC*H*CN$_{(mesityl)}$), 7.12 (m, 3H, *p*-C*H*$_{(2,6\text{-xylyl})}$ + *m*-C*H*$_{(2,6\text{-xylyl})}$), 6.99 (s, 2H, *m*-C*H*$_{(mesityl)}$), 6.97 (d, ^{3}J = 1.8 Hz, 1H, NCC*H*N$_{(mesityl)}$), 2.41 (s, 3H, C*H*$_{3(imine)}$), 2.35 (s, 3H, *p*-C*H*$_{3(mesityl)}$), 2.24 (s, 6H, *o*-C*H*$_{3(2,6\text{-xylyl})}$), 2.10 (s, 6H, *o*-C*H*$_{3(mesityl)}$), 1.11 (CNC(C*H*$_3$)$_{3(isocyanide)}$, 0.01 (s, 3H, Pd–C*H*$_3$). ^{13}C{^{1}H} NMR (100 MHz, $CDCl_3$): δ 177.2 (N*C*N$_{(mesityl)}$), 162.0 (*C*=N), 143.9 (*C*$_{ipso(2,6\text{-xylyl})}$), 140.4 (*p*-*C*$_{(mesityl)}$), 135.0 (*C*NC(CH$_3$)$_{3(isocyanide)}$, 134.3 (*o*-*C*$_{(mesityl)}$), 134.0 (*C*$_{ipso(mesityl)}$), 129.5 (*m*-*C*H$_{(mesityl)}$), 129.4 (*o*-*C*$_{(2,6\text{-xylyl})}$), 128.7 (*m*-*C*H$_{(2,6\text{-xylyl})}$), 126.9 (*p*-*C*H$_{(2,6\text{-xylyl})}$), 124.9 (NC*C*N$_{(mesityl)}$), 120.4 (N*C*CN$_{(mesityl)}$), 57.95 (CN*C*(CH$_3$)$_{3(isocyanide)}$, 29.7 (CNC(*C*H$_3$)$_{3(isocyanide)}$, 21.3 (*p*-*C*H$_{3(mesityl)}$), 18.4 (*o*-*C*H$_{3(2,6\text{-xylyl})}$), 17.8 (*o*-*C*H$_{3(mesityl)}$), 14.5 *C*H$_{3(imine)}$), –12.6 (Pd–*C*H$_3$). FTIR (cast-DCM): ν$_{C=N(ligand)}$ 1656 cm^{-1}, ν$_{C=N(isocyanide)}$ 2208 cm^{-1}. Anal. Calcd for $C_{28}H_{37}F_6N_4PPd$ (%): C, 49.38; H, 5.48; N, 8.23. Found (%): C, 49.14; H, 5.52; N, 7.95.

Compound 22b, [Pd(C^Imine$_{t\text{-Bu}}$)(Me)(*t*-BuNC)]PF$_6$: *tert*-Butyl isocyanide (5.3 μL, 0.047 mmol) was syringed into a solution of **17b** (31.9 mg, 0.0468 mmol) in THF (4 mL) and stirred at room temperature for 1 h. Volatiles were removed under reduced pressure and a pentane wash was performed to give a brown solid (31.2 mg, 0.0431 mmol, 92%). ^{1}H NMR (400 MHz, $CDCl_3$): δ 8.25 (d, ^{3}J = 1.4 Hz, 1H, NC*H*CN$_{(mesityl)}$), 7.08 (m, 3H, *p*-C*H*$_{(2,6\text{-xylyl})}$ + *m*-C*H*$_{(2,6\text{-xylyl})}$), 7.07 (s, 1H, NCC*H*N$_{(mesityl)}$), 6.97 (s, 2H, *m*-C*H*$_{(mesityl)}$), 2.34 (s, 9H, *p*-C*H*$_{3(mesityl)}$ + *o*-C*H*$_{3(2,6\text{-xylyl})}$), 2.10 (s, 6H, *o*-C*H*$_{3(mesityl)}$), 1.41 (s, 9H,

C(C*H*$_3$)$_{3(imine)}$), 1.13 (CNC(C*H*$_3$)$_{3(isocyanide)}$, –0.07 (s, 3H, Pd–C*H*$_3$). ^{13}C{^{1}H} NMR (100 MHz, $CDCl_3$): δ 178.5 (N*C*N$_{(mesityl)}$), 166.1 (*C*=N), 147.0 (*C*$_{ipso(2,6\text{-}xylyl)}$), 140.3 (*p*-*C*$_{(mesityl)}$), 134.7 (*C*NC(CH$_3$)$_{3(isocyanide)}$, 134.3 (*o*-*C*$_{(mesityl)}$), 134.2 (*C*$_{ipso(mesityl)}$), 129.5 (*m*-*C*H$_{(mesityl)}$), 128.2 (*m*-*C*H$_{(2,6\text{-}xylyl)}$), 127.8 (*o*-*C*$_{(2,6\text{-}xylyl)}$), 126.1 (*p*-*C*H$_{(2,6\text{-}xylyl)}$), 124.6 (NC*C*N$_{(mesityl)}$), 122.7 (N*C*CN$_{(mesityl)}$), 57.8 CN*C*(CH*3*)$_{3(isocyanide)}$,40.6 (*C*(CH3*)*$_{3(imine)}$), 29.9 (C(*C*H$_3$*)*$_{3(imine)}$), 29.7 (CNC(*C*H*3*)$_{3(isocyanide)}$, 21.3 (*p*-*C*H$_{3(mesityl)}$), 19.1 (*o*-*C*H$_{3(2,6\text{-}xylyl)}$), 17.8 (*o*-*C*H$_{3(mesityl)}$), –11.4 (Pd-*C*H$_3$). FTIR (cast-DCM): $\nu_{C=N(ligand)}$ 1626 cm^{-1}, $\nu_{C=N(isocyanide)}$ 2211 cm^{-1}. Anal. Calcd for $C_{31}H_{43}N_4F_6PPd$ (%): C, 51.49; H, 5.99; N, 7.75. Found (%): C, 51.58; H, 6.12; N, 8.02.

Compound 22c, [Pd(C^Imine$_{Ph}$)(Me)(*t*-BuNC)]PF$_6$: *tert*-Butyl isocyanide (7.0 μL, 0.062 mmol) was syringed into a solution of **17c** (43.9 mg, 0.0614 mmol) in THF (6 mL) and stirred at room temperature for 1 h. Volatiles were removed under reduced pressure and a pentane wash was performed to give a light brown solid (38.8 mg, 0.0512 mmol, 83%). ^{1}H NMR (400 MHz, $CDCl_3$): δ 7.54 (t, ^3J = 7.5 Hz, 1H, *p*-C*H*$_{(phenyl)}$), 7.46 (t, ^3J = 7.5 Hz, 2H, *m*-C*H*$_{(phenyl)}$), 7.40 (d, ^3J = 7.5 Hz, 2H, *o*-C*H*$_{(phenyl)}$), 7.36 (d, ^3J = 1.8 Hz, 1H, NC*H*CN$_{(azole\text{-}mesityl)}$), 7.03 (s, ^3J = 1.8 Hz, 1H, NCC*H*N$_{(azole\text{-}mesityl)}$), 7.00 (s, 2H, *m*-C*H*$_{(azole\text{-}mesityl)}$), 6.80 (s, 2H, *m*-C*H*$_{(N\text{-}mesityl)}$), 2.36 (s, 3H, *p*-C*H*$_{3(azole\text{-}mesityl)}$), 2.23 (s, 6H, *o*-C*H*$_{3(N\text{-}mesityl)}$), 2.20 (s, 3H, *p*-C*H*$_{3(N\text{-}mesityl)}$), 2.15 (s, 6H, *o*-C*H*$_{3(azole\text{-}mesityl)}$), 1.13 (CNC(C*H*$_3$)$_{3(isocyanide)}$, –0.10 (s, 3H, Pd–C*H*$_3$).^{13}C{^{1}H} NMR (100 MHz, $CDCl_3$): δ 178.2 (N*C*N$_{(mesityl)}$), 160.5 (*C*=N), 141.7 (*C*$_{ipso(N\text{-}mesityl)}$), 140.4 (*p*-*C*$_{(azole\text{-}mesityl)}$), 136.3 (*p*-*C*$_{(N\text{-}mesityl)}$), 134.90 (*C*NC(CH$_3$)$_{3(isocyanide)}$, 134.4 (*o*-*C*$_{(azole\text{-}mesityl)}$), 134.1 (*C*$_{ipso(azole\text{-}mesityl)}$), 133.0

(*p*-*C*H$_{(phenyl)}$), 129.5 (*m*-*C*H$_{(azole\text{-}mesityl)}$), 129.5 (*m*-*C*H$_{(phenyl)}$), 129.1 (*m*-*C*$_{(N\text{-}mesityl)}$), 129.1 (*o*-*C*$_{(N\text{-}mesityl)}$), 128.5 (*o*-*C*H$_{(phenyl)}$), 126.0 (*C*$_{ipso(phenyl)}$), 125.2 (NC*C*N$_{(azole\text{-}mesityl)}$), 121.5 (N*C*CN$_{(azole\text{-}mesityl)}$), 58.0 (CN*C*(CH$_3$)$_{3(isocyanide)}$, 29.6 (CNC(*C*H$_3$)$_{3(isocyanide)}$, 21.3 (*p*-*C*H$_{3(azole\text{-}mesityl)}$), 20.8 (*p*-*C*H$_{3(N\text{-}mesityl)}$), 18.8 (*o*-*C*H$_{3(N\text{-}mesityl)}$), 17.9 (*o*-*C*H$_{3(azole\text{-}mesityl)}$), −12.0 (Pd–*C*H$_3$). FTIR (cast-DCM): $\nu_{C=N(ligand)}$ 1636 cm^{-1}, $\nu_{C=N(isocyanide)}$ 2208 cm^{-1}. Anal. Calcd for $C_{34}H_{41}F_6N_4PPd$ (%): C, 53.94; H, 5.46; N, 7.40. Found (%): C, 54.02; H, 5.71; N, 7.28.

Compound 23a, [Pd(C^Imine$_{Me}$)(Me)(ArNC)]PF$_6$: A solution of 2,6-dimethylphenyl isocyanide (10.7 mg, 0.0816 mmol) in THF (6 mL) was added to a solution of **17a** (52.0 mg, 0.0814 mmol) in THF (4 mL) and stirred at room temperature for 1 h. The solution was filtered through a plug of Celite and the volatiles were removed under reduced pressure. The resulting brown solid was further washed with pentane and dried under reduced pressure to give the desired product (52.7 mg, 0.888 mmol, 89%). ^{1}H NMR (400 MHz, CDCl$_3$): δ 7.99 (d, ^3J = 1.6 Hz, 1H, NC*H*CN$_{(mesityl)}$), 7.19 (t, ^3J = 7.7 Hz, 1H, *p*-C*H*$_{(2,6\text{-}xylyl)}$), 7.09 (m, 3H, *p*-C*H*$_{(2,6\text{-}xylyl)\text{-}isocyanide}$ + *m*-C*H*$_{(2,6\text{-}xylyl)\text{-}isocyanide}$), 7.02 (s, 2H, *m*-C*H*$_{(mesityl)}$), 7.00 (s + br, 3H, NCC*H*N$_{(mesityl)}$ + *m*-C*H*$_{(2,6\text{-}xylyl)}$), 2.42 (s, 3H, C*H*$_{3(imine)}$), 2.37 (s, 3H, *p*-C*H*$_{3(mesityl)}$), 2.29 (s, 6H, *o*-C*H*$_{3(2,6\text{-}xylyl)}$), 2.14 (s, 6H, *o*-C*H*$_{3(mesityl)}$), 1.93 (s, 6H, *o*-C*H*$_{3(2,6\text{-}xylyl)\text{-}isocyanide}$), 0.23 (s, 3H, Pd-C*H*$_3$). ^{13}C{^{1}H} NMR (100 MHz, CDCl$_3$): δ 176.7 (N*C*N$_{(mesityl)}$), 162.5 (*C*=N), 144.2 (*C*$_{ipso(2,6\text{-}xylyl)}$), 140.4 (*p*-*C*$_{(mesityl)}$), 135.7 (*o*-*C*$_{(2,6\text{-}xylyl)\text{-}isocyanide}$), 134.5 (*o*-*C*$_{(mesityl)}$), 134.0 (*C*$_{ipso(mesityl)}$), 130.4 (*p*-*C*H$_{(2,6\text{-}xylyl)}$), 129.5 (*m*-*C*H$_{(mesityl)}$), 129.2 (*o*-*C*$_{(2,6\text{-}xylyl)}$), 129.0 (*m*-*C*H$_{(2,6\text{-}xylyl)\text{-}isocyanide}$), 128.2 (*m*-*C*H$_{(2,6\text{-}xylyl)}$), 127.0

(*p*-*C*H$_{(2,6\text{-xylyl})\text{-isocyanide}}$), 124.1 (NC*C*N$_{(\text{mesityl})}$ + *C*$_{(2,6\text{-xylyl})\text{-isocyanide}}$), 120.6 (N*C*CN$_{(\text{mesityl})}$), 21.3 (*p*-*C*H$_{3(\text{mesityl})}$), 18.4 (*o*-*C*H$_{3(2,6\text{-xylyl})}$), 18.3 (*o*-*C*H$_{3(2,6\text{-xylyl})\text{-isocyanide}}$), 17.8 (*o*-*C*H$_{3(\text{mesityl})}$), 14.5 *C*H$_{3(\text{imine})}$), –11.8 (Pd-*C*H$_3$); *C*N-(2,6-dimethylphenyl) carbon resonances not observed. FTIR (cast-DCM): $\nu_{C=N(\text{ligand})}$ 1653 cm^{-1}, $\nu_{C=N(\text{isocyanide})}$ 2181 cm^{-1}. Anal. Calcd for $C_{32}H_{37}N_4F_6PPd$ (%): C, 52.72; H, 5.12; N, 7.68. Found (%): C, 52.49; H, 5.03; N, 7.41.

Compound 23b, [Pd(C^Imine$_{t\text{-Bu}}$)(Me)(ArNC)]PF$_6$: A solution of 2,6-dimethylphenyl isocyanide (22.3 mg, 0.170 mmol) in THF (8 mL) was added to a solution of **17b** (112 mg, 0.165 mmol) in THF (6 mL) and stirred at room temperature for 1 h. The solution was filtered through a plug of Celite and the volatiles were removed under reduced pressure. The resulting brown solid was further washed with pentane and dried under reduced pressure to the desired product (114 mg, 0.148 mmol, 89%). ^{1}H NMR (400 MHz, $CDCl_3$): δ 8.31 (d, ^3J = 1.8 Hz, 1H, NC*H*CN$_{(\text{mesityl})}$), 7.19 (t, ^3J = 7.8 Hz, 1H, *p*-C*H*$_{(2,6\text{-xylyl})\text{-isocyanide}}$), 7.13 (d, ^3J = 1.8 Hz, 1H, NCC*H*N$_{(\text{mesityl})}$), 7.19 (d, ^3J = 7.8 Hz, 2H, *m*-C*H*$_{(2,6\text{-xylyl})\text{-isocyanide}}$), 7.00 (s, 2H, *m*-C*H*$_{(\text{mesityl})}$), 6.95 (d, ^3J = 7.6 Hz, 2H, *m*-C*H*$_{(2,6\text{-xylyl})}$), 6.80 (t, ^3J = 7.6 Hz, 3H, *p*-C*H*$_{(2,6\text{-xylyl})}$), 2.38 (s, 6H, *o*-C*H*$_{3(2,6\text{-xylyl})}$), 2.35 (s, 3H, *p*-C*H*$_{3(\text{mesityl})}$), 2.14 (s, 6H, *o*-C*H*$_{3(\text{mesityl})}$), 2.04 (s, 6H, *o*-C*H*$_{3(2,6\text{-xylyl})\text{-isocyanide}}$), 1.43 (s, 9H, C(C*H*$_3$)$_{3(\text{imine})}$), 0.11 (s, 3H, Pd–C*H*$_3$). ^{13}C{^{1}H} NMR (100 MHz, $CDCl_3$): δ 177.9 (N*C*N$_{(\text{mesityl})}$), 166.5 (*C*=N), 146.8 (*C*$_{\text{ipso}(2,6\text{-xylyl})}$), 140.4 (*p*-*C*$_{(\text{mesityl})}$), 135.2 (*C*$_{(2,6\text{-xylyl})\text{-isocyanide}}$), 134.3 (*o*-*C*$_{(\text{mesityl})}$), 134.2 (*C*$_{\text{ipso}(\text{mesityl})}$), 130.3 (*p*-*C*H$_{(2,6\text{-xylyl})\text{-isocyanide}}$), 129.6 (*m*-*C*H$_{(\text{mesityl})}$), 128.2 (*m*-*C*H$_{(2,6\text{-xylyl})}$ + *m*-*C*H$_{(2,6\text{-xylyl})\text{-isocyanide}}$), 127.5 (*o*-*C*$_{(2,6\text{-xylyl})}$), 126.1 (*p*-

*C*H$_{(2,6\text{-xylyl})}$), 125.1 (*o*-*C*$_{(2,6\text{-xylyl})\text{-isocyanide}}$), 124.9 (NC*C*N$_{(\text{mesityl})}$ + *o*-*C*$_{(2,6\text{-xylyl})\text{-isocyanide}}$), 123.0 (N*C*CN$_{(\text{mesityl})}$), 40.7 (*C*(CH$_3$)$_{3(\text{imine})}$), 29.9 (C(*C*H$_3$)$_{3(\text{imine})}$), 21.3 (*p*-*C*H$_{3(\text{mesityl})}$), 19.2 (*o*-*C*H$_{3(2,6\text{-xylyl})}$), 18.6 (*o*-*C*H$_{3(2,6\text{-xylyl})\text{-isocyanide}}$), 17.9 (*o*-*C*H$_{3(\text{mesityl})}$), –10.8 (Pd–*C*H$_3$), (*C*N-(2,6-dimethylphenyl) carbon missing. FTIR (cast-DCM): $\nu_{C=N(\text{ligand})}$ 1628 cm^{-1}, $\nu_{C=N(\text{isocyanide})}$ 2184 cm^{-1}. Anal. Calcd for $C_{35}H_{43}F_6N_4PPd$ (%): C, 54.51; H, 5.62; N, 7.27. Found (%): C, 54.26; H, 5.45; N, 7.00.

Compound 23c, [Pd(C^Imine$_{Ph}$)(Me)(ArNC)]PF$_6$: A solution of 2,6-dimethylphenyl isocyanide (9.20 mg, 0.070 mmol) in THF (4 mL) was added to a solution of **17c** (50.0 mg, 0.070 mmol) in THF (6 mL) and stirred at room temperature for 1 h. The solution was filtered through a plug of Celite and the volatiles were removed under reduced pressure. The resulting brown solid was further washed with pentane and dried under reduced pressure to the desired product (48.6 mg, 0.0604 mmol, 86%). ^{1}H NMR (400 MHz, $CDCl_3$): δ 7.53 (t, ^3J = 7.4 Hz, 1H, *p*-C*H*$_{(\text{phenyl})}$), 7.46 (t, ^3J = 7.4 Hz, 2H, *m*-C*H*$_{(\text{phenyl})}$), 7.41 (d, ^3J = 7.4 Hz, 2H, *o*-C*H*$_{(\text{phenyl})}$), 7.39 (d, ^3J = 1.8 Hz, 1H, NC*H*CN$_{(\text{azole-mesityl})}$), 7.20 (t, ^3J = 7.7 Hz, 1H, *p*-C*H*$_{(2,6\text{-xylyl})\text{-isocyanide}}$), 7.07 (s, ^3J = 1.8 Hz, 1H, NCC*H*N$_{(\text{azole-mesityl})}$), 7.03 (s, 2H, *m*-C*H*$_{(\text{azole-mesityl})}$), 7.01 (m, 2H, *m*-C*H*$_{(2,6\text{-xylyl})\text{-isocyanide}}$), 6.72 (s, 2H, *m*-C*H*$_{(N\text{-mesityl})}$), 2.37 (s, 3H, *p*-C*H*$_{3(\text{azole-mesityl})}$), 2.27 (s, 6H, *o*-C*H*$_{3(N\text{-mesityl})}$), 2.20 (s, 6H, *o*-C*H*$_{3(\text{azole-mesityl})}$), 2.11 (s, 3H, *p*-C*H*$_{3(N\text{-mesityl})}$), 1.97 (s, 6H, *o*-C*H*$_{3(2,6\text{-xylyl})\text{-isocyanide}}$), 0.31 (s, 3H, Pd–C*H*$_3$).^{13}C{^{1}H} NMR (100 MHz, $CDCl_3$): δ 177.3 (N*C*N$_{(\text{mesityl})}$), 161.0 (*C*=N), 141.9 (*C*$_{\text{ipso(N-mesityl)}}$), 140.5 (*p*-*C*$_{(\text{azole-mesityl})}$), 136.4 (*p*-*C*$_{(N\text{-mesityl})}$), 135.7 (*C*$_{(2,6\text{-xylyl})\text{-isocyanide}}$), 134.5 (*o*-*C*$_{(\text{azole-mesityl})}$), 134.1 (*C*$_{\text{ipso(azole-mesityl)}}$), 133.0 (*p*-*C*H$_{(\text{phenyl})}$),

130.4 (*p*-*C*H$_{(2,6\text{-xylyl})\text{-isocyanide}}$), 129.6 (*m*-*C*H$_{(\text{azole-mesityl})}$), 129.4 (*m*-*C*H$_{(\text{phenyl})}$), 129.3 (*m*-*C*$_{(N\text{-mesityl})}$), 128.9 (*o*-*C*$_{(N\text{-mesityl})}$), 128.6 (*o*-*C*H$_{(\text{phenyl})}$), 128.2 (*m*-*C*H$_{(2,6\text{-xylyl})\text{-isocyanide}}$), 126.0 (*C*$_{(\text{phenyl})}$), 125.4 (NC*C*N$_{(\text{azole-mesityl})}$), 121.7 (N*C*CN$_{(\text{azole-mesityl})}$), 21.3 (*p*-*C*H$_{3(\text{azole-mesityl})}$), 20.7 (*p*-*C*H$_{3(N\text{-mesityl})}$), 18.9 (*o*-*C*H$_{3(N\text{-mesityl})}$), 18.2 (*o*-*C*H$_{3(2,6\text{-xylyl})\text{-isocyanide}}$), 17.9 (*o*-*C*H$_{3(\text{azole-mesityl})}$), –11.3 (Pd–*C*H$_3$). FTIR (cast-DCM): $\nu_{C=N(\text{ligand})}$ 1635 cm^{-1}, $\nu_{C=N(\text{isocyanide})}$ 2181 cm^{-1}. Anal. Calcd for $C_{38}H_{41}N_4F_6PPd$ (%): C, 56.69; H, 5.13; N, 6.96. Found (%): C, 56.91; H, 4.97; N, 7.10.

Compound 24, Pd(C^Imine$_{t\text{-Bu}}$)(C=OMe)Cl: A Schlenk tube containing a solution of **16b** (32.5 mg, 0.0613 mmol) in 6 mL of THF was back-filled with CO and stirred for 15 mins at atmospheric pressure and room temperature. The reaction was dried under vacuum and brought inside the glove box. The solid residue was dissolved in a minimal amount of THF, filtered through a plug of Celite and the yellow solution was dried under vacuum. The solid was washed with pentane and dried under vacuum to give a yellow-green solid (26.5 mg, 0.0474 mmol, 77%). ^{1}H NMR (400 MHz, $CDCl_3$): δ 7.82 (d, ^3J = 1.3 Hz, 1H, NC*H*CN$_{(\text{mesityl})}$), 6.97 (m, 3H, *p*-C*H*$_{(2,6\text{-xylyl})}$ + *m*-C*H*$_{(2,6\text{-xylyl})}$), 6.94 (m, 2H, *m*-C*H*$_{(\text{mesityl})}$), 6.87 (s + br, 1H, NCC*H*N$_{(\text{mesityl})}$), 2.31 (s, 3H, *p*-C*H*$_{3(\text{mesityl})}$), 2.29 (s, 6H, *o*-C*H*$_{3(2,6\text{-xylyl})}$), 2.14 (s, 6H, *o*-C*H*$_{3(\text{mesityl})}$), 1.71 (s, 3H, Pd–CO–C*H*$_3$), 1.36 (s, 9H, C(C*H*$_3$)$_{3(\text{imine})}$). ^{13}C{^{1}H} NMR (100 MHz, $CDCl_3$): δ 228.5 (Pd-*C*O-CH$_3$), 179.4 (N*C*N$_{(\text{mesityl})}$), 161.7 (*C*=N), 143.1 (*C*$_{(2,6\text{-xylyl})}$), 140.3 (*p*-*C*$_{(\text{mesityl})}$), 135.5 (*o*-*C*$_{(\text{mesityl})}$), 134.4 (*C*$_{(\text{mesityl})}$), 129.4 (*m*-*C*H$_{(\text{mesityl})}$), 127.9 (*o*-*C*$_{(2,6\text{-xylyl})}$), 127.4 (*m*-*C*$_{(2,6\text{-xylyl})}$), 125.2 (*p*-*C*H$_{(2,6\text{-xylyl})}$), 122.2 (NC*C*N$_{(\text{mesityl})}$), 120.0 (N*C*CN$_{(\text{mesityl})}$), 40.2 (*C*(CH$_3$)$_{3(\text{imine})}$), 38.7 (Pd–CO–

CH_3), 29.9 (C(CH_3)$_{3(imine)}$), 21.3 (*p*-$CH_{3(mesityl)}$), 19.6 (*o*-$CH_{3(2,6\text{-xylyl})}$), 18.1 (*o*-$CH_{3(mesityl)}$). FTIR (cast-DCM): $\nu_{C=N}$ 1632 cm^{-1}, $\nu_{C=O}$ 1690 cm^{-1}. Anal. Calcd for $C_{27}H_{34}N_3OClPd$ (%): C, 58.07; H, 6.14; N, 7.52. Found (%): C, 58.19; H, 6.28; N, 7.24.

Scheme 21. Preparation of a Ru(II) benzylidene imino-NHC complex (**25**).

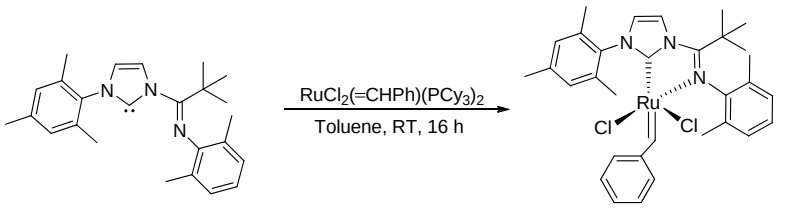

2b

25 (C^Imine$_{t\text{-Bu}}$)Ru(=CHPh)Cl$_2$

Compound 25, Ru(C^Imine$_{t\text{-Bu}}$)(CHPh)Cl$_2$: A solution of C^Imine$_{t\text{-Bu}}$ (**2b**) (65.2 mg, 0.175 mmol) in toluene (10 mL) was added to a solution of $RuCl_2(PCy_3)_2$(CHPh) (119 mg, 0.144 mmol) in toluene (6 mL). The reaction mixture was stirred for 24 h. Volatiles were removed under reduced pressure. The solid was subsequently washed with pentane (2 × 6 mL) and diethyl ether (3 × 6 mL) to give compound **25** as a green solid (67 mg, 0.11 mmol, 76%). ^{1}H NMR (400 MHz, $CDCl_3$): δ = 18.41 (s, 1H, C*H*Ph), 8.65 (s, 1H, NC*H*CN$_{(mesityl)}$), 7.70 (t, ^3J = 7.6 Hz, 1H, *p*-C*H*$_{(phenyl)}$), 7.32 (t, ^3J = 7.6 Hz, 2H, *m*-C*H*$_{(phenyl)}$), 7.08 (d, ^3J = 2.0 Hz, 1H, NCC*H*N$_{(mesityl)}$), 7.06 (br, 2H, *o*-C*H*$_{(phenyl)}$), 6.97 (t, ^3J = 7.5 Hz, 1H, *p*-C*H*$_{(2,6\text{-xylyl})}$), 6.86 (s, 1H, *m*-C*H*$_{(mesityl)}$), 6.84 (s, 1H, *m*-C*H*$_{(2,6\text{-xylyl})}$), 6.73 (d, ^3J = 7.5 Hz, 1H, *m*-C*H*$_{(2,6\text{-xylyl})}$), 6.40 (s, 1H, *m*-C*H*$_{(mesityl)}$), 2.25 (s, 3H, *o*-C*H*$_{3(mesityl)}$), 2.10 (s, 3H, *p*-C*H*$_{3(mesityl)}$), 1.81 (s, 3H, *o*-C*H*$_{3(2,6\text{-xylyl})}$), 1.41 (s, 9H, C(C*H*$_3$)$_{3(imine)}$), 1.22

(s, 3H, *o*-C$H_{3(2,6\text{-xylyl})}$), 1.02 (s, 3H, *o*-C$H_{3(\text{mesityl})}$). $^{13}C\{^{1}H\}$ NMR (100 MHz, $CDCl_3$): δ = 318.4 (*C*HPh), 196.1 (NCN$_{(\text{mesityl})}$), 169.2 (*C*=N), 154.2 ($C_{\text{ipso(phenyl)}}$), 145.2 ($C_{\text{ipso(2,6-xylyl}}$), 138.5 (*p*-$C_{(\text{mesityl})}$), 136.5 ($C_{\text{ipso(mesityl)}}$), 135.2 (*o*-$C_{(\text{mesityl})}$), 134.9 (*o*-$C_{(\text{mesityl})}$), 132.1 (*p*-C$H_{(\text{phenyl})}$), 131.5 (*o*-$C_{(2,6\text{-xylyl})}$), 131.3 (*o*-$C_{(2,6\text{-xylyl})}$), 130.5 (*o*-C$H_{(\text{phenyl})}$), 130.2 (*m*-C$H_{(\text{phenyl})}$), 128.6 (*m*-*C*H$_{(\text{mesityl})}$), 128.5 (*m*-*C*H$_{(\text{mesityl})}$), 128.4 (*m*-*C*H$_{(2,6\text{-xylyl})}$), 127.8 (*m*-*C*H$_{(2,6\text{-xylyl})}$), 126.3 (*p*-*C*H$_{(2,6\text{-xylyl})}$), 124.8 (NC*C*N$_{(\text{mesityl})}$), 120.5 (N*C*CN$_{(\text{mesityl})}$), 40.5 (*C*(CH$_3$)$_{3(\text{imine})}$), 30.0 (C(*C*H$_3$)$_{3(\text{imine})}$), 21.0 (*p*-*C*H$_{3(\text{mesityl})}$), 20.4 (*o*-*C*H$_{3(2,6\text{-xylyl})}$), 20.2 (*o*-*C*H$_{3(2,6\text{-xylyl})}$), 19.8 (*o*-*C*H$_{3(\text{mesityl})}$), 17.6 (*o*-*C*H$_{3(\text{mesityl})}$). Elemental analysis calcd (%) for $C_{32}H_{37}N_3Cl_2Ru$: C 60.47, H 5.87, N 6.61; found C 60.22, H 5.74, N 6.37. After the preparation and characterization of **25**, this work was taken up by another member of the Lavoie group, Tim Larocque, to investigate the potential of this compound in metathesis.[155]

General Procedure for Ethylene Polymerization. Ethylene polymerization was performed at atmospheric pressure and room temperature in a 500-mL Schlenk flask containing a magnetic stir bar. The flask was conditioned in an oven at 160 °C for at least 12 h prior to use. The hot flask was brought to room temperature under dynamic vacuum, and back-filled with ethylene. This cycle was repeated a total of three times. Under an atmosphere of ethylene, the flask was charged with 25 mL of dry toluene and 1000 equivalents of methylaluminoxane (2M in toluene). The solution was stirred for 15 min before the catalyst (10.3 μmol) in 1 mL of toluene was introduced into the flask via syringe. The reaction mixture was vigorously stirred for 10 min after the addition of the catalyst, and subsequently quenched with a 50:50 mixture of concentrated hydrochloric

acid and methanol. The resulting mixture was filtered and any solid collected was washed with distilled water. Solids collected, if any, were dried under vacuum at approximately 60 °C for several hours.

5.4 X-Ray Crystallography

Detailed crystallographic data for all structures including structure refinement parameters, tables of atomic coordinates with isotropic and anisotropic displacement parameters, bond lengths and angles that have been published can be found on the Cambridge Crystallographic Data Centre (CCDC) website. CCDC reference numbers for each compound are given in parentheses: **1a** (759030), **2b** (808924), **3a** (759031), **4** (759032), (**5a** (853927), **5b** (853928), **8** (853926), **12a** (853929), **12b** (853930), **13** (853931), **16a** (940711), **16b** (940712), **16c** (940713), **17a** (940714), **18** (940715), **21** (940716), **24** (940717). Structure refinement parameters for structures **9**, **10**, **14** and **15b** are listed in the tables below.

X-ray crystallographic data for **1a, 2b, 3a, 4, 6a, 6b, 8, 12a, 12b, 16a–c, 17b, 18** and **21** were collected at the University of Toronto on a Bruker-Nonius Kappa-CCD diffractometer using monochromated Mo-Kα radiation (λ = 0.71073 Å) at 150K and were measured using a combination of ϕ scans and ω scans with κ offsets, to fill the Ewald sphere. Intensity data were processed using the Denzo-SMN package. Absorption corrections were carried out using SORTAV.[156] Structures **1a, 2b, 3a, 4** and **6a, 12a, 16a–c, 17b, 18** and **21** were solved and refined using SHELXTL V6.1[157] for full-matrix

least-squares refinement was based on F^2. Structures **6b** and **12b** were solved and refined using Superflip[158] and refined with SHELXS-97[159] for full-matrix least-squares refinement that was based on F^2. All H atoms were included in calculated positions and allowed to refine in riding-motion approximation with U_{iso} tied to the carrier atom.

X-ray crystallographic data for **17b** and **24** were collected at the University of Toronto on a Bruker Kappa APEX-DUO diffractometer using monochromated Mo-Kα radiation (Bruker Triumph) and were measured using a combination of ϕ scans and ω scans. The data were processed using APEX2 and SAINT. Absorption corrections were carried out using SADABS. Structures were solved and refined using Superflip[158] and refined with SHELXS-97[159] for full-matrix least-squares refinement that was based on F^2. All H atoms were included in calculated positions and allowed to refine in riding-motion approximation with U_{iso} tied to the carrier atom.

X-Ray crystallographic data for **13** was collected at McMaster University on a Bruker APEX2 diffractometer diffractometer using monochromated Mo-Kα radiation (λ = 0.71073 Å) at 100K and were measured using ϕ and ω scans. Unit cell parameters were determined using at least 50 frames from three different orientations. Data were processed using SAINT, and corrected for absorption with accurate face-indexing as well as redundant data (SADABS). Structure **13** was solved and refined using Superflip[158] and refined with SHELXS-97[159] for full-matrix least-squares refinement that was based on F^2. All H atoms were included in calculated positions and allowed to refine in riding-motion approximation with U_{iso} tied to the carrier atom.

Table 2. Crystal data and structure refinement for Compound **9**.

Empirical formula	C23 H27 Cl4 N3 Zn	
Formula weight	552.65	
Temperature	150(1) K	
Wavelength	0.71073 Å	
Crystal system	Orthorhombic	
Space group	Pcab	
Unit cell dimensions	a = 13.8221(6) Å	α= 90°.
	b = 14.6035(4) Å	β= 90°.
	c = 26.3013(10) Å	γ = 90°.
Volume	5308.9(3) $Å^3$	
Z	8	
Density (calculated)	1.383 Mg/m^3	
Absorption coefficient	1.343 mm^{-1}	
F(000)	2272	
Crystal size	0.30 x 0.20 x 0.06 mm^3	
Theta range for data collection	2.55 to 27.49°.	
Index ranges	-17<=h<=17, -16<=k<=18, -34<=l<=34	
Reflections collected	32679	
Independent reflections	6063 [R(int) = 0.0806]	
Completeness to theta = 27.49°	99.7 %	
Absorption correction	Semi-empirical from equivalents	
Max. and min. transmission	0.939 and 0.791	
Refinement method	Full-matrix least-squares on F^2	
Data / restraints / parameters	6063 / 0 / 286	
Goodness-of-fit on F^2	1.040	
Final R indices [I>2sigma(I)]	R1 = 0.0613, wR2 = 0.1541	
R indices (all data)	R1 = 0.1329, wR2 = 0.1871	
Largest diff. peak and hole	0.555 and -0.916 e.$Å^{-3}$	

Table 3. Crystal data and structure refinement for Compound **10**.

Empirical formula	C47 H50 Cl10 Fe2 N6	
Formula weight	1165.13	
Temperature	293(2) K	
Wavelength	0.71073 Å	
Crystal system	Monoclinic	
Space group	P 21/a	
Unit cell dimensions	a = 15.9310(4) Å	α= 90°.
	b = 14.1817(5) Å	β= 105.802(2)°.
	c = 26.1895(9) Å	γ = 90°.
Volume	5693.3(3) $Å^3$	
Z	4	
Density (calculated)	1.359 Mg/m^3	
Absorption coefficient	1.015 mm^{-1}	
F(000)	2384	
Crystal size	0.2 x 0.24 x 0.28 mm^3	
Theta range for data collection	2.56 to 27.46°.	
Index ranges	-20<=h<=20, -18<=k<=18, -27<=l<=33	
Reflections collected	37540	
Independent reflections	12878 [R(int) = 0.1155]	
Completeness to theta = 27.46°	98.8 %	
Refinement method	Full-matrix least-squares on F^2	
Data / restraints / parameters	12878 / 15 / 572	
Goodness-of-fit on F^2	1.120	
Final R indices [I>2sigma(I)]	R1 = 0.0996, wR2 = 0.2242	
R indices (all data)	R1 = 0.2385, wR2 = 0.2832	
Extinction coefficient	0.0000(2)	
Largest diff. peak and hole	1.374 and -1.308 $e.Å^{-3}$	

Table 4. Crystal data and structure refinement for Compound **14**.

Empirical formula	C33 H43 N3 Ni	
Formula weight	497.07	
Temperature	150(2) K	
Wavelength	0.71073 Å	
Crystal system	Triclinic	
Space group	P -1	
Unit cell dimensions	a = 10.7987(7) Å	α= 92.936(4)°.
	b = 11.3719(5) Å	β= 100.271(3)°.
	c = 13.9439(9) Å	γ = 90.580(4)°.
Volume	1682.36(17) $Å^3$	
Z	2	
Density (calculated)	0.981 Mg/m^3	
Absorption coefficient	0.595 mm^{-1}	
F(000)	494	
Crystal size	0.45 x 0.24 x 0.10 mm^3	
Theta range for data collection	2.60 to 27.46°.	
Index ranges	-13<=h<=13, -14<=k<=14, -15<=l<=18	
Reflections collected	17297	
Independent reflections	7555 [R(int) = 0.0954]	
Completeness to theta = 27.46°	98.2 %	
Refinement method	Full-matrix least-squares on F^2	
Data / restraints / parameters	7555 / 2 / 372	
Goodness-of-fit on F^2	1.030	
Final R indices [I>2sigma(I)]	R1 = 0.0880, wR2 = 0.1824	
R indices (all data)	R1 = 0.1595, wR2 = 0.2236	
Largest diff. peak and hole	0.798 and -0.494 e.$Å^{-3}$	

Table 5. Crystal data and structure refinement for Compound **15b**.

Empirical formula	C28 H36 B F4 N3 Pd	
Formula weight	607.81	
Temperature	293(2) K	
Wavelength	0.71073 Å	
Crystal system	Monoclinic	
Space group	P *21/c*	
Unit cell dimensions	a = 12.7101(4) Å	α= 90°.
	b = 11.6376(3) Å	β= 101.353(2)°.
	c = 19.3405(5) Å	γ = 90°.
Volume	2804.77(14) $Å^3$	
Z	4	
Density (calculated)	1.439 Mg/m^3	
Absorption coefficient	0.710 mm^{-1}	
F(000)	1248	
Crystal size	0.3 x 0.22 x 0.08 mm^3	
Theta range for data collection	2.75 to 27.44°.	
Index ranges	-16<=h<=16, -14<=k<=15, -25<=l<=25	
Reflections collected	26260	
Independent reflections	6381 [R(int) = 0.0560]	
Completeness to theta = 27.44°	99.7 %	
Refinement method	Full-matrix least-squares on F^2	
Data / restraints / parameters	6381 / 9 / 352	
Goodness-of-fit on F^2	1.036	
Final R indices [I>2sigma(I)]	R1 = 0.0563, wR2 = 0.1496	
R indices (all data)	R1 = 0.0857, wR2 = 0.1689	
Largest diff. peak and hole	1.089 and -0.560 e.$Å^{-3}$	

References

(1) Natta, G.; Pino, P.; Corradini, P.; Danusso, F.; Mantica, E.; Mazzanti, G.; Moraglio, G. *Journal of the American Chemical Society* **1955**, *77*, 1708.

(2) Janas, Z. *Coordination Chemistry Reviews* **2010**, *254*, 2227.

(3) Rodrigues, A.-S.; Carpentier, J.-F. *Coordination Chemistry Reviews* **2008**, *252*, 2137.

(4) Gibson, V. C.; Spitzmesser, S. K. *Chemical Reviews* **2002**, *103*, 283.

(5) Sinn, H.; Kaminsky, W.; Vollmer, H.-J.; Woldt, R. *Angewandte Chemie International Edition in English* **1980**, *19*, 390.

(6) Brintzinger, H. H.; Fischer, D.; Mülhaupt, R.; Rieger, B.; Waymouth, R. M. *Angewandte Chemie International Edition in English* **1995**, *34*, 1143.

(7) Johnson, L. K.; Killian, C. M.; Brookhart, M. *Journal of the American Chemical Society* **1995**, *117*, 6414.

(8) Johnson, L. K.; Mecking, S.; Brookhart, M. *Journal of the American Chemical Society* **1996**, *118*, 267.

(9) Van Asselt, R.; Elsevier, C. J. *Organometallics* **1992**, *11*, 1999.

(10) Van Asselt, R.; Gielens, E. E. C. G.; Rulke, R. E.; Vrieze, K.; Elsevier, C. J. *Journal of the American Chemical Society* **1994**, *116*, 977.

(11) Vrieze, K. *Journal of Organometallic Chemistry* **1986**, *300*, 307.

(12) van Asselt, R.; Elsevier, C. J.; Smeets, W. J. J.; Spek, A. L.; Benedix, R. *Recueil des Travaux Chimiques des Pays-Bas* **1994**, *113*, 88.

(13) Gates, D. P.; Svejda, S. A.; Oñate, E.; Killian, C. M.; Johnson, L. K.; White, P. S.; Brookhart, M. *Macromolecules* **2000**, *33*, 2320.

(14) Popeney, C.; Guan, Z. *Organometallics* **2005**, *24*, 1145.

(15) Chen, E. Y.-X.; Marks, T. J. *Chemical Reviews* **2000**, *100*, 1391.

(16) Kaminsky, W.; Miri, M.; Sinn, H.; Woldt, R. *Die Makromolekulare Chemie, Rapid Communications* **1983**, *4*, 417.

(17) Tempel, D. J.; Johnson, L. K.; Huff, R. L.; White, P. S.; Brookhart, M. *Journal of the American Chemical Society* **2000**, *122*, 6686.

(18) Deng, L.; Margl, P.; Ziegler, T. *Journal of the American Chemical Society* **1997**, *119*, 1094.

(19) Shultz, L. H.; Tempel, D. J.; Brookhart, M. *Journal of the American Chemical Society* **2001**, *123*, 11539.

(20) Froese, R. D. J.; Musaev, D. G.; Morokuma, K. *Journal of the American Chemical Society* **1998**, *120*, 1581.

(21) Svoboda, M.; Dieck, H. t. *Journal of Organometallic Chemistry* **1980**, *191*, 321.

(22) Ittel, S. D.; Johnson, L. K.; Brookhart, M. *Chemical Reviews* **2000**, *100*, 1169.

(23) Daugulis, O.; Brookhart, M. *Organometallics* **2002**, *21*, 5926.

(24) Guan, Z.; Marshall, W. J. *Organometallics* **2002**, *21*, 3580.

(25) Peuckert, M.; Keim, W. *Organometallics* **1983**, *2*, 594.

(26) Keim, W.; Behr, A.; Limbäcker, B.; Krüger, C. *Angewandte Chemie International Edition in English* **1983**, *22*, 503.

(27) Keim, W.; Kowaldt, F. H.; Goddard, R.; Krüger, C. *Angewandte Chemie International Edition in English* **1978**, *17*, 466.

(28) Kuhn, P.; Semeril, D.; Matt, D.; Chetcuti, M. J.; Lutz, P. *Dalton Transactions* **2007**, 515.

(29) Gibson, V. C.; Tomov, A.; White, A. J. P.; Williams, D. J. *Chemical Communications* **2001**, 719.

(30) Wang, C.; Friedrich, S.; Younkin, T. R.; Li, R. T.; Grubbs, R. H.; Bansleben, D. A.; Day, M. W. *Organometallics* **1998**, *17*, 3149.

(31) Drent, E.; van Dijk, R.; van Ginkel, R.; van Oort, B.; Pugh, R. I. *Chemical Communications* **2002**, 744.

(32) Luo, S.; Vela, J.; Lief, G. R.; Jordan, R. F. *Journal of the American Chemical Society* **2007**, *129*, 8946.

(33) Skupov, K. M.; Piche, L.; Claverie, J. P. *Macromolecules* **2008**, *41*, 2309.

(34) Skupov, K. M.; Marella, P. R.; Simard, M.; Yap, G. P. A.; Allen, N.; Conner, D.; Goodall, B. L.; Claverie, J. P. *Macromolecular Rapid Communications* **2007**, *28*, 2033.

(35) Wanzlick, H. W. *Angewandte Chemie International Edition in English* **1962**, *1*, 75.

(36) Wanzlick, H. W.; Schönherr, H. J. *Angewandte Chemie International Edition in English* **1968**, *7*, 141.

(37) Öfele, K. *Journal of Organometallic Chemistry* **1968**, *12*, P42.

(38) Arduengo, A. J.; Harlow, R. L.; Kline, M. *Journal of the American Chemical Society* **1991**, *113*, 361.

(39) Hahn, F. E.; Jahnke, M. C. *Angewandte Chemie International Edition* **2008**, *47*, 3122.

(40) Lee, M.-T.; Hu, C.-H. *Organometallics* **2004**, *23*, 976.

(41) Cavallo, L.; Correa, A.; Costabile, C.; Jacobsen, H. *Journal of Organometallic Chemistry* **2005**, *690*, 5407.

(42) Chianese, A. R.; Li, X.; Janzen, M. C.; Faller, J. W.; Crabtree, R. H. *Organometallics* **2003**, *22*, 1663.

(43) Dorta, R.; Stevens, E. D.; Scott, N. M.; Costabile, C.; Cavallo, L.; Hoff, C. D.; Nolan, S. P. *Journal of the American Chemical Society* **2005**, *127*, 2485.

(44) Gusev, D. G. *Organometallics* **2009**, *28*, 6458.

(45) Gusev, D. G. *Organometallics* **2009**, *28*, 763.

(46) Kelly Iii, R. A.; Clavier, H.; Giudice, S.; Scott, N. M.; Stevens, E. D.; Bordner, J.; Samardjiev, I.; Hoff, C. D.; Cavallo, L.; Nolan, S. P. *Organometallics* **2007**, *27*, 202.

(47) Crabtree, R. H. *Journal of Organometallic Chemistry* **2005**, *690*, 5451.

(48) Dorta, R.; Stevens, E. D.; Hoff, C. D.; Nolan, S. P. *Journal of the American Chemical Society* **2003**, *125*, 10490.

(49) Becker, E.; Stingl, V.; Dazinger, G.; Puchberger, M.; Mereiter, K.; Kirchner, K. *Journal of the American Chemical Society* **2006**, *128*, 6572.

(50) McGuinness, D. S.; Saendig, N.; Yates, B. F.; Cavell, K. J. *Journal of the American Chemical Society* **2001**, *123*, 4029.

(51) McGuinness, D. S.; Saendig, N.; Yates, B. F.; Cavell, K. J. *Journal of the American Chemical Society* **2001**, *123*, 4029.

(52) Simms, R. W.; Drewitt, M. J.; Baird, M. C. *Organometallics* **2002**, *21*, 2958.

(53) Douthwaite, R. E.; Haüssinger, D.; Green, M. L. H.; Silcock, P. J.; Gomes, P. T.; Martins, A. M.; Danopoulos, A. A. *Organometallics* **1999**, *18*, 4584.

(54) Douthwaite, R. E.; Green, M. L. H.; Silcock, P. J.; Gomes, P. T. *Organometallics* **2001**, *20*, 2611.

(55) Larocque, T. G.; Lavoie, G. G. *Journal of Organometallic Chemistry* **2012**, *715*, 26.

(56) Herrmann, W. A.; Elison, M.; Fischer, J.; Köcher, C.; Artus, G. R. J. *Angewandte Chemie International Edition in English* **1995**, *34*, 2371.

(57) Badaj, A. C.; Lavoie, G. G. *Organometallics* **2012**, *31*, 1103.

(58) Al Thagfi, J.; Dastgir, S.; Lough, A. J.; Lavoie, G. G. *Organometallics* **2010**, *29*, 3133.

(59) Wang, H. M. J.; Lin, I. J. B. *Organometallics* **1998**, *17*, 972.

(60) Grundemann, S.; Albrecht, M.; Kovacevic, A.; Faller, J. W.; Crabtree, R. H. *Journal of the Chemical Society, Dalton Transactions* **2002**, 2163.

(61) Marion, N.; Nolan, S. P. *Accounts of Chemical Research* **2008**, *41*, 1440.

(62) McGuinness, D. *Dalton Transactions* **2009**, *0*, 6915.

(63) Zhou, X.; Jordan, R. F. *Organometallics* **2011**, *30*, 4632.

(64) Coleman, K. S.; Chamberlayne, H. T.; Turberville, S.; Green, M. L. H.; Cowley, A. R. *Dalton Transactions* **2003**, *0*, 2917.

(65) Tulloch, A. A. D.; Winston, S.; Danopoulos, A. A.; Eastham, G.; Hursthouse, M. B. *Dalton Transactions* **2003**, 699.

(66) Chen, J. C. C.; Lin, I. J. B. *Organometallics* **2000**, *19*, 5113.

(67) Khlebnikov, V.; Meduri, A.; Mueller-Bunz, H.; Montini, T.; Fornasiero, P.; Zangrando, E.; Milani, B.; Albrecht, M. *Organometallics* **2012**, *31*, 976.

(68) César, V.; Bellemin-Laponnaz, S.; Gade, L. H. *Organometallics* **2002**, *21*, 5204.

(69) Frøseth, M.; Netland, K. A.; Rømming, C.; Tilset, M. *Journal of Organometallic Chemistry* **2005**, *690*, 6125.

(70) Gade, L. H.; César, V.; Bellemin-Laponnaz, S. *Angewandte Chemie International Edition* **2004**, *43*, 1014.

(71) Venkatachalam, G.; Heckenroth, M.; Neels, A.; Albrecht, M. *Helvetica Chimica Acta* **2009**, *92*, 1034.

(72) Dastgir, S.; Coleman, K. S.; Cowley, A. R.; Green, M. L. H. *Organometallics* **2005**, *25*, 300.

(73) Badaj, A. C.; Dastgir, S.; Lough, A. J.; Lavoie, G. G. *Dalton Transactions* **2010**, *39*, 3361.

(74) Larocque, T. G.; Badaj, A. C.; Dastgir, S.; Lavoie, G. G. *Dalton Transactions* **2011**, *40*, 12705.

(75) Alvarado, E.; Badaj, A. C.; Larocque, T. G.; Lavoie, G. G. *Chemistry – A European Journal* **2012**, *18*, 12112.

(76) Coleman, K. S.; Dastgir, S.; Barnett, G.; Alvite, M. J. P.; Cowley, A. R.; Green, M. L. H. *Journal of Organometallic Chemistry* **2005**, *690*, 5591.

(77) Steiner, G.; Kopacka, H.; Ongania, K.-H.; Wurst, K.; Preishuber-Pflügl, P.; Bildstein, B. *European Journal of Inorganic Chemistry* **2005**, *2005*, 1325.

(78) Garrison, J. C.; Youngs, W. J. *Chemical Reviews* **2005**, *105*, 3978.

(79) Ramnial, T.; Abernethy, C. D.; Spicer, M. D.; McKenzie, I. D.; Gay, I. D.; Clyburne, J. A. C. *Inorganic Chemistry* **2003**, *42*, 1391.

(80) Matsumoto, K.; Matsumoto, N.; Ishii, A.; Tsukuda, T.; Hasegawa, M.; Tsubomura, T. *Dalton Transactions* **2009**, *0*, 6795.

(81) Edworthy, I. S.; Rodden, M.; Mungur, S. A.; Davis, K. M.; Blake, A. J.; Wilson, C.; Schröder, M.; Arnold, P. L. *Journal of Organometallic Chemistry* **2005**, *690*, 5710.

(82) Kaur, H.; Zinn, F. K.; Stevens, E. D.; Nolan, S. P. *Organometallics* **2004**, *23*, 1157.

(83) Tulloch, A. A. D.; Danopoulos, A. A.; Kleinhenz, S.; Light, M. E.; Hursthouse, M. B.; Eastham, G. *Organometallics* **2001**, *20*, 2027.

(84) Cordero, B.; Gomez, V.; Platero-Prats, A. E.; Reves, M.; Echeverria, J.; Cremades, E.; Barragan, F.; Alvarez, S. *Dalton Transactions* **2008**, *0*, 2832.

(85) Duan, H.; Sengupta, S.; Petersen, J. L.; Akhmedov, N. G.; Shi, X. *Journal of the American Chemical Society* **2009**, *131*, 12100.

(86) Sivaram, H.; Jothibasu, R.; Huynh, H. V. *Organometallics* **2012**, *31*, 1195.

(87) Frey, G. D.; Dewhurst, R. D.; Kousar, S.; Donnadieu, B.; Bertrand, G. *Journal of Organometallic Chemistry* **2008**, *693*, 1674.

(88) Busetto, L.; Cristina Cassani, M.; Femoni, C.; Macchioni, A.; Mazzoni, R.; Zuccaccia, D. *Journal of Organometallic Chemistry* **2008**, *693*, 2579.

(89) Su, H.-L.; Pérez, L. M.; Lee, S.-J.; Reibenspies, J. H.; Bazzi, H. S.; Bergbreiter, D. E. *Organometallics* **2012**, *31*, 4063.

(90) Mecking, S. *Angewandte Chemie International Edition* **2001**, *40*, 534.

(91) Takeuchi, D. *Dalton Transactions* **2010**, *39*, 311.

(92) Schmid, M.; Eberhardt, R.; Klinga, M.; Leskelä, M.; Rieger, B. *Organometallics* **2001**, *20*, 2321.

(93) Britovsek, G. J. P.; Bruce, M.; Gibson, V. C.; Kimberley, B. S.; Maddox, P. J.; Mastroianni, S.; McTavish, S. J.; Redshaw, C.; Solan, G. A.; Strömberg, S.; White, A. J. P.; Williams, D. J. *Journal of the American Chemical Society* **1999**, *121*, 8728.

(94) Mecking, S.; Johnson, L. K.; Wang, L.; Brookhart, M. *Journal of the American Chemical Society* **1998**, *120*, 888.

(95) Khramov, D. M.; Lynch, V. M.; Bielawski, C. W. *Organometallics* **2007**, *26*, 6042.

(96) Trnka, T. M.; Grubbs, R. H. *Accounts of Chemical Research* **2000**, *34*, 18.

(97) Vougioukalakis, G. C.; Grubbs, R. H. *Chemical Reviews* **2009**, *110*, 1746.

(98) Samojłowicz, C.; Bieniek, M.; Grela, K. *Chemical Reviews* **2009**, *109*, 3708.

(99) Nagai, Y.; Kochi, T.; Nozaki, K. *Organometallics* **2009**, *28*, 6131.

(100) Waltman, A. W.; Grubbs, R. H. *Organometallics* **2004**, *23*, 3105.

(101) Steinke, T.; Shaw, B. K.; Jong, H.; Patrick, B. O.; Fryzuk, M. D. *Organometallics* **2009**, *28*, 2830.

(102) Grundemann, S.; Albrecht, M.; Kovacevic, A.; Faller, J. W.; Crabtree, R. H. *Journal of the Chemical Society, Dalton Transactions* **2002**, *0*, 2163.

(103) Huang, Y.-P.; Tsai, C.-C.; Shih, W.-C.; Chang, Y.-C.; Lin, S.-T.; Yap, G. P. A.; Chao, I.; Ong, T.-G. *Organometallics* **2009**, *28*, 4316.

(104) Matsubara, K.; Ueno, K.; Shibata, Y. *Organometallics* **2006**, *25*, 3422.

(105) Herrmann, W. A.; Gerstberger, G.; Spiegler, M. *Organometallics* **1997**, *16*, 2209.

(106) Furst, M. R. L.; Cazin, C. S. J. *Chemical Communications* **2010**, *46*, 6924.

(107) Al Thagfi, J.; Lavoie, G. G. *Organometallics* **2012**, *31*, 2463.

(108) Winston, S.; Stylianides, N.; Tulloch, A. A. D.; Wright, J. A.; Danopoulos, A. A. *Polyhedron* **2004**, *23*, 2813.

(109) Bonnet, L. G.; Douthwaite, R. E.; Hodgson, R.; Houghton, J.; Kariuki, B. M.; Simonovic, S. *Dalton Transactions* **2004**, *0*, 3528.

(110) Froseth, M.; Dhindsa, A.; Roise, H.; Tilset, M. *Dalton Transactions* **2003**, *0*, 4516.

(111) Collado, A.; Balogh, J.; Meiries, S.; Slawin, A. M. Z.; Falivene, L.; Cavallo, L.; Nolan, S. P. *Organometallics* **2013**, *32*, 3249.

(112) Herrmann, W. A.; Goossen, L. J.; Artus, G. R. J.; Köcher, C. *Organometallics* **1997**, *16*, 2472.

(113) McGuinness, D. S.; Cavell, K. J.; Skelton, B. W.; White, A. H. *Organometallics* **1999**, *18*, 1596.

(114) Schaub, T.; Radius, U. *Chemistry – A European Journal* **2005**, *11*, 5024.

(115) Badaj, A. C.; Lavoie, G. G. *Organometallics* **2013**, *32*, 4577.

(116) Tamao, K.; Kiso, Y.; Sumitani, K.; Kumada, M. *J. Amer. Chem. Soc.* **1972**, *94*, 9268.

(117) Suzuki, A. *J. Organomet. Chem.* **1999**, *576*, 147.

(118) Sekiya, A.; Ishikawa, N. *J. Organomet. Chem.* **1976**, *118*, 349.

(119) Nicolaou, K. C.; Bulger, P. G.; Sarlah, D. *Angew. Chem., Int. Ed.* **2005**, *44*, 4442.

(120) Miyaura, N.; Suzuki, A. *Chem. Rev. (Washington, D. C.)* **1995**, *95*, 2457.

(121) Jessop, P. G.; Joo, F.; Tai, C.-C. *Coord. Chem. Rev.* **2004**, *248*, 2425.

(122) Herrmann, W. A. *Angew. Chem., Int. Ed.* **2002**, *41*, 1290.

(123) Breit, B. *Acc. Chem. Res.* **2003**, *36*, 264.

(124) Johnson, J. R.; Cuny, G. D.; Buchwald, S. L. *Angew. Chem., Int. Ed. Engl.* **1995**, *34*, 1760.

(125) Yamamoto, Y. *Coordination Chemistry Reviews* **1980**, *32*, 193.

(126) Yamamoto, Y.; Yamazaki, H. *Coordination Chemistry Reviews* **1972**, *8*, 225.

(127) Canovese, L.; Visentin, F.; Santo, C.; Levi, C.; Dolmella, A. *Organometallics* **2007**, *26*, 5590.

(128) Delis, J. G. P.; Aubel, P. G.; van Leeuwen, P. W. N. M.; Vrieze, K.; Veldman, N.; Spek, A. L. *Journal of the Chemical Society, Chemical Communications* **1995**, 2233.

(129) Delis, J. G. P.; Aubel, P. G.; Vrieze, K.; van Leeuwen, P. W. N. M.; Veldman, N.; Spek, A. L.; van Neer, F. J. R. *Organometallics* **1997**, *16*, 2948.

(130) Vicente, J.; Abad, J.-A.; MartÃ-nez-Viviente, E. s.; Jones, P. G. *Organometallics* **2002**, *21*, 4454.

(131) Owen, G. R.; Vilar, R. n.; White, A. J. P.; Williams, D. J. *Organometallics* **2002**, *21*, 4799.

(132) Onitsuka, K.; Yanai, K.; Takei, F.; Joh, T.; Takahashi, S. *Organometallics* **1994**, *13*, 3862.

(133) Veya, P.; Floriani, C.; Chiesi-Villa, A.; Rizzoli, C. *Organometallics* **1993**, *12*, 4899.

(134) Crociani, B.; Sala, M.; Polo, A.; Bombieri, G. *Organometallics* **1986**, *5*, 1369.

(135) Yamamoto, Y.; Tanase, T.; Yanai, T.; Asano, T.; Kobayashi, K. *Journal of Organometallic Chemistry* **1993**, *456*, 287.

(136) Han, Y.; Yuan, D.; Teng, Q.; Huynh, H. V. *Organometallics* **2011**, *30*, 1224.

(137) WÃrtz, S.; Glorius, F. *Accounts of Chemical Research* **2008**, *41*, 1523.

(138) Diez-Gonzalez, S.; Marion, N.; Nolan, S. P. *Chemical Reviews* **2009**, *109*, 3612.

(139) Carrow, B. P.; Nozaki, K. *Journal of the American Chemical Society* **2012**, *134*, 8802.

(140) Popeney, C. S.; Camacho, D. H.; Guan, Z. *Journal of the American Chemical Society* **2007**, *129*, 10062.

(141) Khlebnikov, V.; Meduri, A.; Mueller-Bunz, H.; Milani, B.; Albrecht, M. *New Journal of Chemistry* **2012**, *36*, 1552.

(142) Cavell, K. J.; McGuinness, D. S. *Coordination Chemistry Reviews* **2004**, *248*, 671.

(143) McGuinness, D. S.; Cavell, K. J. *Organometallics* **2000**, *19*, 4918.

(144) Liu, Y.-M.; Lin, Y.-C.; Chen, W.-C.; Cheng, J.-H.; Chen, Y.-L.; Yap, G. P. A.; Sun, S.-S.; Ong, T.-G. *Dalton Transactions* **2012**, *41*, 7382.

(145) Lee, J.-H.; Jeon, H.-T.; Kim, Y.-J.; Lee, K.-E.; Ok Jang, Y.; Lee, S. W. *European Journal of Inorganic Chemistry* **2011**, *2011*, 1750.

(146) Peñafiel, I.; Pastor, I. M.; Yus, M.; Esteruelas, M. A.; Oliván, M.; Oñate, E. *European Journal of Organic Chemistry* **2011**, *2011*, 7174.

(147) Fliedel, C.; Braunstein, P. *Organometallics* **2010**, *29*, 5614.

(148) Ray, L.; Shaikh, M. M.; Ghosh, P. *Organometallics* **2007**, *26*, 958.

(149) Veya, P.; Floriani, C.; Chiesi-Villa, A.; Rizzoli, C. *Organometallics* **1994**, *13*, 441.

(150) Dupont, J.; Pfeffer, M. *Journal of the Chemical Society, Dalton Transactions* **1990**, 3193.

(151) Warsink, S.; de Boer, S. Y.; Jongens, L. M.; Fu, C.-F.; Liu, S.-T.; Chen, J.-T.; Lutz, M.; Spek, A. L.; Elsevier, C. J. *Dalton Transactions* **2009**, 7080.

(152) Ketz, B. E.; Cole, A. P.; Waymouth, R. M. *Organometallics* **2004**, *23*, 2835.

(153) Brindley, J. C.; Caldwell, J. M.; Meakins, G. D.; Plackett, S. J.; Price, S. J. *Journal of the Chemical Society, Perkin Transactions 1* **1987**, *0*, 1153.

(154) Schwab, P.; Grubbs, R. H.; Ziller, J. W. *Journal of the American Chemical Society* **1996**, *118*, 100.

(155) Larocque, T. G.; Badaj, A. C.; Lavoie, G. G. *Dalton Transactions* **2013**, *42*, 14955.

(156) Blessing, R. *Acta Crystallographica Section A* **1995**, *51*, 33.

(157) Sheldrick, G. *Acta Crystallographica Section A* **2008**, *64*, 112.

(158) Palatinus, L.; Chapuis, G. *Journal of Applied Crystallography* **2007**, *40*, 786.

(159) Sheldrick, G. *Acta Crystallographica Section A* **1990**, *46*, 467.